

VAPOUR FILMS ON LIQUID METALS

by

DAVID TUDOR HUGHES

Submitted for the Degree of  
DOCTOR OF PHILOSOPHY  
at the University of Aston in Birmingham

January 1984

# VAPOUR FILMS ON LIQUID METALS

DAVID TUDOR HUGHES

Submitted for the Degree of PhD

January 1984

## SUMMARY

Vapour explosions resulting from the interaction of molten metals with water have been violent enough to cause loss of life. Widespread research has been initiated to study the cause of these explosions.

In this work, vapour films are examined to provide information relevant to vapour explosion phenomena.

Experiments have been performed to gain information on film boiling heat transfer from solid and liquid metals to coolants and to examine the physical characteristics and stability of vapour films. The bulk of the experiments involved the quenching of solid copper in water and organic (methanol, ethanol, n-propanol, acetone, chloroform and carbon tetrachloride) coolants and the quenching of liquid tin and liquid copper in water.

Transient calorimetry techniques were used to gain heat transfer data, and electrical techniques were used to examine the stability of vapour films. The capacitative properties of vapour films were examined, and estimates of vapour film thicknesses were made.

Results from the experiments were discussed in the context of self-triggered (spontaneous) explosions and externally triggered explosions.

VAPOUR  
FILMS  
LIQUID  
METAL  
EXPLOSIONS

### ACKNOWLEDGEMENTS

I would like to thank Professor F.M.Page,  
Professor W.O.Alexander, Dr.A.T.Chamberlain  
and Dr.J.F.W.Bell for their kind help and  
support during my research at Aston.

I would also like to thank the European Coal  
and Steel Commission for sponsoring my work.

LIST OF TABLES

Table 5.1	Values Of $\bar{s}$ And S	109
Table 6.1	Coolants In Which Explosions Were Not Recorded	134

## LIST OF FIGURES

Fig 2.1	The Boiling Curve	9
Fig 2.2	The Film Boiling Model Of Hsu And Westwater	20
Fig 3.1	The Copper Probe	40
Fig 3.2	The Probe Assembly	40
Fig 3.3	The Quenching Of The Probe	40
Fig 3.4	Film Boiling Data For Acetone	45
Fig 3.5	Film Boiling Data For Carbon Tetrachloride	46
Fig 3.6	Film Boiling Data For Chloroform	47
Fig 3.7	Film Boiling Data For Ethanol	48
Fig 3.8	Film Boiling Data For Methanol	49
Fig 3.9	Film Boiling Data For n-propanol	50
Fig 3.10	Minimum Temperatures For The Organic Coolants	51
Fig 3.11	The Apparatus Used To Quench The Probe In Water	53
Fig 3.12	Film Boiling Data For Water	55
Fig 3.13	Minimum Heat Fluxes For Water	55
Fig 3.14	Minimum Temperatures For Water	56

Fig 4.1	The D.C. Circuit	59
Fig 4.2	D.C. Analysis Of The Probe Cooling In n-propanol	60
Fig 4.3	A Trial Experiment	64
Fig 4.4	The Electrical Analogue	64
Fig 4.5	The Waveforms $F_1$ And $F_0$	68
Fig 4.6	The Capacitance-Resistance Transducer	72
Fig 4.7	Vapour Film Collapse In $70^{\circ}\text{C}$ Water	78
Fig 4.8	Vapour Film Collapse In $90^{\circ}\text{C}$ Water	79
Fig 4.9	A Trace Of $X_{Cv}$ And $R_w$	81
Fig 4.10	Film Boiling In n-propanol	86
Fig 4.11	The Film Thickness At Collapse In n-propanol	89
Fig 4.12	The Film Thicknesses At Collapse In Water	90
Fig 5.1	A Vertical Surface Undergoing Film Boiling	94
Fig 5.2	A Program To Calculate Heat Fluxes	103
Fig 5.3	Film Boiling Curves For Water	105
Fig 5.4	The Vapour Flow Reynolds Numbers	107

Fig 5.5	The Heat Flux $q_2$	111
Fig 6.1	D.C. Analysis Of Boxley's Apparatus	113
Fig 6.2	The Trial Apparatus	117
Fig 6.3	Liquid Metal Heat Transfer Apparatus	120
Fig 6.4	The Crucible Arrangement	121
Fig 6.5	Quenching Of The High-Walled Crucible	125
Fig 6.6	Heat Transfer Data For Liquid Metal-Water Systems	127
Fig 6.7	Minimum Temperatures In The Tin-Water System	132
Fig 7.1	The Electric Circuit Corresponding To Contact Across The Vapour Film	144
Fig 8.1	Apparatus For Measuring Heat Flux From A Liquid Surface	160

## LIST OF CONTENTS

Title Page		i
Summary		ii
Acknowledgements		iii
List of Tables		iv
List of Figures		v
CHAPTER ONE	INTRODUCTION	1
CHAPTER TWO	THEORETICAL ASPECTS OF VAPOUR EXPLOSIONS	7
2.1	Boiling Heat Transfer	8
2.2	Fragmentation Models	29
2.2.1	Impact Breakup	29
2.2.2	Coolant Entrapment	30
2.2.3	Dissolved Gas	31
2.2.4	Metal Solidification	32
2.2.5	Spontaneous Nucleation	33
2.2.6	Vapour Film And Vapour Bubble Collapse	35
2.3	Objectives Of The Present Work	37
CHAPTER THREE	PRELIMINARY HEAT TRANSFER EXPERIMENTS	39
3.1	Introduction	39

3.2	Experiments With Organic Coolants	39
3.3	Experiments With Water As A Coolant	44
3.4	Visual Observations	57
CHAPTER FOUR VAPOUR FILM ANALYSIS		58
4.1	Direct Current Analysis	58
4.2	Vapour Films As Capacitors	62
4.3	The Capacitance-Resistance Transducer	66
4.4	Experiments With The Transducer	76
4.4.1	Preliminary Experiments	76
4.4.2	Vapour Film Thickness At Collapse	84
4.5	The Effect Of The Transducer	91
CHAPTER FIVE A MODEL FOR FILM BOILING		92
5.1	Introduction	92
5.2	Heat Transfer Equations	93
5.3	Solution Of The Equations	102
5.4	The Vapour Flow Reynolds Number	104
5.5	The Mean Film Thickness	106
5.6	Film Boiling Over A Cooling Surface	108

CHAPTER SIX	HEAT TRANSFER FROM LIQUID METALS	112
6.1	Vapour Films On Liquid Metals	112
6.2	The Liquid Copper-Water System	119
6.3	Minimum Temperature Experiments	131
6.4	Small Scale Interactions	131
CHAPTER SEVEN	DISCUSSION	135
7.1	Discussion Of The Experimental Apparatus	135
7.2	Discussion Of Boiling Terminology	137
7.3	Discussion Of The Experimental Results	140
7.3.1	Thermal Experiments With The Copper Probe	140
7.3.2	Electrical Experiments With The Copper Probe	141
7.3.3	Experiments With Liquid Metals	145
7.4	Discussion Of The Model For Film Boiling	147
7.5	Discussion Of The Results In The Context Of Vapour Explosion Phenomena	149

7.5.1	Spontaneous Explosions	149
7.5.2	Externally Triggered Explosions	151
7.6	Suggestion For Further Work	158
APPENDIX		159
REFERENCES		162

## CHAPTER ONE

### INTRODUCTION

When a hot liquid comes into contact with a cold vaporisable liquid, a violent explosion may occur. These explosions are known as vapour explosions or fuel-coolant interactions, the hot liquid being the fuel and the cold liquid being the coolant. Interactions in which the fuel is molten metal, and the coolant is water have become a source of concern due to the number of molten metal-water explosions in industry which have been violent enough to cause loss of life. An early example of one such accident can be seen in a casualty list printed in 1826<sup>(1)</sup> which records the deaths of fifteen people. Records of these explosions are incomplete but the scope of the problem can be appreciated by noting that in 1975 there were 327 reported molten metal-water explosions in the UK, the most violent of these being at the British Steel's plant at Scunthorpe<sup>(2)</sup> in which eleven people were killed. The explosion was thought to have occurred due to an interaction between molten steel and water.

The Aluminium Association of America collected records,

which they acknowledge as being incomplete, for the years 1944 to 1975<sup>(3)</sup>. Their list shows that during these years in North America, there were 75 molten metal-water explosions in which a total of 32 people were killed. These explosions were usually the product of interactions between water and molten aluminium. The records do however include interactions involving molten iron, steel, copper and zinc.

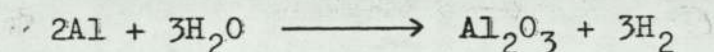
Research programmes have been initiated in an attempt to find the cause of molten metal-water explosions. The first empirical work was published by Long<sup>(4)</sup> in 1957.

Long performed experiments in which molten aluminium (usually 50 lb) was dropped into water held in a steel tank. The explosions that occurred were characterised by a violent bursting action, closely followed by a loud noise and a shock wave. Quantities of finely divided aluminium were formed along with a small white cloud of aluminium oxide.

It was noted that in order for an explosion to occur, the molten aluminium had to reach the base of the water tank. When the base of the tank had been intentionally covered in oil, grease or paint,

explosions never occurred, whereas coatings of rust or lime increased the likelihood of an explosion. It was found that no explosions occurred when the temperature of the water was above 60°C. Explosions that occurred at lower water temperatures could be prevented by the addition of soluble oil to the water.

In the experiments, there was no visible flash and never more than a slight cloud of aluminium oxide. Therefore, the exothermic reaction



was not considered to be significantly involved in the interactions.

Epstein<sup>(5)</sup> studied the kinetics involved in the system of a condensed metal phase with water vapour, and the calculations indicate that the only way the timescale of a vapour explosion (less than 10 ms) could chemically occur would be for every water molecule striking the metal surface to react, forming metal oxide and hydrogen. Since this is a limiting case, it is unlikely to occur. Vapour explosions are generally held to be physical in nature. The energy for the interaction is assumed to come from

the excess heat in the metal, which is transferred with rapid vapourisation of the coolant, and the formation of finely divided metal debris.

Large scale interactions (metal mass between 2.5 and 7 kg) have been investigated by Alexander, Chamberlain and Page<sup>(6)</sup>. Molten aluminium, brass, copper and cast iron were poured into water held in a steel tank. The metal-water interactions were initiated by the detonation of a cordtex charge attached to the outside of the water tank. The cordtex could be detonated whilst the metal was falling through the water, or when the metal arrived at the tank base. It was found that the efficiency of the explosion, measured by the deformation of a crush block upon which the water tank rested, was not dependent on the amount of cordtex used, as long as the amount had been sufficient to start the explosive process. The efficiency of the explosions was found to increase as the metal superheat increased and as the water temperature increased.

Large scale experiments, whilst providing situations similar to those found in industry, and giving scope for experiments involving high energy triggers, are extremely expensive. Research programmes in which

small scale interactions are observed in the laboratory are more numerous than large scale interaction programmes.

Many small scale experiments have been performed in which quantities of liquid metal (often less than 20g) were dropped into water, the resulting interaction being observed photographically. Konuray<sup>(7)</sup> performed experiments in which liquid tin was used, and observed that the liquid tin could spontaneously explode as it fell through the water. Such explosions were not found to occur when the water temperature was above 60°C (sometimes called the coolant cut-off temperature). This temperature behaviour has been confirmed by Dullforce, Buchanan and Peckover<sup>(8)</sup> and by Pool<sup>(9)</sup>. Konuray noted similar behaviour with other low melting point metals (Thallium, Indium and Bismuth). Pool observed that lead could spontaneously explode in room temperature water, in contrast to the higher melting point metals copper and aluminium. Pool also noted that molten tin did not spontaneously explode in carbonated water, formamide or n-propanol.

Some idea of the extent of the fragmentation that can occur during vapour explosions is given by experiments performed by Nelson and Duda<sup>(10)</sup>, in which an iron oxide drop, 2.9 mm in diameter, initially at 2000<sup>o</sup>K, is dropped into water and then made to undergo a vapour explosion by triggering the explosive process using an exploding bridgewire held in the water. Their experiments show that an iron oxide particle can fragment into about two million particles in a few milliseconds.

## CHAPTER TWO

### THEORETICAL ASPECTS OF VAPOUR EXPLOSIONS

It is assumed that the energy for a vapour explosion comes from the excess heat in the molten metal.

This energy is transferred from the metal in a few milliseconds, with rapid vapourisation of the coolant and fragmentation of the metal.

In order to examine vapour explosion phenomena, the way in which heat can be transferred from a metal to a coolant and the way in which a liquid metal can fragment have to be examined.

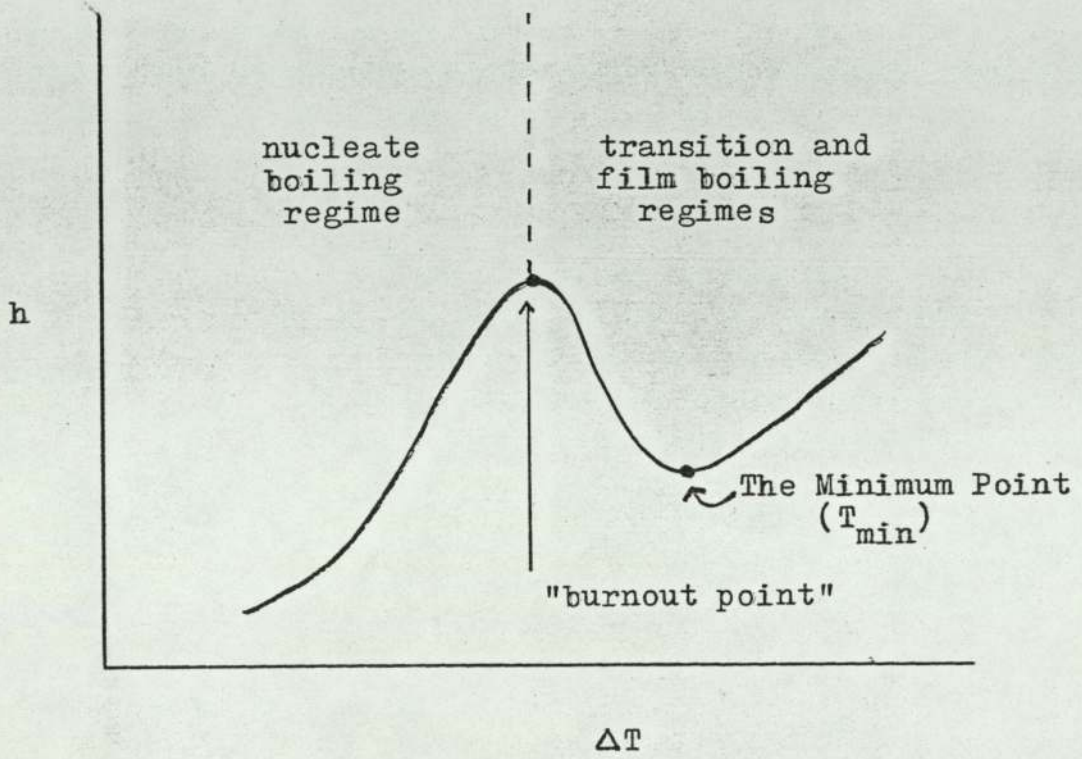
In this chapter, the theories of boiling heat transfer with particular reference to the film boiling regime and the experiments which have given information on the appearance, stability and thermal characteristics of vapour films are discussed. The fragmentation models are discussed in section 2.2, the objectives of this thesis being presented in section 2.3.

## 2.1 Boiling Heat Transfer

When a surface is submerged in a liquid such that the surface has a temperature in excess of the liquid saturation temperature, boiling may occur. It has been found that the amount of heat that travels from a surface to a boiling liquid depends on the temperature difference between the surface and the liquid. The relationship between the rate of heat transfer from the surface and the temperature difference has been studied by Nukiyama<sup>(11)</sup> and Farber and Scoriah<sup>(12)</sup>. Their experiments show that different regimes of boiling are identifiable. A graph showing the general relationship between the heat transfer coefficient ( $h$ ) and the temperature difference ( $\Delta T$ ) between the surface and the saturated liquid is shown in Fig 2.1. For low values of  $\Delta T$ , any vapour that is formed exists as vapour bubbles. At high values of  $\Delta T$ , a distinct vapour phase between the surface and the liquid forms.

In order for a bubble to form in a liquid, a surface of separation has to be formed. Kelvin has shown that as a result of surface tension, the pressure inside such a bubble  $p_v$ , and the liquid pressure outside  $p_l$  are related by the equation

Fig 2.1 The Boiling Curve



$$p_v - p_l = \frac{2\sigma}{r} \quad \dots(2.1)$$

where  $r$  is the radius of the bubble and  $\sigma$  is the surface tension of the liquid. This equation implies that it is impossible for bubbles to be created, since as  $r$  tends to zero,  $p_v - p_l$  tends to infinity. Vapour bubbles can however be created by homogeneous and heterogeneous nucleation (Cole<sup>(13)</sup>).

Homogeneous nucleation is a process in which molecules of liquid which have high energy compared to the average, cluster together through collision and initiate the formation of a vapour bubble. Kenrick, Gilbert and Wismer<sup>(14)</sup> have experimentally measured the maximum superheat of water to be 170°C. Buchanan and Dullforce<sup>(15)</sup> note that generally, water is extremely difficult to superheat. In order to superheat water by more than 10°C requires careful preparation, i.e. the water has to be boiled for several hours and has to be kept under vacuum. This is because heterogeneous nucleation invariably occurs, due to dust and dissolved gas present in the liquid and imperfections in the heater surface, which can provide sites for the nucleation of vapour bubbles. Thus, unless the heater surface is scrupulously clean and the liquid completely degassed, heterogeneous

nucleation will occur. In the following discussion of nucleate boiling, it is assumed that the vapour bubbles are formed by heterogeneous nucleation.

If the heater is a few degrees above the liquid (also referred to as the coolant) saturation temperature, vapour bubbles are formed. An increase in the temperature of the surface causes more bubbles to be formed from more nucleation sites. When the surface loses heat by this process, i.e. effecting a change of phase of the coolant at preferred nucleation sites, the system is said to be in the nucleate boiling regime.

In this regime, any liquid which is directly in contact with the heater surface exists in a superheated condition. Rohsenow and Clark<sup>(16)</sup> postulate that the vapour bubbles agitate the quiescent regions of liquid adjacent to the heater surface. This results in high heat transfer rates from the surface to the liquid.

Cryder and Finalborgo<sup>(17)</sup> boiled a number of liquids on a horizontal brass plate and showed that for a variety of liquids boiling in the nucleate boiling regime, the heat transfer coefficient  $h$ , could be

related to the temperature difference  $\Delta T$  by the expression

$$h = \text{const} \cdot \Delta T^{2.5} \quad \dots(2.2)$$

In this regime, the heat transfer rate is a function of the surface roughness. Berenson<sup>(18)</sup> boiled pentane on horizontal copper plates of varying surface roughness, and observed that for a given temperature difference between the plate and the pentane, a plate which had a rougher surface resulted in heat being transferred from the plate at a higher rate.

When the temperature difference between the submerged surface and the coolant reaches a sufficiently high value, the bubbles are formed so rapidly that they cannot all get away from the surface, and they start to coalesce. This coalescence means that less liquid is able to flow onto the surface to take any major part in the heat transfer, and thus the heat transfer coefficient starts to fall.

The point of maximum heat flux is sometimes called the "First Crisis" or "Burnout" point, since when heaters such as electrically heated filaments reach

this point, a rise in temperature causes a decrease in heat flux sometimes causing the heater to burnout.

Zuber<sup>(19)</sup> assumed that the burnout point corresponded to a Helmholtz instability which occurred due to the relative velocities of the liquid streams flowing onto the surface and the vapour streams going away from the surface. From this assumption, Zuber obtained an expression for the maximum heat flux on horizontal heaters such that

$$q_{\max} = \frac{\pi}{24} \rho_v^{\frac{1}{2}} L \left\{ \sigma g (\rho_l - \rho_v) \right\}^{1/4} \left\{ 1 + \rho_v / \rho_l \right\}^{\frac{1}{2}} \dots(2.3)$$

where

$q_{\max}$  = the maximum heat flux

$\rho_v$  = density of the vapour

$L$  = latent heat of vapourisation of the coolant

$\sigma$  = surface tension between the liquid and the vapour

$g$  = acceleration due to gravity

$\rho_l$  = density of the liquid

This equation estimates that at atmospheric pressure, the burnout heat flux in saturated water from a horizontal heater is  $1.1 \text{ MWm}^{-2}$ .

Ded and Lienhard<sup>(20)</sup> took Zuber's approach and applied

it to spheres and showed that the ratio ( $q_{\max}/q_{\max F}$ ), of the burnout heat flux for spheres and the burnout heat flux for horizontal surfaces could, for saturated coolants, be expressed as

$$\frac{q_{\max}}{q_{\max F}} = \frac{1.734}{r^{\frac{1}{2}}} \quad \text{when } 0.1 \lesssim r \lesssim 4.26$$

and

$$\frac{q_{\max}}{q_{\max F}} = 0.84 \quad \text{when } r \geq 4.26$$

where

$$r = R \left\{ g(\rho_l - \rho_v) / \sigma \right\}^{\frac{1}{2}} \quad \dots(2.4)$$

and R is the radius of the sphere

When the temperature difference increases from the temperature difference corresponding to the maximum heat flux, the resulting boiling becomes unstable. This unstable region of boiling is referred to as transition boiling or partial film boiling. Berenson<sup>(18)</sup> describes this region of boiling as a mixture of unstable film boiling and unstable nucleate boiling. Westwater and Santangelo<sup>(21)</sup> observed this regime

of boiling using high speed photography. Their observations show that the vapour is formed by explosive bursts at random locations. The decreasing heat flux of this regime reaches a minimum referred to as the "Second Crisis". This point corresponds to the onset of film boiling, the situation in which the heater is separated from the coolant by a film of vapour.

An example of film boiling is the Leidenfrost<sup>(22)</sup> phenomenon, in which water droplets can "dance" on a very hot surface. The droplets do not evaporate quickly since an insulating vapour layer forms between the hot surface and the droplet.

Once a stable vapour film (sometimes called a vapour blanket) forms, a rise in heater surface temperature produces a rise in the heat flux leaving the heater surface. The heat leaving the surface is conducted across the vapour film by the vapour molecules, the conducted heat being capable of producing vapour. As the surface temperature increases, the contribution made by radiative heat transfer can become important.

Bromley<sup>(23)</sup> derived a theory for film boiling in a

saturated coolant, using assumptions and equations similar to those used by Nusselt, who theoretically estimated the heat transfer rates present when vapours condense on cold surfaces. An account of Nusselts theory is given by Monrad and Badger<sup>(24)</sup>. Bromley considered the heat transfer rates that would be expected from horizontal and vertical tubes submerged in saturated coolants. The assumptions used by Bromley were

- 1 The liquid is separated from the hot tube by a continuous vapour film.
- 2 Heat travels through the film by conduction and radiation.
- 3 Vapour rises under the action of buoyant forces.
- 4 The vapour-liquid interface is smooth in the section where most of the heat is transferred.
- 5 The rise of the vapour is retarded by the viscous drag of the tube.
- 6 The latent heat of vapourisation is the major item in the heat supplied to the vapour film.
- 7 The kinetic energy of the film is negligible.
- 8 The vapour-liquid interface is smooth and continuous and is not affected by a variation in the vapour-liquid surface tension.

- 9 It is permissible to use an average value for the temperature difference between the hot tube and the boiling liquid, and treat it as a constant around the tube.
- 10 The coolant is at its boiling point at the vapour-liquid interface.
- 11 It is satisfactory to evaluate all physical properties of the vapour at the arithmetic mean temperature of the hot surface and the boiling liquid.

The equation for the heat transfer coefficient obtained by Bromley for a vertical tube undergoing film boiling in a saturated coolant was

$$h = 0.943 \left\{ \frac{k_v^3 \rho_v (\rho_L - \rho_v) g \lambda'}{L_o \mu_v \Delta T} \right\}^{1/4} \dots(2.5)$$

where

- $h$  = heat transfer coefficient
- $k_v$  = vapour thermal conductivity
- $\rho_v$  = vapour density
- $\rho_L$  = liquid density
- $g$  = acceleration due to gravity
- $L_o$  = height of the tube undergoing film boiling
- $\mu_v$  = vapour viscosity
- $\Delta T$  = temperature difference between the tube and the coolant

and

$$\lambda' = L \left\{ 1 + \frac{0.34 C_v \Delta T}{L} \right\}^2$$

where

$C_v$  = specific heat capacity of the vapour

$L$  = latent heat of vapourisation of the coolant

Bromley performed experiments using various heater surfaces, and concluded that the heat transfer coefficients were independent of the nature of the heater surface as long as the contributions made to the overall heat transfer coefficient by radiative heat transfer were neglected. Similarly, Berenson<sup>(18)</sup> concluded that the surface roughness does not affect the heat transfer as long as the film thickness is greater than the surface roughness height.

When using horizontal tubes, Bromley noted that horizontal tubes submerged one inch below the coolant surface gave the same heat transfer coefficients as those which were not totally submerged (one sixth part being exposed) in the coolant. The vapour escaped freely from the horizontal tube

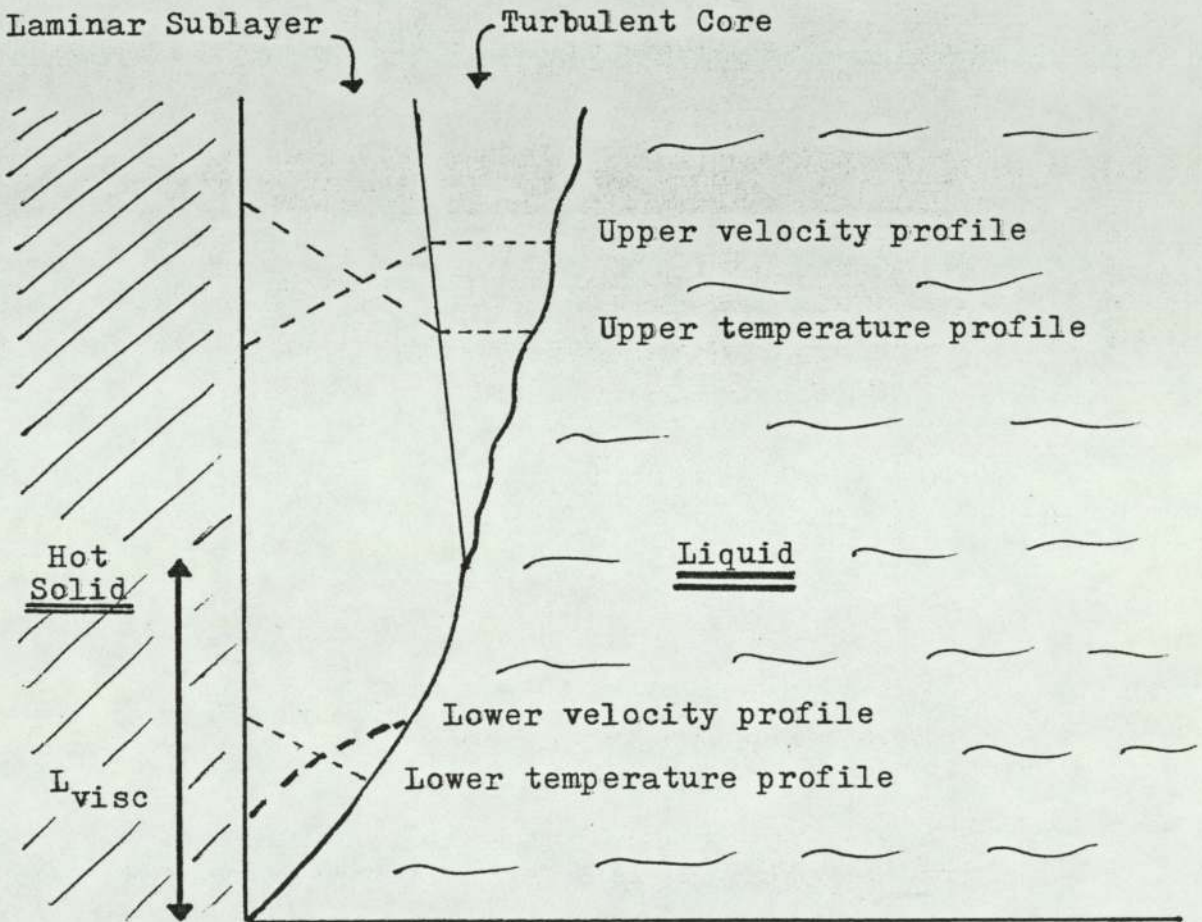
partially submerged, in contrast to the totally submerged tube where the vapour left the vapour-liquid interface as vapour bubbles, which set up convection currents in the coolant.

Hsu and Westwater<sup>(25)</sup> observed that equation (2.5) predicted heat fluxes that were too low if turbulence of the vapour in the film occurred. They suggested that when using Bromley's model, it is only reasonable to assume that the flow of vapour is viscous when the height of the vertical tube is less than  $L_{\text{visc}}$  where

$$L_{\text{visc}} = \frac{\mu_v \lambda'}{2k_v \Delta T} \left\{ \frac{2 \mu_v^2 \text{Re}^{*4}}{g \rho_v (\rho_l - \rho_v)} \right\}^{\frac{1}{2}} \quad \dots(2.6)$$

$\text{Re}^*$  was taken to be 100 and was assumed to correspond to the vapour flow Reynolds number which had to be exceeded for turbulence of the vapour to occur. They obtained this value for  $\text{Re}^*$  by considering the Prandtl-Nikuradse universal velocity profile. An account of this profile can be found in reference (26). Fig 2.2 is a diagram showing the postulated film boiling model of Hsu and Westwater. In the laminar sublayer, the temperature was assumed to fall linearly, and the vapour velocity follow the relation put forward by Bromley. In the turbulent

Fig 2.2 The Film Boiling Model Of Hsu And Westwater



core, the vapour velocity was considered to be a constant, the temperature of this vapour assumed to be equal to the boiling point of the coolant.

The models of Bromley and Hsu and Westwater only considered the situation where the coolant was at its boiling point.

Awberry<sup>(27)</sup> considered the case of a thin submerged horizontal plate undergoing film boiling in sub-cooled coolants. Heat was assumed to travel across the vapour film by conduction and radiation, the heat arriving at the vapour-liquid interface being carried away by convection into the coolant. The vapour in the film was assumed to condense rather than evaporate during the process.

The equation obtained for this film boiling was

$$q = B ( T_b - T_o )^{4/3} ( k^2 \alpha g c / \nu )^{1/3} \dots(2.7)$$

where

$q$  = heat flux

$T_b$  = boiling point of the coolant

$T_o$  = bulk temperature of the coolant

- k = thermal conductivity of the coolant
- $\alpha$  = cubic expansivity of the coolant
- g = acceleration due to gravity
- c = specific heat of the coolant
- $\nu$  = kinematic viscosity of the coolant
- B = 0.0015 when the thermal quantities are measured in calories

All the variables associated with the coolant are estimated at the temperature  $\frac{1}{2}(T_o + T_b)$ . The right hand side of equation (2.7) is a function of the rate of heat transfer from the vapour-liquid interface to the coolant.

The film boiling models discussed do not give any information on vapour film stability. They imply, in contrast to experiment, that a heater with a temperature only slightly above the coolant boiling point will be capable of sustaining a vapour film.

The question of vapour stability was considered by Berenson<sup>(28)</sup> who formulated an analysis based on a Taylor instability near the minimum film boiling point on a horizontal surface submerged in a saturated coolant. Berenson's expression for the heat transfer coefficient ( $h_{crit}$ ) near the minimum heat flux is

$$h_{\text{crit}} = 0.425 \left\{ \frac{k_v^3 (\rho_L - \rho_v) L g \rho_v}{\mu_v \Delta T (g_0 \sigma / g (\rho_L - \rho_v))^{\frac{1}{2}}} \right\}^{1/4} \dots(2.8)$$

$g_0$  is a conversion factor,  $32.2 \text{ lb}_m \text{ ft} / \text{lb sec}^2$ , and  $\sigma$  is the surface tension of the coolant.

This result differs from Bromley's in that the term  $(g_0 \sigma / g (\rho_L - \rho_v))^{\frac{1}{2}}$  is present in place of  $L_0$  for the vertical tube.

Spiegler<sup>(29)</sup> considered the film destabilisation temperature ( $T_D$ ) in terms of thermodynamics rather than hydrodynamics by assuming that  $T_D$  corresponded to the maximum metastable temperature to which the coolant can be heated. This temperature, computed from the Van der Waals equation of state is

$$T_{\text{max}} = \frac{27}{32} T_c \dots(2.9)$$

where  $T_c$  is the critical temperature of the coolant.

Experiments to provide information on film boiling heat fluxes, and film destabilisation temperatures, have been performed by many workers using quenching techniques. Heaters, often spheres, with a thermo-

couple mounted inside, have been quenched in the coolant. The heater cools initially surrounded by a vapour film which collapses at temperature  $T_D$ . The heat fluxes from such experiments are computed using the equation

$$q = \frac{m C_p}{A} \cdot \frac{dT}{dt} \quad \dots(2.10)$$

where

- q = heat flux
- m = mass of the heater
- $C_p$  = specific heat capacity of the heater
- A = area of the heater exposed to the coolant
- $\frac{dT}{dt}$  = cooling rate of the heater in the coolant

Dullforce<sup>(30)</sup>, who quenched a 19.5 mm diameter steel sphere in water at various subcoolings, correlated his data to show that in the film boiling regime

$$\left( \frac{dT}{dt} \right)_{1000} = 21.563 \exp ( 0.0724 T_{sub} )$$

and

$$\left( \frac{dT}{dt} \right)_{750} = 10.753 \exp ( 0.0965 T_{sub} )$$

where  $(dT/dt)_{1000}$  is the cooling rate of the sphere when the sphere temperature was  $1000^{\circ}\text{K}$ ,  $(dT/dt)_{750}$  being the corresponding value at  $750^{\circ}\text{K}$ .  $T_{\text{sub}}$  is the subcooling of the water.

Dullforce noted that the film destabilisation temperature was higher in cold water than in hot water. From Dullforce's data, it can be seen that the mean film breakdown temperature was approximately  $540^{\circ}\text{C}$  in  $20^{\circ}\text{C}$  water, the corresponding temperature being about  $320^{\circ}\text{C}$  in  $80^{\circ}\text{C}$  water. A linear relationship between the mean vapour collapse temperature and the water subcooling was observed.

This linear relationship has also been observed by Konuray<sup>(7)</sup> who quenched a one inch diameter stainless steel sphere in water. The film breakdown temperature in  $50^{\circ}\text{C}$  water was found to be about  $610^{\circ}\text{C}$ , the corresponding temperature for  $80^{\circ}\text{C}$  water was roughly  $330^{\circ}\text{C}$ . Konuray noted that the addition of a small amount of Teepol to the water slightly lowered the film collapse temperatures.

Experiments on the heat transfer from liquid metals to water have been performed by Boxley<sup>(31)</sup> in which the cooling rate of liquid tin, lead and aluminium

held in a crucible have been recorded. An account of Boxley's experiment is presented in the Appendix. It was noted that the heat transfer rates were not dependent on the metal used.

In order to examine the nature of vapour films during quenching, Bradfield<sup>(32)</sup> connected the vapour film into an electric circuit and observed the current flow which occurred when the coolant contacted the metal. Bradfield quenched a 2.375" diameter, 538°C, chrome plated copper sphere in 80°C water and noted that intermittent liquid-solid contact could occur during stable film boiling. Bradfield also observed that the area of the sphere in contact with the coolant decreased as the sphere cooled in the nucleate boiling regime. This decrease was assumed to be due to the onset of bubble formation.

Experiments have been performed to observe the cooling of spheres as they travel through water. Walford<sup>(33)</sup> performed experiments in which a 6.35 mm diameter nickel sphere was quenched in water, the relative velocity between the sphere and the water being 1.2 to 1.5 ms<sup>-1</sup>. The highest heat flux recorded in these experiments was 8.9 MWm<sup>-2</sup>, obtained with an oxidised sphere (initially at 800°C) in 40°C water. At high water subcoolings, Walford observed three different types of vapour film.

These were

- 1 A smooth and stable laminar film which in some tests changed to
- 2 A fine turbulent film in which the vapour layer became opaque and less than 15 microns thick in the direction of sphere travel. On further cooling this changed to
- 3 A coarse turbulent film in which there were large disturbances at the vapour-liquid interface. This collapsed into violent nucleate boiling.

At low water subcoolings ( $5-20^{\circ}\text{C}$ ), with the initial sphere temperature less than  $500^{\circ}\text{C}$ , it was found that a large spherical cavity formed around the sphere. The sphere moved through this cavity until it touched the vapour-liquid interface at which point, vapour production produced another cavity.

Oscillating vapour films were observed by Board et Al<sup>(34,35)</sup> who investigated transient film boiling over a 0.01 mm thick nickel foil which was heated by a pulsed ruby laser. When the foil temperature was below  $450^{\circ}\text{C}$ , an oscillating vapour film was observed. The frequency of oscillation increased linearly from 5 to 15 kHz as the water subcooling was varied from  $25^{\circ}\text{C}$  to  $75^{\circ}\text{C}$ .

For temperatures above 400°C, and moderate subcoolings, a thin vapour film with "rapidly moving irregularities", was observed. As the level of subcooling was further decreased, a stable thick blanket was observed. At low subcoolings, the heat fluxes observed were consistent with conduction across a pure laminar film, given by

$$q = \frac{k_v (T_w - T_{sat})}{\delta} \quad \dots(2.11)$$

where

$q$  = heat flux

$k_v$  = thermal conductivity of the vapour

$T_w$  = temperature of the foil

$T_{sat}$  = boiling point of water

$\delta$  = vapour film thickness

At high subcoolings, the observed heat fluxes were up to an order of magnitude greater than those given by equation (2.11). They suggested that the vapour film was in the form of a two phase layer.

## 2.2 Fragmentation Models

In this section, the models which have been put forward for the fragmentation of liquid metals are outlined and discussed. Their number and diversity show that little is known about the process. The overall fragmentation mechanism may vary between explosions, and could be a combination of some of the models presented.

### 2.2.1 Impact Breakup

In this model for fragmentation, it is assumed that when liquid metal falls onto a coolant, the breakup of the metal occurs due to the surface tension forces holding the metal together being overcome by inertial forces. The ratio governing this instability is the Weber number (We), which is given by

$$We = \frac{\rho_c R V^2}{\gamma} \quad \dots(2.12)$$

where

$\rho_c$  = density of the coolant

R = radius of the molten metal drop

V = molten drop velocity

$\gamma$  = molten metal surface tension

An analysis of this fragmentation has been carried out by Hinze<sup>(36)</sup>. Witte and Cox<sup>(37)</sup> note that the critical range of Weber numbers for this fragmentation has been established as being between 10 and 20.

Nelson and Duda<sup>(10)</sup> noted in their experiments observing the interaction of molten iron oxide drops with water, that the extensive fragmentation of the drops that they sometimes observed could not satisfactorily be accounted for by this impact breakup model. They point out that the time taken for the iron oxide drops to fragment, (a few milliseconds), is significantly shorter than would be expected if the fragmentation was wholly due to a Weber instability.

### 2.2.2 Coolant Entrapment

The concept of coolant entrapment was put forward by Long<sup>(4)</sup> after observing the behaviour of molten aluminium when it was poured into water held in steel tanks. He suggested that the trigger for the large explosions that were observed had been generated by a smaller explosion due to the sudden vapourisation of a very thin layer of water trapped in between the molten aluminium and the tank base. It was suggested

that the small explosion had dispersed the metal into small droplets, which because of their small size and high speed, could not support vapour films, thus resulting in heat being transferred from the metal at high rates. These high rates of heat transfer would generate large amounts of steam and consequently cause a vapour explosion. Long suggested that coatings of grease, oil or paint on the tank base which were found to prevent explosions did not allow water to be trapped between the molten aluminium and the tank base.

Experiments performed by Alexander, Chamberlain and Page<sup>(6)</sup> in which 2.5 kg of aluminium was poured into water held in steel tanks have shown that explosions can occur before the aluminium reaches the base of the tank, if the molten aluminium-water system is externally triggered by a cordtex charge attached to the outside of the tank. They conclude that the function of the base is to generate the trigger and not to generate the explosion.

### 2.2.3 Dissolved Gas

A model for fragmentation of the liquid metal by the violent release of gas dissolved in the liquid metal

has been put forward by Epstein<sup>(38)</sup>. In this model, it is assumed that as the metal is quenched, any dissolved gas in the metal becomes supersaturated, causing high pressures to be generated in the liquid metal which are capable of causing the liquid metal to fragment.

In order for this model to apply, the metal must be capable of dissolving gas without forming a stable phase, and the solubility of the gas in the metal must increase with temperature. Many laboratory explosions have occurred under conditions where the metal was only in contact with inert gas. Johnson and Shuttleworth<sup>(39)</sup> have shown that the amount of krypton that can be dissolved in liquid tin and lead is very small.

#### 2.2.4 Metal Solidification

In this model, it is assumed that the metal surface freezes, forming a surface skin which pressurises the inner molten metal core. The pressurisation is assumed to cause the skin to rupture and fragment the metal. Hsaio<sup>(40)</sup> theoretically analysed the cooling of an aluminium alloy sphere, and predicted that rupture of the frozen surface would occur for high cooling rates of the sphere.

Zyskowski<sup>(41)</sup> observed the behaviour of small amounts of liquid copper (0.5 to 2g) in room temperature water, and suggested that the pressures induced by the freezing metal surface caused jets of liquid copper to be ejected from the main liquid copper mass. It was assumed that these jets bridged the vapour film, giving rise to fast solidification of the copper in or near the jet. Zyskowski assumed that this period of fast phase transformation caused the fragmentation.

This model, based on pressurisation of the metal due to surface solidification, cannot account for the explosions observed in the bismuth-water system observed by Flory, Paoli and Messler<sup>(42)</sup>, since bismuth expands on freezing.

#### 2.2.5 Spontaneous Nucleation

In this model proposed by Fauske<sup>(43)</sup>, it is assumed that contact between the liquid metal and coolant occurs in such a way that the interface temperature between the molten metal and coolant is in excess of the spontaneous nucleation temperature of the coolant. This contact is assumed to give rise to explosive vapourisation of the coolant.

The interface temperature  $T_{int}$  is calculated from the equation

$$\frac{T_{int} - T_{cl}}{T_m - T_{int}} = \left\{ \frac{k_m \rho_m C_m}{k_{cl} \rho_{cl} C_{cl}} \right\}^{\frac{1}{2}} \quad \dots(2.13)$$

where

- $T$  = temperature
- $k$  = thermal conductivity
- $\rho$  = density
- $C$  = specific heat capacity

and for the subscripts

- int = interface
- m = metal
- cl = coolant

The spontaneous nucleation temperature,  $T_{spon}$ , can take any temperature between the coolant saturation temperature and the coolant homogeneous nucleation temperature,  $T_{hom}$ . If there are few nucleation sites available,  $T_{spon}$  will take a value near  $T_{hom}$ . This model is not capable of giving a direct explanation for the existence of the coolant cut-off temperatures that are observed when low melting point metals interact with water.

### 2.2.6 Vapour Film And Vapour Bubble Collapse

A sufficiently hot liquid metal in a coolant, will cool surrounded by a vapour film. At a certain temperature, the vapour film will collapse and contact between the molten metal and the coolant may occur. Whilst this sequence of events is compatible with initiation of the metal pressurisation models, (metal solidification and dissolved gas models), it may account for fragmentation of the liquid metal by vapour bubble collapse.

Buchanan and Dullforce<sup>(44)</sup> suggest that the contact between the metal and the coolant produces a vapour bubble. This is the first stage of a five stage process, the subsequent stages being

Stage 2 The vapour bubble expands and collapses within the coolant. The collapse is asymmetric and a high velocity jet of cold coolant is directed towards the molten metal

Stage 3 The cold jet penetrates the molten metal and disintegrates

Stage 4 During the breakup of the jet, heat is transferred to the coolant, and the contact area between the coolant and the molten

metal increases rapidly.

Stage 5. Once the jet has reached a certain temperature, it evaporates suddenly and a high pressure bubble is formed and it disperses the surrounding molten metal in the form of small droplets into the coolant, and the process continues again from Stage 2.

Nelson and Duda<sup>(10)</sup> believe that the best explanation for the fragmentation of the iron oxide drops in water that they observed is related to the destabilisation of film boiling. They find the hypothesis of jet formation due to bubble collapse near a surface to be "attractive". They saw evidence of such collapse adjacent to the iron drops in several of their films, followed by strong asymmetric ejection of melt.

Witte and Cox<sup>(37)</sup> note that generally, the presence of vapour inhibits fragmentation, but the collapse of the vapour film leads to fragmentation. They conclude that, "this observation adds credence to the notion... that the precipitous collapse of a vapour film may be the key to molten metal fragmentation".

### 2.3 Objectives Of The Present Work

Whilst no one is in a position to say that the precipitous collapse of a vapour film is the key to molten metal fragmentation, there is no doubt that in order to examine vapour explosions, additional information on vapour films is desirable.

The objectives of the present work are to gain information on film boiling heat transfer from solid and liquid metals to coolants and to look at the physical characteristics and stability of vapour films.

In these experiments, the differences in behaviour of vapour films generated over solid copper in water and organic coolants are examined. These experiments record the thermal and electrical properties of the films. The preliminary electrical analyses are based on the experiments of Bradfield<sup>(32)</sup>. The results from these experiments are used to investigate the observation made by Pool<sup>(9)</sup>, that liquid tin spontaneously explodes in room temperature water, but not in n-propanol.

The experiments of Boxley<sup>(31)</sup> are analysed, and experiments are performed to estimate the heat fluxes

that are present in the liquid copper-water system. The results from these experiments are used to discuss the possibility of molten copper-water interactions being simple steam explosions.

A model for film boiling in subcooled coolants is also presented.

## CHAPTER THREE

### PRELIMINARY HEAT TRANSFER EXPERIMENTS

#### 3.1 Introduction

Heat flux data during film boiling were obtained using a quenching technique, based on the method used by Ded and Lienhard<sup>(20)</sup>. The cooling rates of a copper probe submerged in a variety of sub-cooled coolants were recorded.

The probe used was a cylinder with a hemispherical base (Fig 3.1). A hole from the upper plane face to the equatorial plane was drilled to enable a thermocouple junction to be positioned at the probe centre. A magnesia-packed inconel-sheathed chromel-alumel thermocouple was used to record the cooling rate of the probe. To ensure a fast response, the inconel and magnesia around the thermocouple hot junction was removed and replaced with a small quantity of copper.

#### 3.2 Experiments With Organic Coolants

The thermocouple was passed through a brass collar and a loose fitting pyrophyllite ring, and then

Fig 3.1 The Copper Probe

Fig 3.2 The Probe Assembly

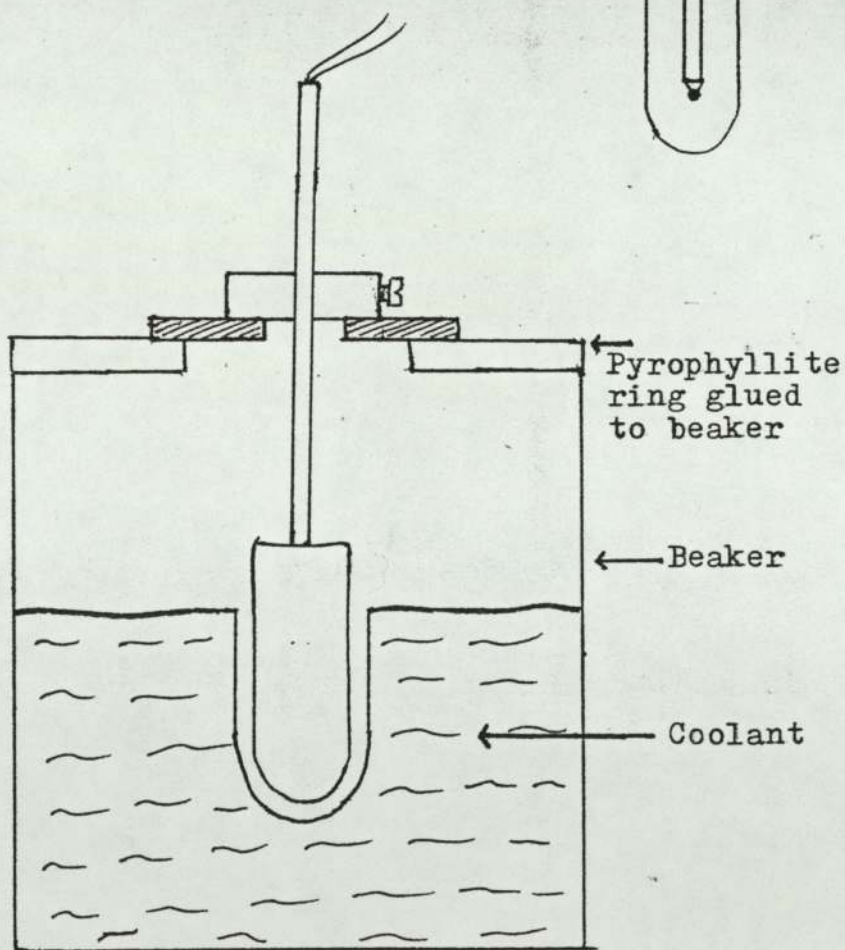
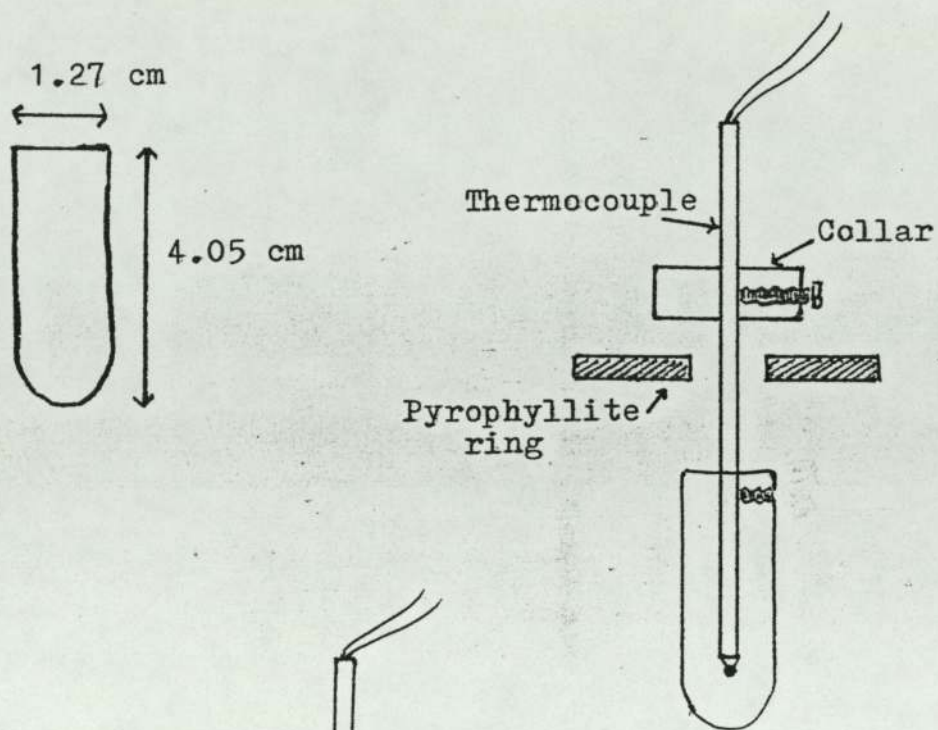


Fig 3.3 The Quenching Of The Probe

forced down into the centre of the probe. The screw on the collar was tightened to give the structure shown in Fig 3.2.

The probe was heated in an electric furnace which was flushed through with argon prior to and during the heating of the probe. The probe was held in the furnace by a 1/4" thick pyrophyllite ring resting on the furnace top. When the probe had reached the desired initial temperature, it was manually transferred to a 600 ml beaker containing 300 ml of the coolant. A 1/4" thick pyrophyllite ring was attached with silicone rubber glue to the top of the beaker, to allow the cooling probe to be held in place in the coolant. Any vapour that was produced during the quenching was able to escape through a hole drilled in the ring. The situation during quenching is shown in Fig 3.3. The thermocouple was connected to a switch by co-axial cable. Using the switch, the thermocouple could either be connected to a digital voltmeter (DVM) or to a chart recorder.

The chart recorder was calibrated using the following procedure. The probe was placed in the furnace and the probe temperature established by noting the

reading displayed on the DVM. The switch was then used to transfer the output of the thermocouple from the DVM to the chart recorder, and the chart recorder pen position was noted. This procedure was repeated with several probe temperatures, thus giving the required calibration.

The coolants used in these experiments were acetone, carbon tetrachloride, chloroform, ethanol, methanol, and n-propanol. The unheated probe was placed in the coolant, and the area of the probe submerged in the coolant was adjusted by varying the position of the collar on the inconel sheath. In all experiments, the area of the copper probe submerged was held constant by ensuring that the upper plane face of the probe was held 1 cm above the coolant surface. The submerged area was  $12.2 \text{ cm}^2$ . The probe was removed from the coolant and the surface was cleaned using fine emery cloth and acetone. The probe was then placed in the furnace. The coolant was then heated to the required initial temperature using an immersion heater. Just before the probe reached the desired initial temperature, as measured by the DVM, the chart recorder drive was switched on. When the probe reached the desired initial temperature, the

probe was manually transferred to the coolant and the output of the thermocouple was transferred from the DVM to the chart recorder using the switch. The probe was left to cool in the coolant, the temperature-time graph being plotted by the recorder.

In the experiments performed with the organic coolants, the initial probe temperature was approximately 270°C. The heat fluxes during quenching were evaluated using the equation

$$q = \frac{m C_p}{A} \cdot \frac{dT}{dt} \quad \dots(3.1)$$

where

$q$  = heat flux

$m$  = mass of the probe (40.93 g )

$C_p$  = specific heat capacity of copper

$A$  = area of the probe submerged (12.2 cm<sup>2</sup>)

$\frac{dT}{dt}$  = cooling rate of the probe taken from the temperature-time graphs

Analysis of the temperature-time graphs show that in each experiment, the heat flux from the probe passed through a minimum. The probe temperature corresponding to this point is referred to as  $T_{\min}$ .

The results from these experiments are shown in Figs 3.4 to 3.9, which record the heat fluxes from the probe at temperatures above  $T_{\min}$ , at 140, 190 and 240°C. The heat fluxes at  $T_{\min}$  are also recorded. The temperatures  $T_{\min}$  are plotted on a graph (Fig 3.10) of  $(T_{\min} - T_{\text{sat}})$  versus the coolant subcooling.  $T_{\text{sat}}$  is the boiling point of the coolant.

### 3.3 Experiments With Water As A Coolant

When the probe was heated above 300°C, removed from the furnace, and held in air for a few seconds, interference fringes were observed to form and disappear on the probe surface leaving the surface dark brown in colour. This was due to the formation of an oxide layer. When the probe temperature was below 300°C, no interference fringes were observed. At elevated temperatures, (over 500°C), large amounts of flaky copper oxide were observed on the probe surface. Since the probe was to be heated above 500°C in the experiments using water as the coolant, it was decided that the previous experimental procedure which employed a manual transference of the probe through air, was unsuitable. Experiments had shown that the flaky oxide layer seriously affected the formation of a stable vapour film.

Fig 3.4 Film Boiling Data For Acetone

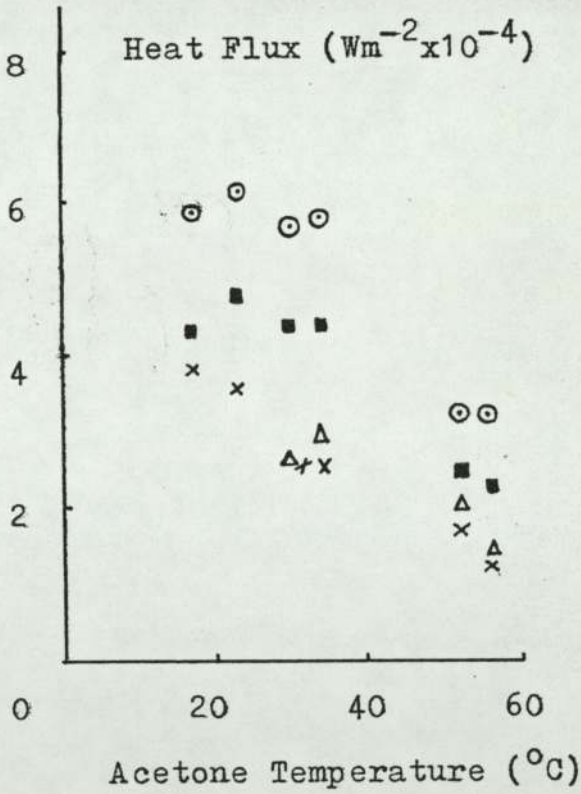
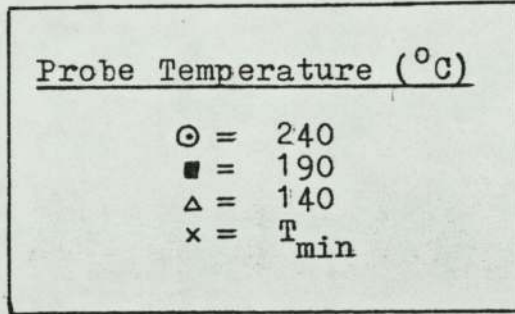


Fig 3.5 Film Boiling Data For Carbon Tetrachloride

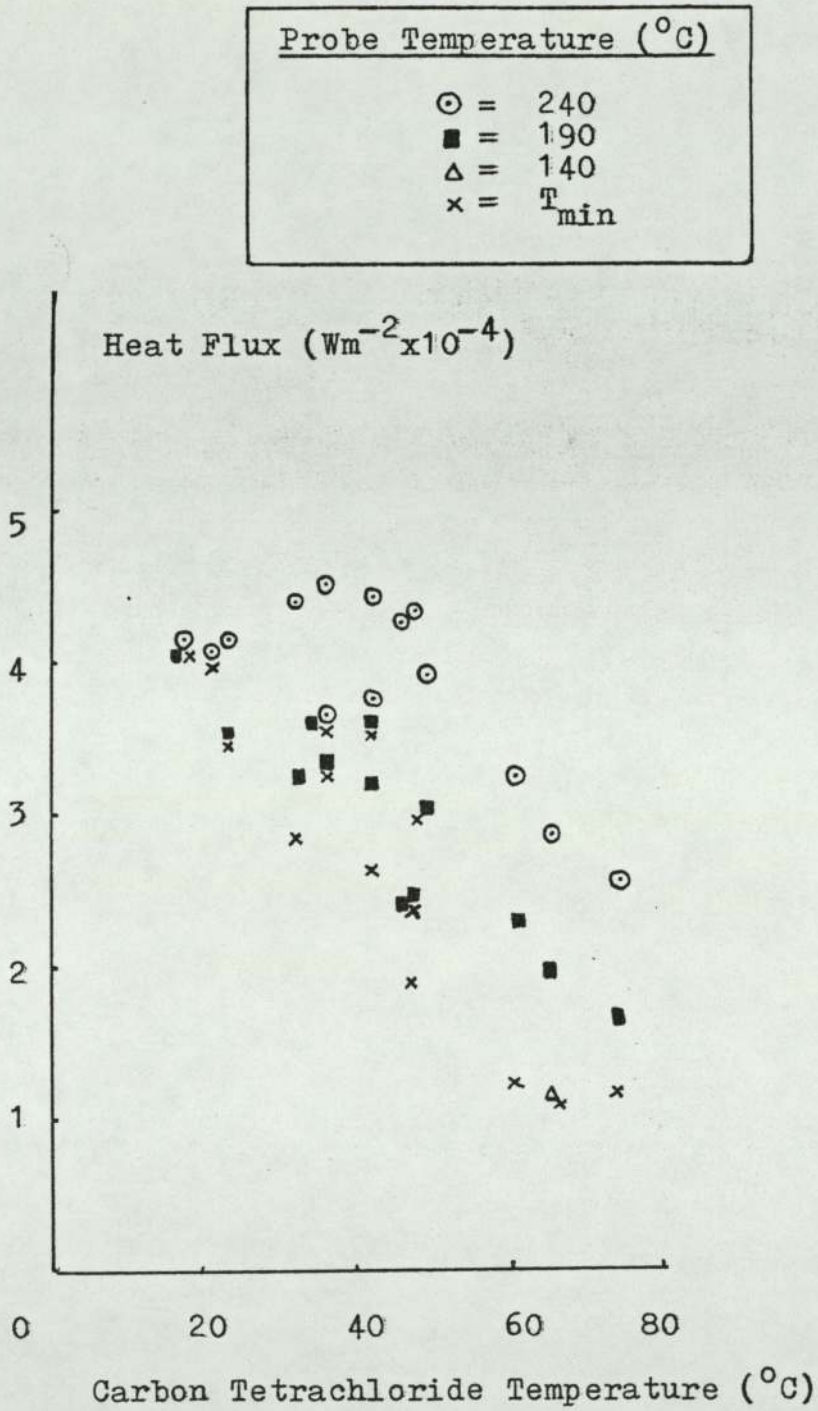


Fig 3.6 Film Boiling Data For Chloroform

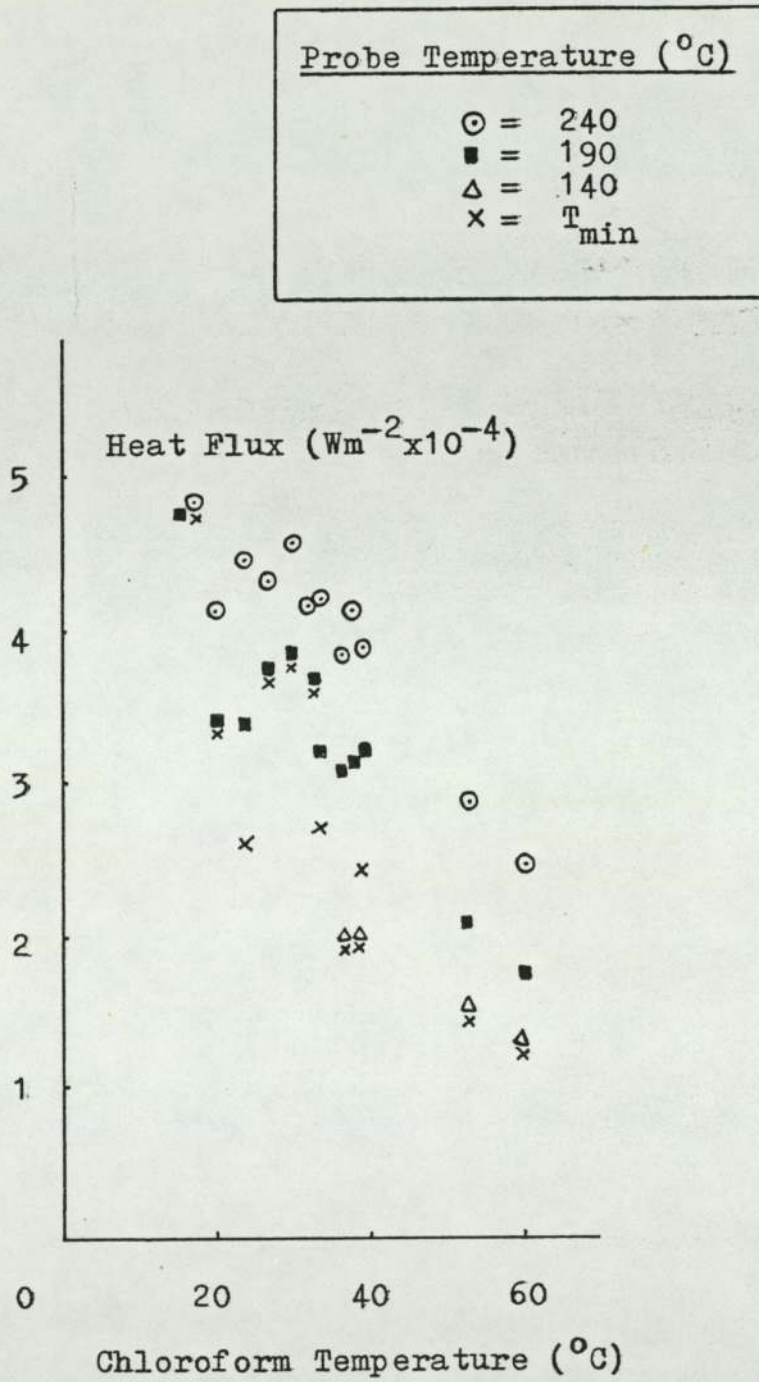


Fig 3.7 Film Boiling Data For Ethanol

Probe Temperature ( $^{\circ}\text{C}$ )	
$\odot$	= 240
$\blacksquare$	= 190
$\triangle$	= 140
$\times$	= $T_{\text{min}}$

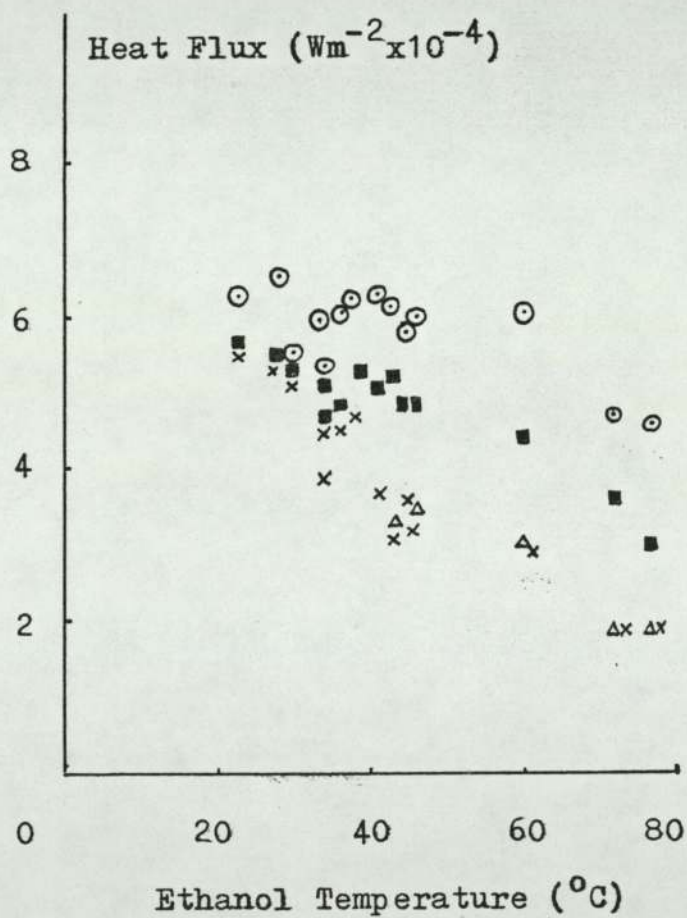


Fig 3.8

Film Boiling Data For Methanol

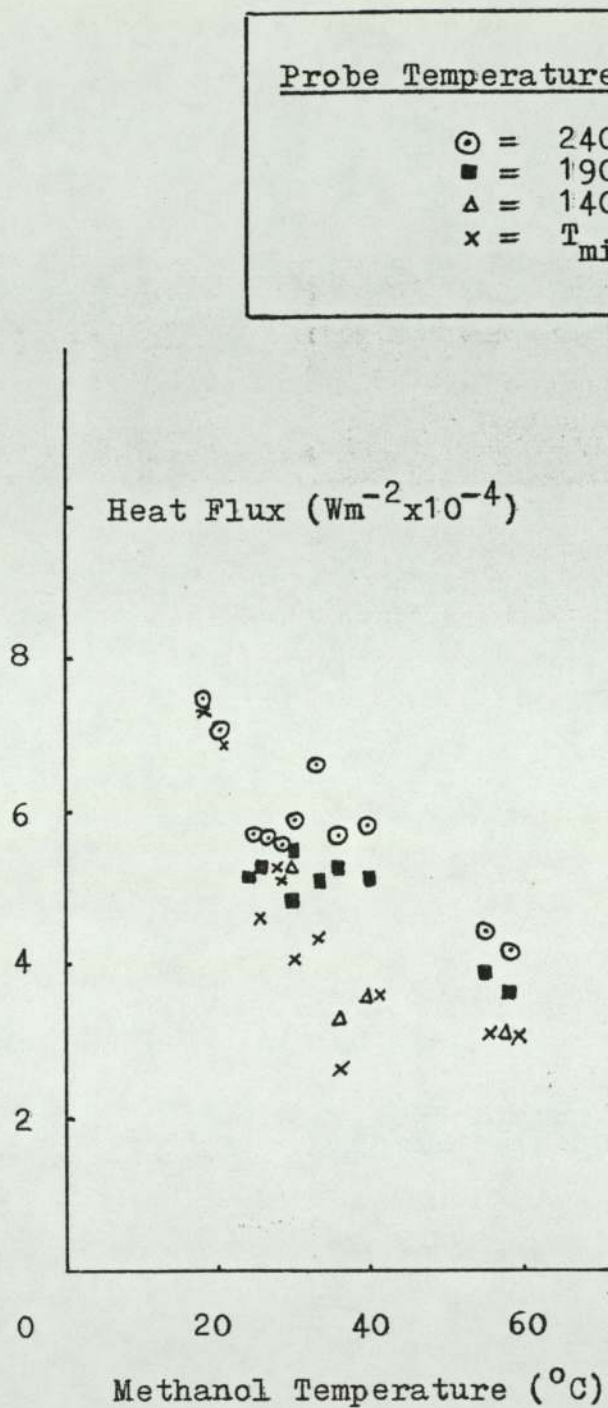


Fig 3.9 Film Boiling Data For n-propanol

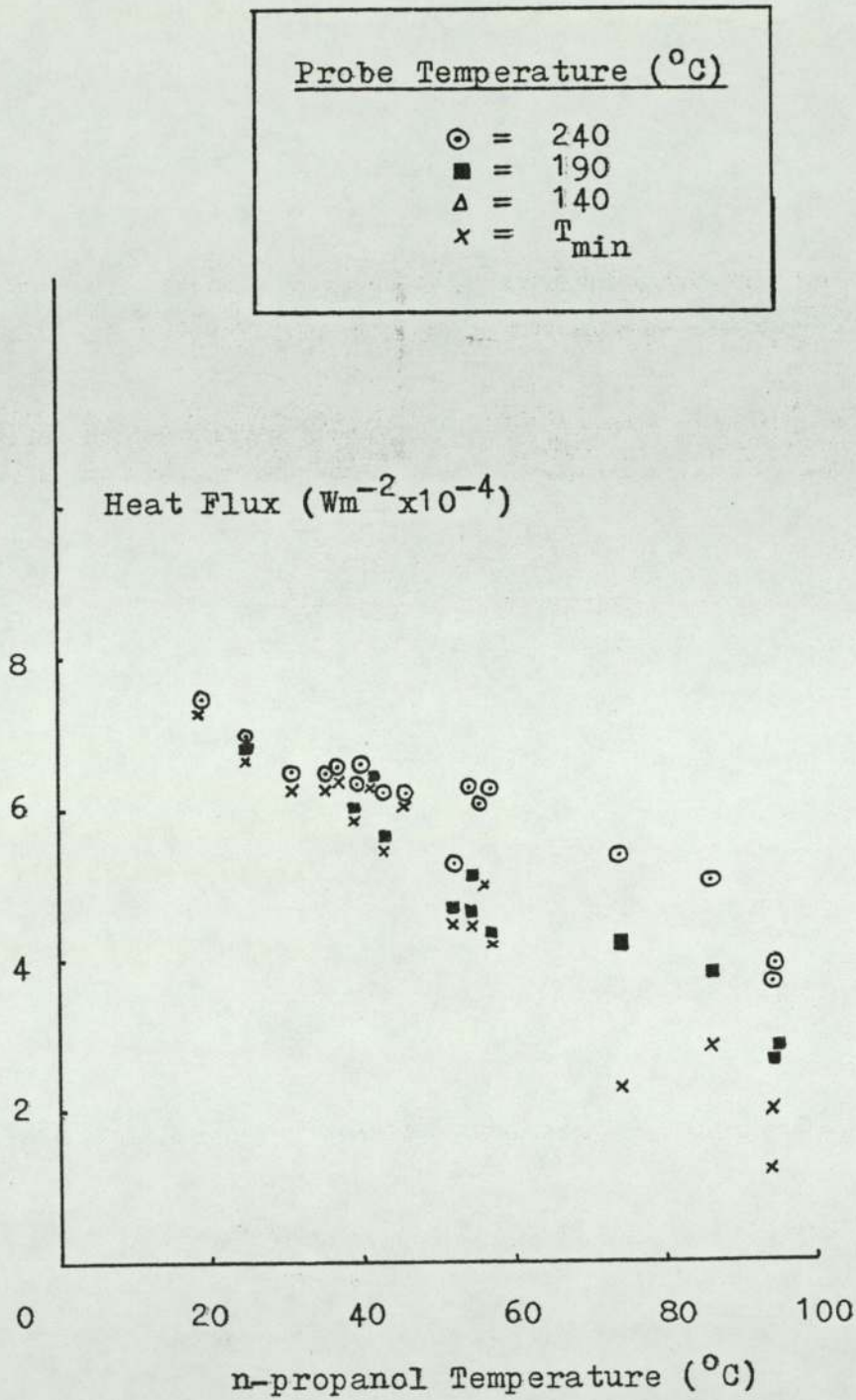
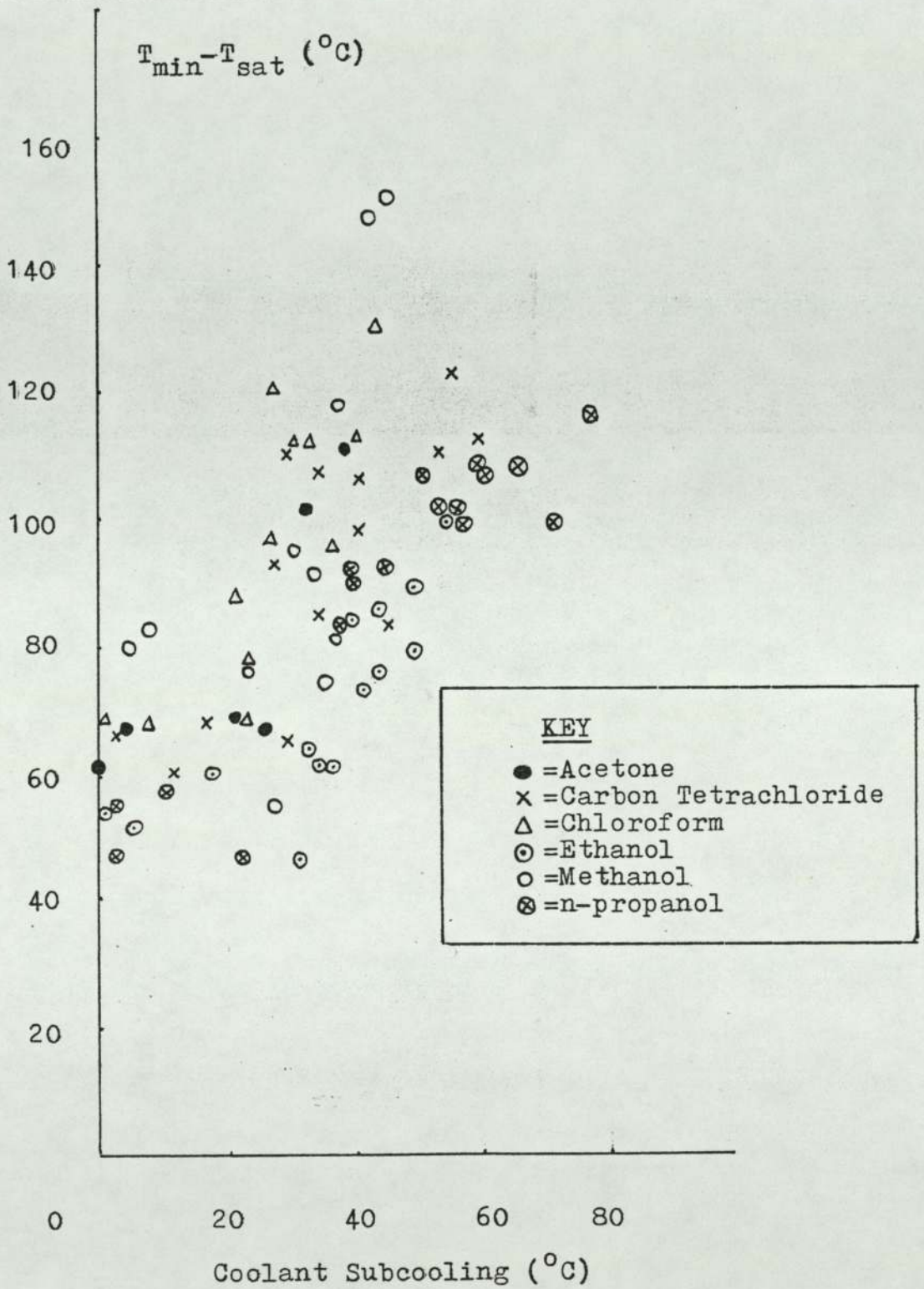


Fig 3.10 Minimum Temperatures For The Organic Coolants



Therefore, it was decided that the experimental technique to be used with water would have to ensure that the probe was both heated and transferred in an inert atmosphere. This prompted the use of an induction furnace.

The apparatus used to quench the probe in water is shown in Fig 3.11. A silica tube was passed through two 10" square sections of Sindanyo horizontally held  $2\frac{1}{2}$ " apart by four OBA bolts symmetrically positioned  $6\frac{1}{3}$ " from the axis of the tube. Around the silica (held in position by a clamp resting on the upper Sindanyo section) between the two sections was an induction coil from a Raydyne C50 furnace. The lower Sindanyo section was held in position parallel to a wooden base by Dexion frame. A Pyrex tube was glued to the lower face of the lower Sindanyo section with silicone rubber glue. An inconel-sheathed cromel-alumel thermocouple was passed through a 1" diameter brass collar and then through a pyrophyllite bung at the top of the silica tube. The thermocouple was then forced down into the probe. The probe could now be raised and lowered in the silica tube by an external wire. The water which was held in a glass tank, sealed the apparatus.

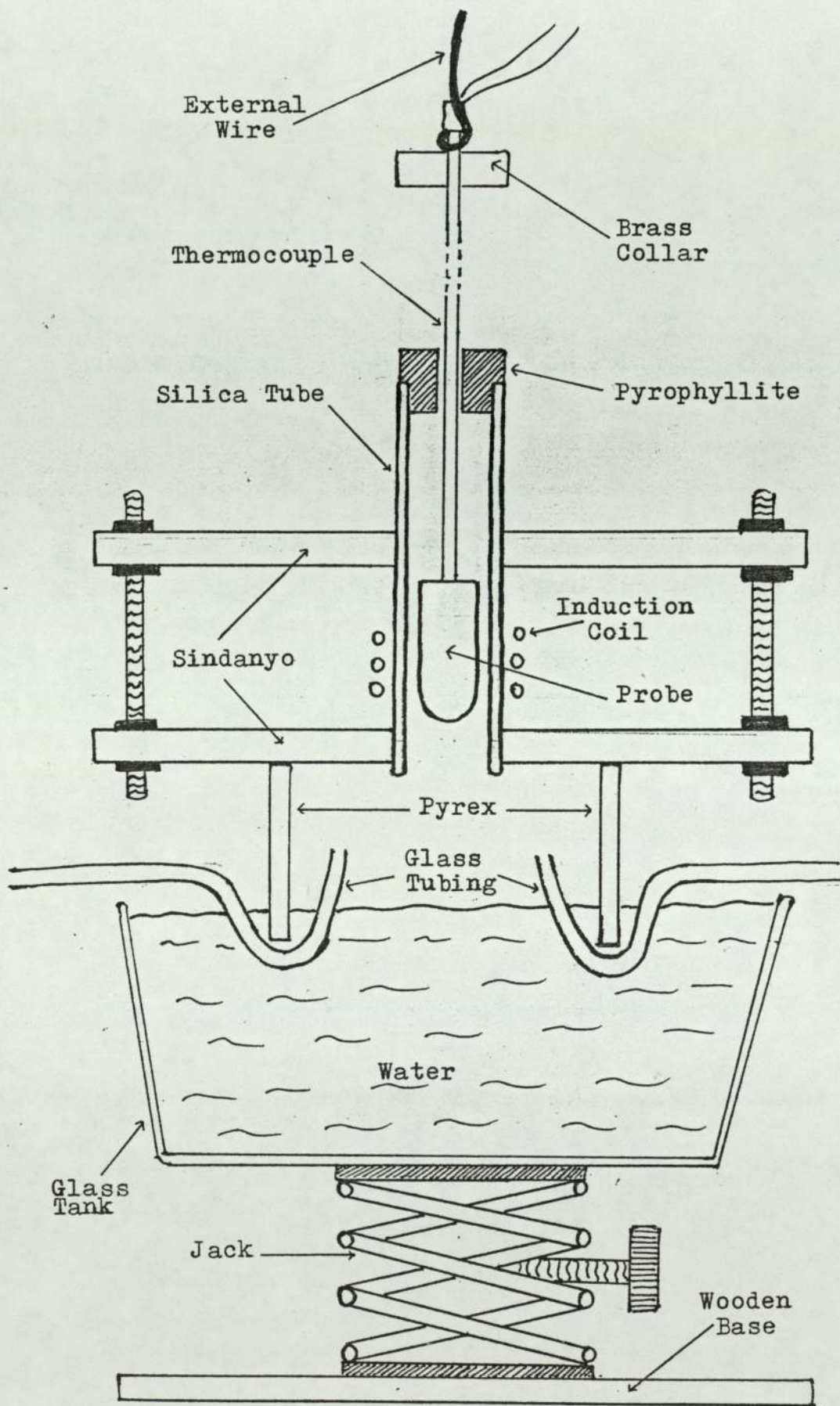


Fig 3.11 The Apparatus Used To Quench The Probe In Water

The tank could be raised and lowered by a jack resting on the wooden base. Argon entered and was able to leave the system via glass tubing.

The system was flushed out with argon and the probe (held in position by the external wire) heated in the induction coil to about  $800^{\circ}\text{C}$ . The power to the coil was cut and the probe allowed to cool to  $700^{\circ}\text{C}$ , at which temperature it was dropped into the water (500 ml) by releasing the external wire. The area of the probe submerged was held at  $12.2\text{ cm}^2$ . The probe was allowed to cool in the water which had previously been heated to the desired initial temperature using an immersion heater. The thermocouple output was recorded on magnetic tape using an Ampex FR 1300 tape recorder. The signal from the thermocouple was amplified before being recorded on an FM channel of the tape recorder. The data recorded was replayed to a chart recorder after the experiment. The heat fluxes from the probe, calculated as before, that were observed when the probe temperature was  $650^{\circ}\text{C}$  are displayed in Fig 3.12 for various initial water temperatures. The corresponding heat fluxes for the probe at  $450^{\circ}\text{C}$  are also shown. The minimum heat fluxes (the heat fluxes at  $T_{\min}$ ) are shown in Fig 3.13, the values of  $T_{\min}$  being recorded in Fig 3.14.

Fig 3.12 Film Boiling Data For Water

(Probe Temperature,  $\odot = 650^{\circ}\text{C}$ ,  $\otimes = 450^{\circ}\text{C}$ )

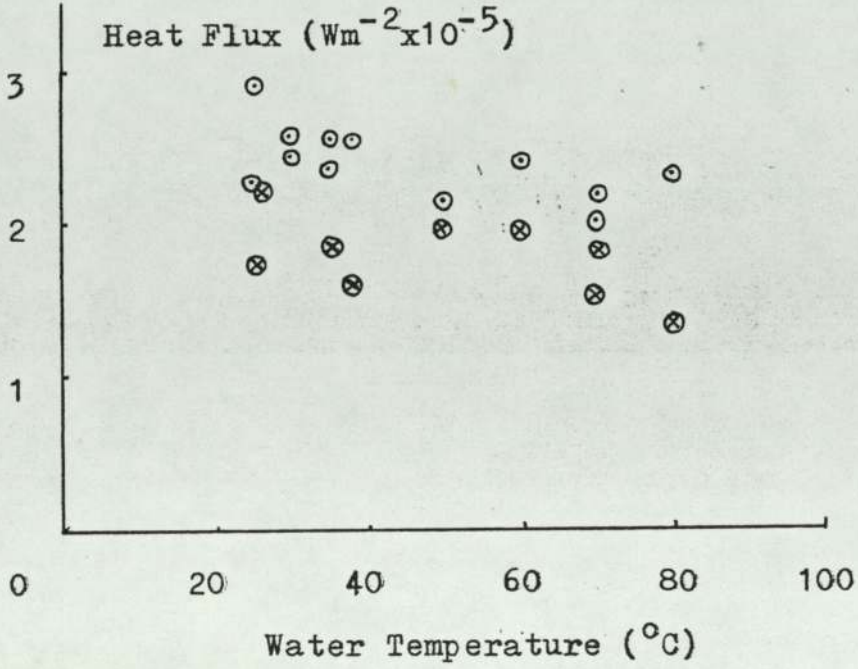


Fig 3.13 Minimum Heat Fluxes For Water

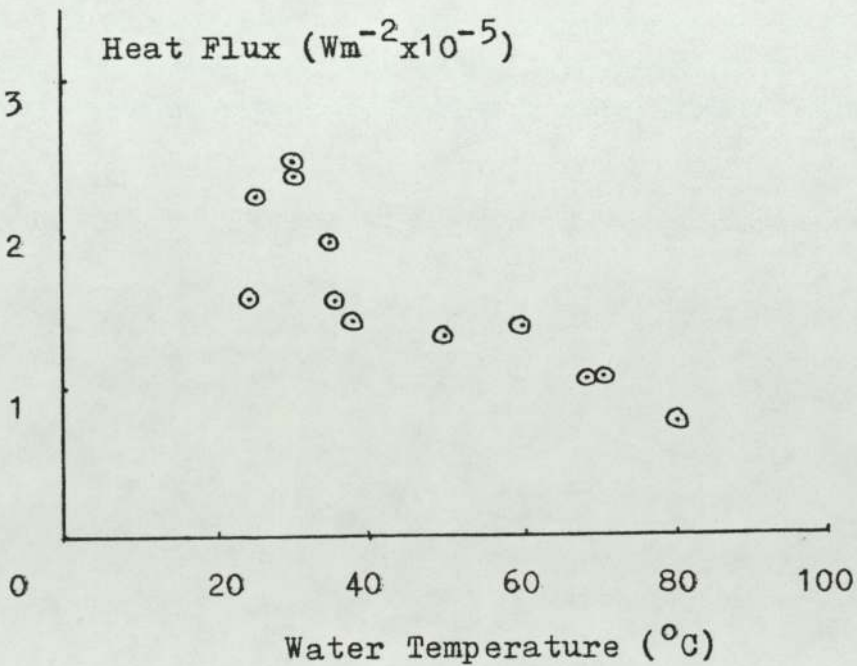
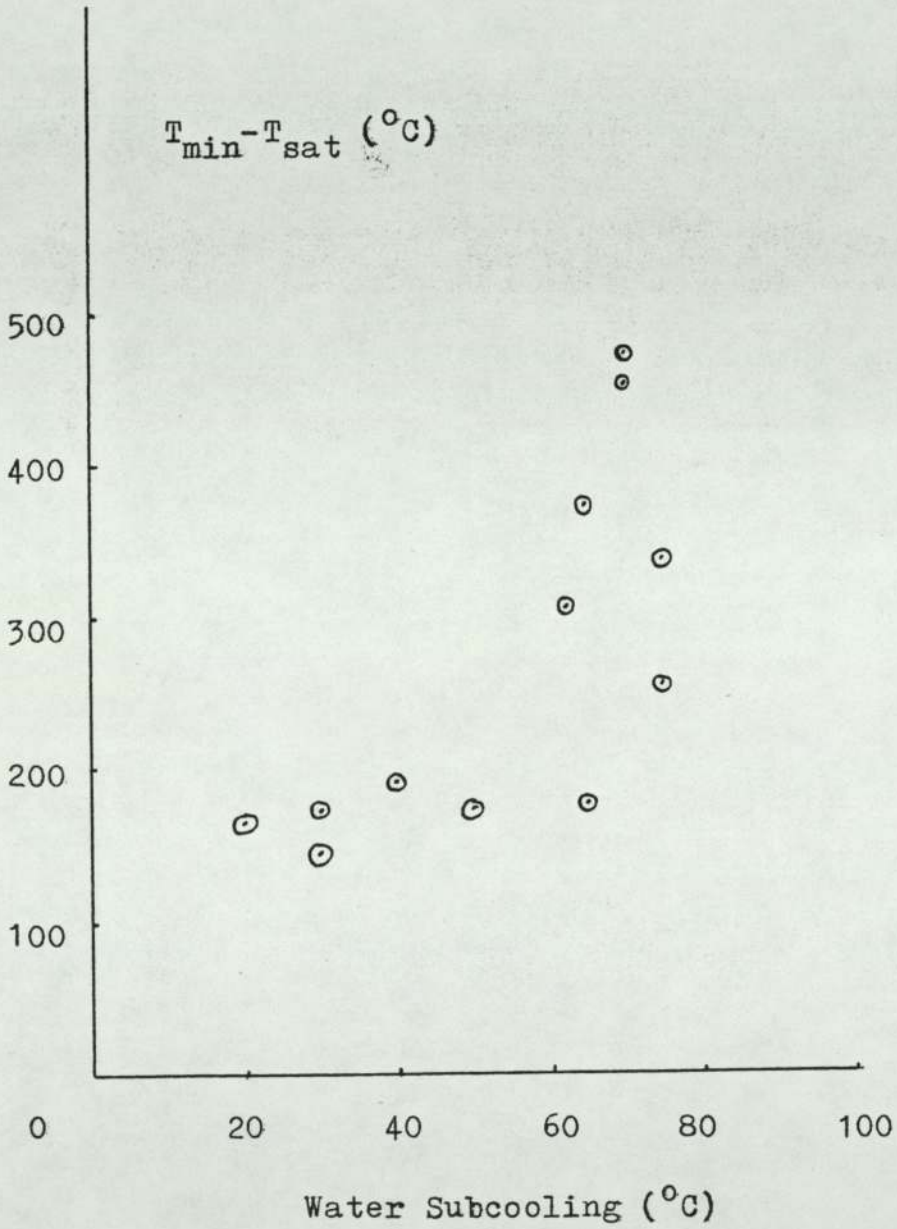


Fig 3.14 Minimum Temperatures For Water



### 3.4 Visual Observations

All coolants appeared to behave in the same way. When the probe was first placed in the coolant, a stable vapour film was seen to exist. In highly subcooled coolants, the vapour film was observed to be glassy smooth. At high coolant temperatures and high probe temperatures, irregularities in the film were observed. The vapour-liquid interface appeared to oscillate in a direction normal to the probe surface. This behaviour was more pronounced near the coolant surface. In all experiments, the vapour film, which appeared to decouple the probe from the coolant, was seen to thin as the probe cooled. The collapse of the film into transition boiling started at the base of the probe and worked its way up the probe so as to cover the whole probe surface. When the cooling rate and the vapour film could be simultaneously observed, it was found, for room temperature coolants, that  $T_{\min}$  corresponded well with the point at which the film was seen to collapse.

## CHAPTER FOUR

### VAPOUR FILM ANALYSIS

#### 4.1 Direct Current Analysis

Experiments based on those of Bradfield<sup>(32)</sup> were performed to gain information on vapour films. The experimental procedure of the previous chapter was used, and the vapour films generated were incorporated into a series electric circuit. This circuit, shown schematically in Fig 4.1, consisted of a battery (9V), a resistor ( $33k\Omega$ ), nickel foil electrode, coolant, vapour film, probe and inconel thermocouple sheath. The nickel foil electrode which covered the base of the beaker was connected to the resistor by a wire which ran through a hole in the pyrophyllite ring. A chart recorder was connected across the  $33k\Omega$  resistor, the voltage across which, indicated the amount of contact that was present between the probe and the coolant. When a stable vapour film existed, no current flowed round the circuit, which resulted in the potential difference across the resistor being zero. Fig 4.2 shows the voltage across the resistor as a function of time, recorded in an experiment in which the copper probe cooled from  $260^{\circ}\text{C}$  in  $40^{\circ}\text{C}$  n-propanol. 15mg of potassium iodide was added

Fig 4.1 The D.C. Circuit

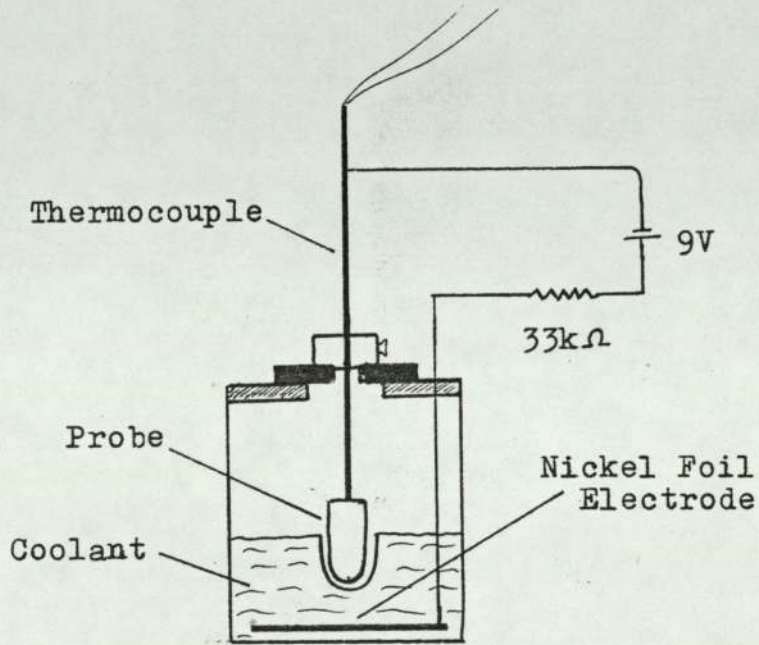


Fig 4.2 D.C. Analysis Of The Probe Cooling In n-propanol

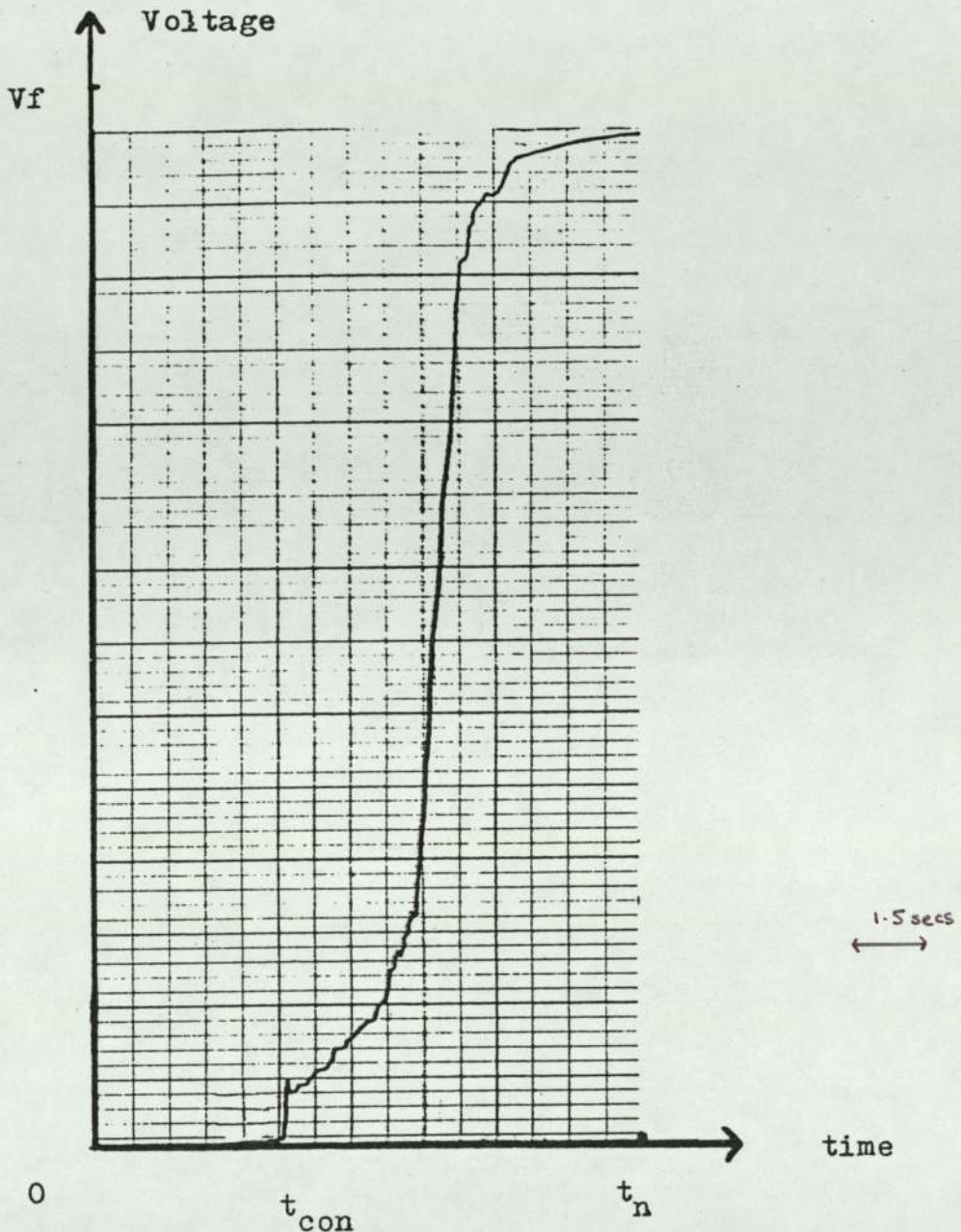


Figure Notes

This graph records the voltage across the resistor as a function of time as the copper probe cooled from 260 degrees centigrade in 40 degree centigrade n-propanol. The zero of the voltage axis corresponds to zero volts across the resistor. The zero of the time axis corresponds to the probe having been in the n-propanol for 5 seconds. The voltage across the resistor during these 5 seconds was zero. One centimetre on the time axis corresponds to 1.5 seconds. The final voltage on the voltage axis (Vf) was reached approximately 10 seconds after time t<sub>n</sub>.

to the n-propanol in order to raise the electrical conductivity of the coolant. The graph shows that initially there was a stable vapour film. At  $t_{con}$ , there was contact between the probe and the coolant. After  $t_{con}$ , the amount of contact between the probe and coolant steadily increased. Contact between the probe and coolant was visually observed a short time after  $t_{con}$ .

This experiment was typical of the experiments performed in which acetone, ethanol and n-propanol were used as coolants. In the experiments, potassium iodide was added to the acetone and ethanol to raise their electrical conductivity. In many experiments, it was observed that there was contact at temperatures well above the temperature corresponding to the minimum heat flux. There was always contact at temperatures below  $T_{min}$ . A steady increase in the amount of contact between the probe and coolant was observed as the probe cooled in the transition and nucleate boiling regimes.

## 4.2 Vapour Films As Capacitors

Bradfield<sup>(32)</sup> refers to vapour films as capacitors. In order to find out whether vapour films could be reasonably analysed as capacitors, a trial experiment was set up. The aim of the experiment was to observe the nature of vapour films generated in water.

The apparatus and experimental method of this trial experiment ensured that the experiment would be simple and quick to perform, and that the vapour film would be physically accessible.

A magnesia-packed inconel-sheathed cromel-alumel thermocouple was passed through a brass collar and then forced down into a stainless steel probe (of similar dimensions to the copper probe). The collar was put into position about six inches away from the probe and held in this position by tightening the collar screw.

The probe was heated in a gas flame to about  $700^{\circ}\text{C}$ , at which point, the connections between the thermocouple and the digital voltmeter which read the temperature were broken and the thermocouple sheath was connected to a large resistor  $R_A$  ( $2.2\text{ M}\Omega$ ) using a

crocodile clip. This resistor had previously been connected in series to an oscillator (operating in the low radio frequency range, at an RMS voltage of approximately 70V) and a steel water tank containing the water coolant. The probe was then partially submerged in the water ( $\sim 80^{\circ}\text{C}$ ), the submerged area being approximately  $10\text{ cm}^2$ . The probe was held in position in the water by the collar which rested on a wooden support.

The probe cooled in the water surrounded by a vapour film. The situation during quenching is shown in Fig 4.3. The vapour film was now present as a capacitor in a series A.C. circuit. A first approximation to the electrical analogue of the physical situation of Fig 4.3 is shown in Fig 4.4. The points A and B are connection points.  $C_v$  is the capacitance of the vapour film and  $R_w$  is the resistance of the water coolant. Since  $R_A$  is a very large resistor, the alternating current that flowed around the circuit was to a high degree of accuracy governed by this resistor, and so the current was unaffected by changes in  $C_v$  or  $R_w$ . The current flowing round the circuit is given by

$$I = I_0 \sin 2\pi ft$$

Fig 4.3 A Trial Experiment

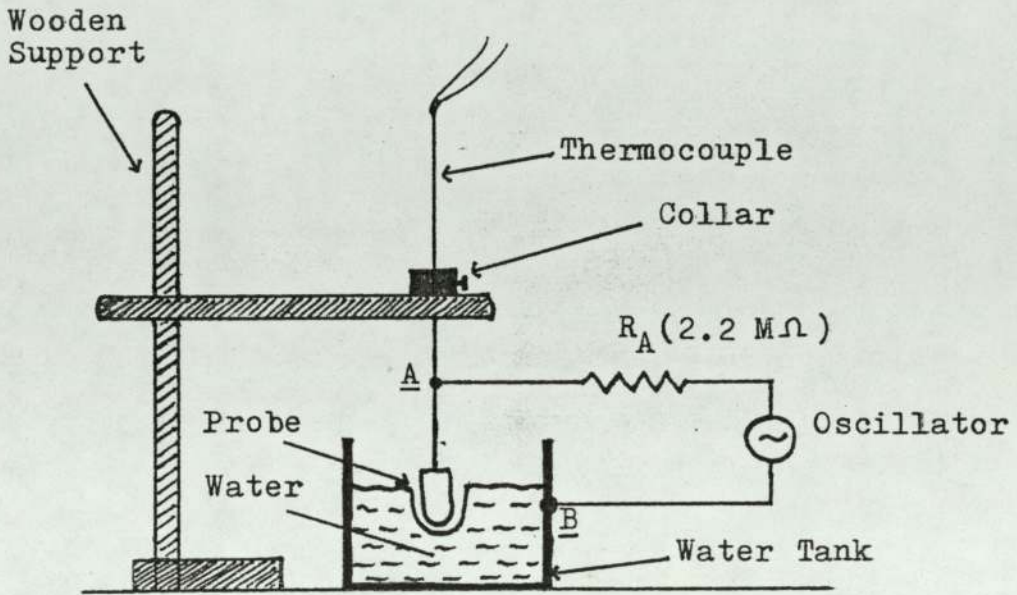
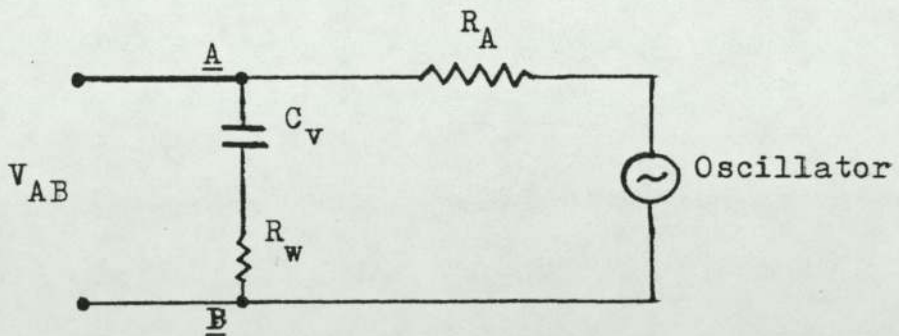


Fig 4.4 The Electrical Analogue



where

$I_0$  = a constant

$f$  = frequency of the oscillator

$t$  = time

While the probe was cooling, the voltage  $V_{AB}$  (the voltage between points A and B) was observed on an oscilloscope. The voltage  $V_{AB}$  was passed through a voltage follower before coming to the oscilloscope, so that  $V_{AB}$  would not be affected by the relatively low impedance of the oscilloscope.

The frequency of the oscillator was manually varied in the low radio frequency range, and  $V_{AB}$  was noted to change simultaneously (over and above the natural change in  $V_{AB}$  that was observed as the probe cooled). The RMS value of  $V_{AB}$  was seen to decrease as the frequency was increased. It was concluded from this experiment that the vapour film was behaving as a capacitor, and that the capacitances provided by this film boiling were such that they could be readily measured.

### 4.3 The Capacitance-Resistance Transducer

It was considered to be useful to look at the capacitive properties of vapour films since, for simple geometries, the relationships between capacitance and geometry are well known.

Further experiments were performed in which the stainless steel probe was quenched in hot water. The experimental method of the previous section was used except that the oscillator frequency was held constant at 100 kHz during the quenching. The RMS output of the oscillator was approximately 70V. These experiments showed that the RMS value of  $V_{AB}$  decreased as the probe cooled. However, it was impossible to make estimates of the vapour film capacitances purely from observation of  $V_{AB}$ . Further circuitry had to be connected to this experiment to enable information concerning the vapour film and coolant to be obtained.

The following is an account of the circuits that were used and the operations that they performed. (The electrical analogue of the physical situation is assumed to be as shown in Fig 4.4).

The voltage ( $V_{AB}$ ) across the coolant and vapour film was used as the input to two separate channels, channel C and channel R. The operations performed by the channels on  $V_{AB}$  were:

Channel C:

$V_{AB}$  was multiplied by a unit square wave ( $F_1$ )  $90^\circ$  out of phase with the current  $I$  (see Fig 4.5), and the resulting signal was low pass filtered, giving the output signal of Channel C,  $V_{\text{chan C}}$ .

Channel R:

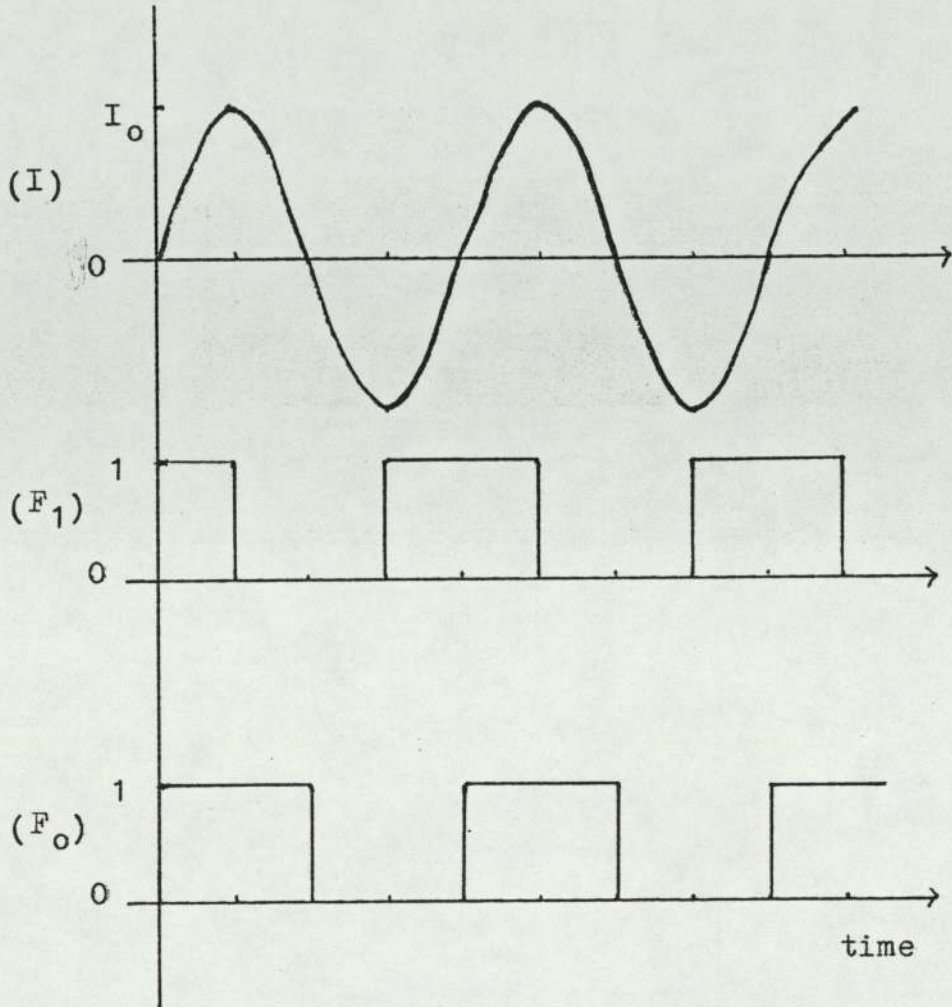
$V_{AB}$  was multiplied by a unit square wave ( $F_0$ ) in phase with the current  $I$  (see Fig 4.5), and the resulting signal was low pass filtered, giving the output signal of Channel R,  $V_{\text{chan R}}$ .

The result of the operations performed by these two channels on  $V_{AB}$  is now theoretically examined. This examination provides an interpretation of the voltages  $V_{\text{chan R}}$  and  $V_{\text{chan C}}$  in terms of  $R_w$  and  $X_{Cv}$  (the capacitive reactance of the vapour film).

When the current  $I$ , given by  $I = I_0 \sin 2\pi ft$  where  $I_0$  is a constant flows around the series circuit, the voltage across the coolant  $V_{Rw}$  is given by



Fig 4.5 The Waveforms  $F_1$  and  $F_o$



The current  $I$  is given by

$$I = I_o \sin 2\pi ft$$

where

$I_o =$  a constant

$f =$  frequency of the oscillator

$t =$  time

$$V_{Rw} = I_o R_w \sin 2\pi ft \quad \dots(4.1)$$

The voltage across the vapour film  $V_{Cv}$  is

$$V_{Cv} = \frac{\int I dt}{C_v} = \frac{-I_o \cos 2\pi ft}{2\pi f C_v}$$

$$= -I_o X_{Cv} \cos 2\pi ft \quad \dots(4.2)$$

where the capacititive reactance of the vapour film is given by

$$X_{Cv} = \frac{1}{2\pi f C_v} \quad \dots(4.3)$$

The voltage  $V_{AB}$  is the instantaneous addition of the voltages  $V_{Rw}$  and  $V_{Cv}$ , and is therefore given by

$$V_{AB} = I_o R_w \sin 2\pi ft - I_o X_{Cv} \cos 2\pi ft \quad \dots(4.4)$$

If  $2\pi ft$  is represented by the variable  $\theta$  then

$$V_{AB} = I_o ( R_w \sin \theta - X_{Cv} \cos \theta ) \quad \dots(4.5)$$

When  $V_{AB}$  is multiplied by the square wave  $F_1$  which is  $90^\circ$  out of phase with the current  $I$ , as in channel C, the resulting voltage  $V_1$  is

$$V_1 = I_o F_1 (R_w \sin \theta - X_{Cv} \cos \theta) \quad \dots(4.6)$$

The square wave  $F_1$  is given by the partial Fourier series

$$F_1 = \frac{1}{2} + \frac{2}{\pi} \left\{ \cos \theta - \frac{\cos 3\theta}{3} + \frac{\cos 5\theta}{5} \dots \right\} \quad \dots(4.7)$$

If  $V_1$  is low pass filtered i.e. averaged over each cycle, the resulting voltage  $V_{chan C}$  is

$$V_{chan C} = \frac{1}{2\pi} \int_0^{2\pi} V_1 d\theta \quad \dots(4.8)$$

Thus

$$V_{chan C} = \frac{I_o}{2\pi} \int_0^{2\pi} \left\{ \frac{1}{2} + \frac{2}{\pi} \left( \cos \theta - \frac{\cos 3\theta}{3} + \frac{\cos 5\theta}{5} \dots \right) \right\} \times \left\{ R_w \sin \theta - X_{Cv} \cos \theta \right\} d\theta \quad \dots(4.9)$$

$$= \frac{-I_o X_{Cv}}{\pi} \quad \dots(4.10)$$

Thus the output voltage from Channel C is proportional to  $X_{Cv}$ , the capacitive reactance of the vapour film, and is independent of  $R_w$ , the resistance of the coolant.

For channel R,  $V_{AB}$  is multiplied by a square wave  $F_o$ , which is in phase with the current I, where

$$F_o = \frac{1}{2} + \frac{2}{\pi} \left\{ \sin\theta + \frac{\sin 3\theta}{3} + \frac{\sin 5\theta}{5} \dots \right\} \dots(4.11)$$

The resulting voltage is averaged, the averaged voltage being  $V_{chan R}$ . This voltage is therefore given by

$$V_{chan R} = \frac{I_o R_w}{\pi} \dots(4.12)$$

The output voltage from Channel R is proportional to the resistance of the coolant, and is **independent** of the capacitative reactance of the vapour film.

The operations that have been described were realised practically using the circuitry shown in Fig 4.6. The circuitry shown is referred to as the capacitance-resistance transducer. The circled capital letters in the figure are positioned next to points in the circuit referred to in the text by underlined capital letters.

The voltage  $V_{AB}$  (the voltage between the points A and B) was passed through a voltage follower, the output of which (point C) was high pass filtered (points C to D) to remove any unwanted mains effects.



For the capacitance channel, the multiplication stage (D to E) was performed by a switch. The switch (equivalent to LF 398H) had  $V_{AB}$  as an input (point D) and was closed during the first and last quarter of each cycle of the current  $I$ , thus allowing selected portions of  $V_{AB}$  to pass. This operation effectively multiplied  $V_{AB}$  by a unit square wave  $90^\circ$  out of phase with the current  $I$ . The resulting signal (point E) was low pass filtered, the filter output (point F) being the output of the capacitance channel.

For the resistance channel, the multiplication stage (D to H) was again performed by a switch. The switch (equivalent to LF 398H) had  $V_{AB}$  as an input and was closed for the first half of each cycle of the current  $I$ . This operation effectively multiplied  $V_{AB}$  by a unit square wave in phase with the current  $I$ . The resulting signal (point H) was low pass filtered, the filter output (point I) being the output of the resistance channel.

The switches were instructed as to whether they should be open or closed by external TTL logic (present at point Q for the capacitance channel, point R for the resistance channel). The two sets of logic were

generated from clock pulses (point P) which were sympathetic to the phase of the current I. That is, at a preset phase angle of each cycle of the current I, a TTL pulse was fired. These pulses were produced using the circuitry between points K and P. The output of the oscillator (point K) was attenuated and passed into a voltage follower, the output of which (point M) was amplified (using an amplifier from Kemo Ltd, Beckenham, Kent) 1000 times to produce a near square wave (point N). The signal at point N was a near square wave since, for most of the cycle, the high amplification caused the amplified signal to bump the voltage rails. This signal was rectified by passing it through a precision diode (points N to O). The diode output was cleaned up using a Schmitt trigger inverter (points O to P), point P being the output of the clock circuit.

For each channel, the transition from the clock pulses to the required external logic was effected by two monostables in series, the first being responsible for phase alligning the external logic to the current I, the second for making sure that the switch was open and closed for the required amount of time.

The circuits were soldered onto veroboard, the connection to point A being made by a fine copper wire, one end of which was soldered to point A, the other being soldered to a crocodile clip. The analogue chips were supplied by voltage rails of +10 and -10 volts. The logic chips were supplied by a +5 volt rail. The voltage rails which were decoupled from ground, were supplied by voltage regulators.

This capacitance-resistance transducer gave a D.C. voltage between points F and G ( $V_{\text{chan C}}$ ) which was proportional to the capacitive reactance between points A and B, and a D.C. voltage between points I and J ( $V_{\text{chan R}}$ ) proportional to the resistance between points A and B. This statement concerning the output of the two channels is valid as long as the resistance and capacitance are in series between the points A and B.

## 4.4 Experiments With The Transducer

### 4.4.1 Preliminary Experiments

In this first series of experiments, the aim was to gain experience in using the transducer and to observe the general behaviour of vapour films over a cooling surface. The first series of experiments concentrated on the information supplied by the capacitance channel.

The experiments with the stainless steel probe were continued using the experimental method of section 4.3. The probe was quenched from 700°C in hot (70°C to 90°C) water. Point A of the capacitance-resistance transducer was connected to the inconel sheath of the thermocouple, and point B was connected to the steel water tank.

The output of the capacitance channel was connected to a chart recorder, and  $V_{\text{chan C}}$  was recorded as the probe cooled. In these experiments, the oscillator frequency was held at 100 kHz, the RMS voltage of the oscillator being approximately 70V. The capacitance channel had previously been calibrated

by recording the output of the capacitance channel when capacitors of known value were connected between the points A and B, thus giving a value of  $k_{AB}$  in the equation

$$V_{\text{chan C}} = k_{AB} X_{Cv} \quad \dots(4.13)$$

Results from these experiments which are representative of the experiments performed are shown in Figs 4.7 and 4.8. The graphs shown have been presented in terms of capacitive reactance versus time. The capacitive reactance between A and B has been assumed to be solely due to the capacitive reactance of the vapour film, and is given by

$$X_{Cv} = \frac{1}{2\pi f C_v}$$

The vapour film is thin compared to the dimensions of the probe and therefore the capacitance of the film can be written as

$$C_v = \frac{A \epsilon_0 \epsilon_r}{\delta} \quad \dots(4.14)$$

where

$A$  = area of the probe submerged

$\epsilon_0$  = permittivity of free space

Fig 4.7 Vapour Film Collapse In 70°C Water

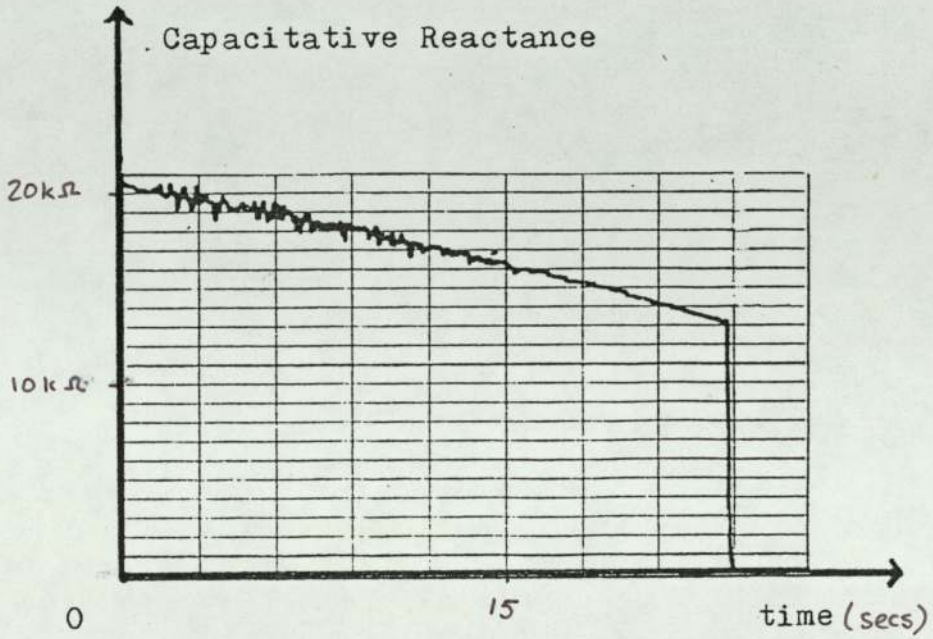


Figure Notes

This graph records the capacitive reactance between points A and B as the probe cooled from 700 degrees centigrade in 70 degree centigrade water. One inch on the capacitive reactance axis is approximately 10 kΩ. One centimetre on the time axis corresponds to 3 seconds.

Fig 4.8 Vapour Film Collapse In 90°C Water

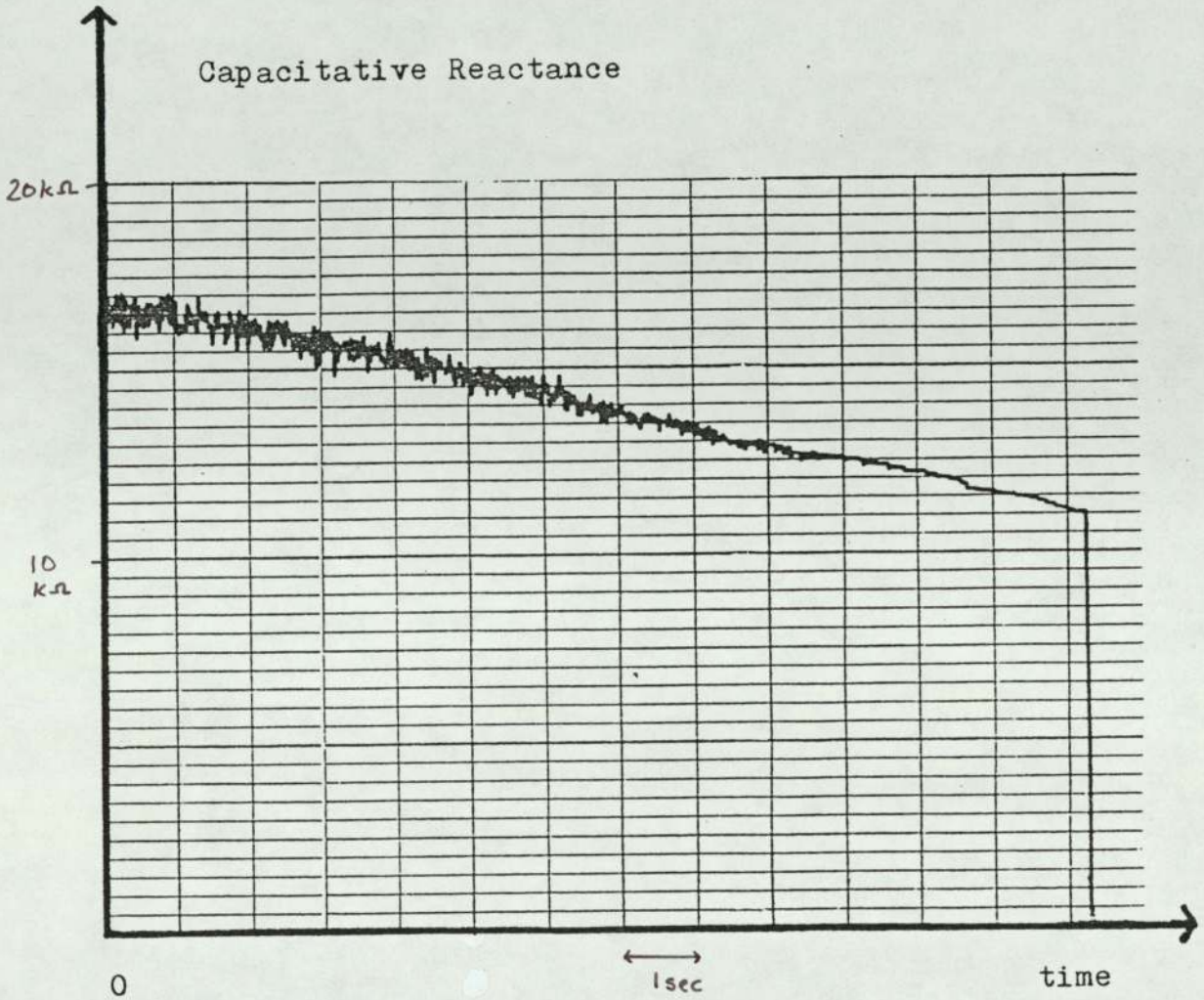


Figure Notes

This graph records the capacitative reactance as a function of time between the points A and B as the stainless steel probe cooled in 90 degree centigrade water. The probe was first partially submerged in the water when the probe temperature was 700 degrees centigrade. The zero of the time axis corresponds to the probe having been in the water for 16 seconds. One inch on the capacitative reactance axis is approximately 5 kΩ. One centimetre on the time axis corresponds to one second.

$\epsilon_r$  = permittivity of the vapour

$\delta$  = mean thickness of the vapour film

and therefore

$$X_{CV} = \frac{\delta}{2\pi f A \epsilon_0 \epsilon_r} \dots(4.15)$$

Thus the graphs in Figs 4.7 and 4.8 can be considered to show how the mean thickness of the vapour film changes with time, since the denominator of equation (4.15) is a constant.

From these experiments, the following observations were noted

- 1 As the probe cools, the vapour film thins.
- 2 The collapse of the vapour film is sudden.
- 3 The vapour film oscillates. The amplitude of oscillation is greater, the higher the water temperature and the higher the probe temperature.

An example of the traces obtained when both the resistance and capacitance channels were in operation is shown in Fig 4.9. The traces record  $V_{\text{chan C}}$  and  $V_{\text{chan R}}$  as the stainless steel probe cooled from

Fig 4.9 A Trace Of  $X_{Cv}$  and  $R_w$

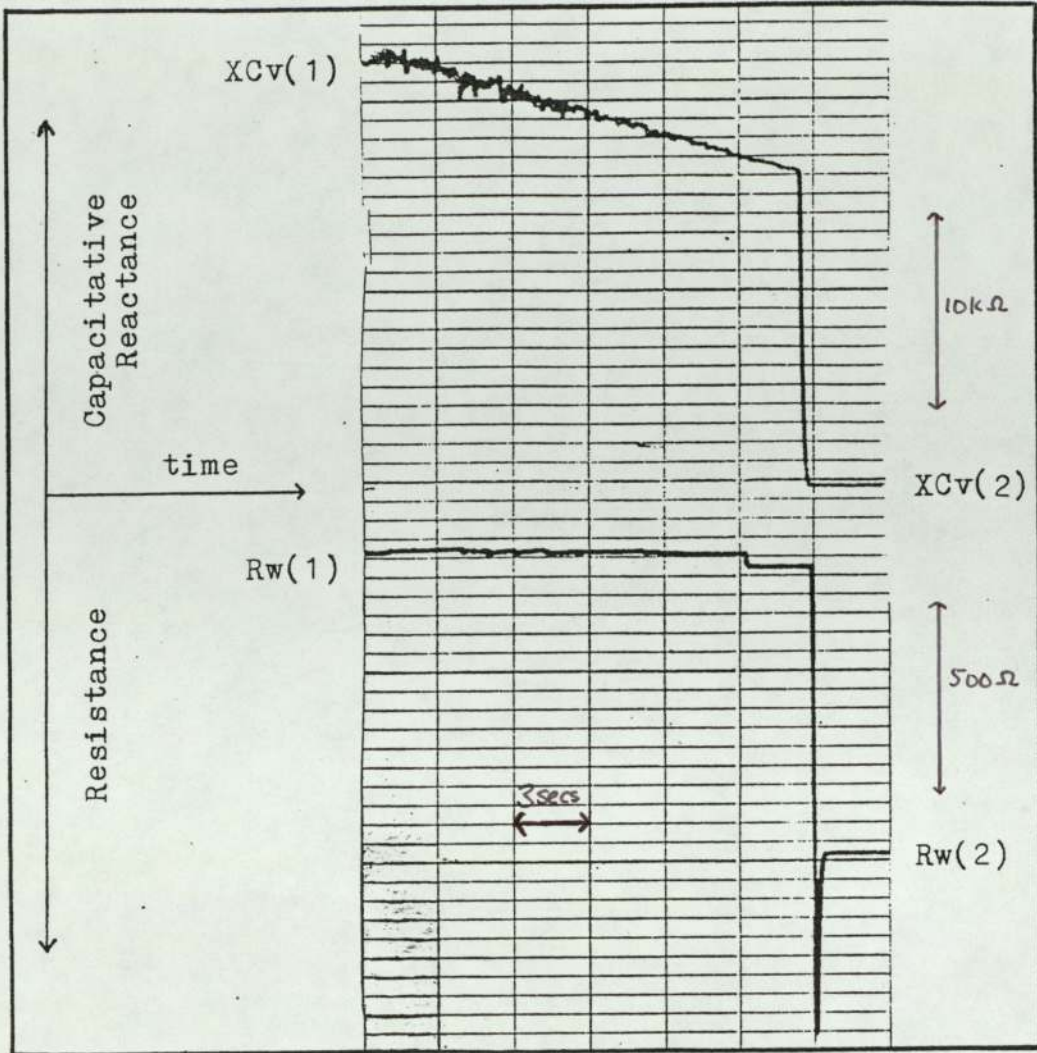


Figure Notes

(For convenience,  $X_{Cv}$  is written as  $X_{Cv}$  and  $R_w$  written as  $R_w$ ).

In this figure, the capacitive reactance  $X_{Cv}$  and resistance  $R_w$  between the points A and B are simultaneously recorded as the stainless steel probe cooled from 700 degrees centigrade in 70 degree centigrade water. The values of  $X_{Cv}$  and  $R_w$  when the probe was first placed in the water are  $X_{Cv}(1)$  and  $R_w(1)$ . The values of  $X_{Cv}$  and  $R_w$  after the collapse of the vapour film are  $X_{Cv}(2)$  and  $R_w(2)$ . The arrows show the directions of increasing capacitive reactance, resistance and time. One inch on the capacitive reactance axis is approximately  $10k\Omega$ . The value of  $X_{Cv}(2)$  is zero. One inch on the resistance axis is approximately  $500\Omega$ . One centimetre on the time axis corresponds to 3 seconds. The large changes in  $X_{Cv}$  and  $R_w$  occurred at the same time. The apparent difference in time between these changes is due to the separation of the recording pens of the chart recorder.

700°C in 70°C water. The outputs  $V_{\text{chan C}}$  and  $V_{\text{chan R}}$  of the figure are plotted in terms of  $X_{\text{Cv}}$  and  $R_w$ .

From the figure it can be seen that initially the probe cooled surrounded by a vapour film. This film became thinner and oscillated less as the probe cooled. During this time, there was no significant change in  $R_w$ , indicating that there was no contact between the probe and the water. This explanation is supported by separate D.C. experiments performed on the same system. After 15 seconds, there was a step increase in the value of  $R_w$ , probably indicating that contact between the probe and the water had been made. The rate of film collapse before and after the step change in  $R_w$  are approximately equal. After about 18 seconds, there was a sudden collapse of the vapour film, together with a large increase in  $R_w$ . The final recorded resistance was larger than the resistance recorded during the initial film collapse.

When these experiments had been performed, two points concerning the resistance channel were noted

- 1 Qualitatively, the resistance channel could provide little new information
- 2 Quantitatively, the resistance channel was limited, firstly because the physical

situation associated with the resistance between points A and B is complex, and secondly because during quenching, the change in the value of  $R_w$  is small compared to the change in the value of the capacitative reactance  $X_{Cv}$ . Thus the value of  $R_w$  was hard to obtain accurately, since the values of  $R_w$  and  $X_{Cv}$  were superposed in the signal  $V_{AB}$  (see equation 4.4).

In the light of these two points, it was considered best to continue by concentrating on the information that could be supplied by the capacitance channel.

#### 4.4.2 Vapour Film Thickness At Collapse

The performance of the capacitance channel was improved by reducing the frequency of operation of the transducer to 25 kHz. This reduced the error caused by the finite amount of time needed to open and close the switch, and raised the impedance of the vapour films generated. The RMS voltage of the oscillator was lowered to approximately 20V. The transducer was now used in conjunction with vapour films generated by the methods described in Chapter Three.

Experiments were performed to estimate the mean vapour film thickness at collapse in n-propanol solutions of varying initial temperature. The apparatus shown in Fig 4.1 was used, the resistor-battery combination being replaced by the points A and B of the transducer. A solution containing 15 mg of potassium iodide in 300 ml of n-propanol was placed in the 600 ml beaker which had the nickel foil electrode at its base. The wire from the electrode which ran through the pyrophyllite ring was connected to point A of the transducer. Point B was connected to the inconel sheath of the chromel-alumel thermocouple embedded in

the probe. The probe was heated to about 300°C in the electric furnace and subsequently quenched in the n-propanol. The output of the capacitance channel was connected to a chart recorder, and  $V_{\text{chan C}}$  was recorded as the probe cooled.

In these experiments, an attempt was made to take account of stray capacitance, the capacitance between points A and B other than the capacitance of the vapour film. The stray capacitance  $C_s$  was estimated in separate experiments by recording the capacitance reactance  $X_s$  between points A and B when the probe was a long way away from the coolant. The stray capacitance was then calculated from

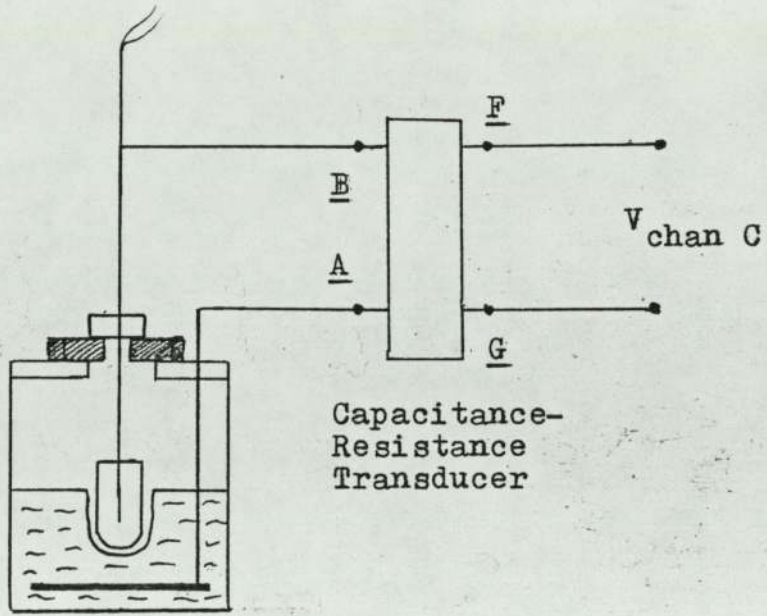
$$X_s = \frac{1}{2\pi f C_s}$$

The capacitance  $C_s$  (estimated as 15 pF) was assumed to be in parallel with the vapour film.

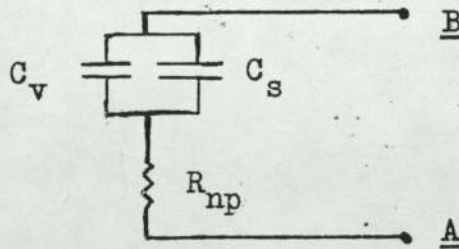
The experimental arrangement and assumed electrical analogue are shown in Fig 4.10.  $R_{\text{np}}$  is the resistance of the n-propanol. The output of channel C is

$$V_{\text{chan C}} = k_{\text{AB}} X_{\text{Cv}}^1$$

Fig 4.10 Film Boiling In n-propanol



The Electrical Analogue



where

$$X_{Cv}^* = \frac{1}{2\pi f(C_v + C_s)}$$

The value of  $k_{AB}$  was again found by recording the voltage  $V_{chan C}$  when capacitors of known value were connected between points A and B of the transducer.

The resulting graphs which recorded  $V_{chan C}$  against time as the probe cooled were similar to those shown in Figs 4.7 and 4.8, except that the vapour film collapse was not always so sudden. The point of film collapse was taken to be the point at which the  $V_{chan C}$  versus time graph was most curved. Mathematically, this point corresponds to the point at which  $\rho$  is a minimum, where

$$\rho = \frac{\left\{ 1 + \left( \frac{dV_{chan C}}{dt} \right)^2 \right\}^{3/2}}{\left\{ \frac{d^2V_{chan C}}{dt^2} \right\}}$$

In using this definition of the point of film collapse, the  $V_{chan C}$  versus time plots were smoothed, i.e. oscillation of the film was neglected.

The film capacitances at the point of film collapse were converted into mean vapour film thicknesses using equation (4.14). The area of the probe submerged was  $12.2 \text{ cm}^2$ , the permittivity of the vapour was taken as unity. The results of these experiments and calculations are shown in Fig 4.11. The film thicknesses at collapse are plotted as a function of the initial n-propanol temperature.

Experiments were also performed in which the mean vapour film thicknesses at collapse in water were estimated. The apparatus of Fig 3.11 was used in conjunction with the transducer. Point A was connected to a nickel foil electrode which was positioned at the base of the glass tank, and point B was connected to the thermocouple sheath. The initial probe temperature was approximately  $700^\circ\text{C}$ , the submerged area being  $12.2 \text{ cm}^2$ . The stray capacitance was found to be 24 pF. Fig 4.12 shows the results of these experiments.

Some experiments were performed in which both the cooling rate and capacitative reactance of the vapour film were recorded. These experiments showed that for water and room temperature n-propanol, the point of film collapse was close to the point of minimum heat flux.

Fig 4.11 The Film Thicknesses At Collapse In n-propanol

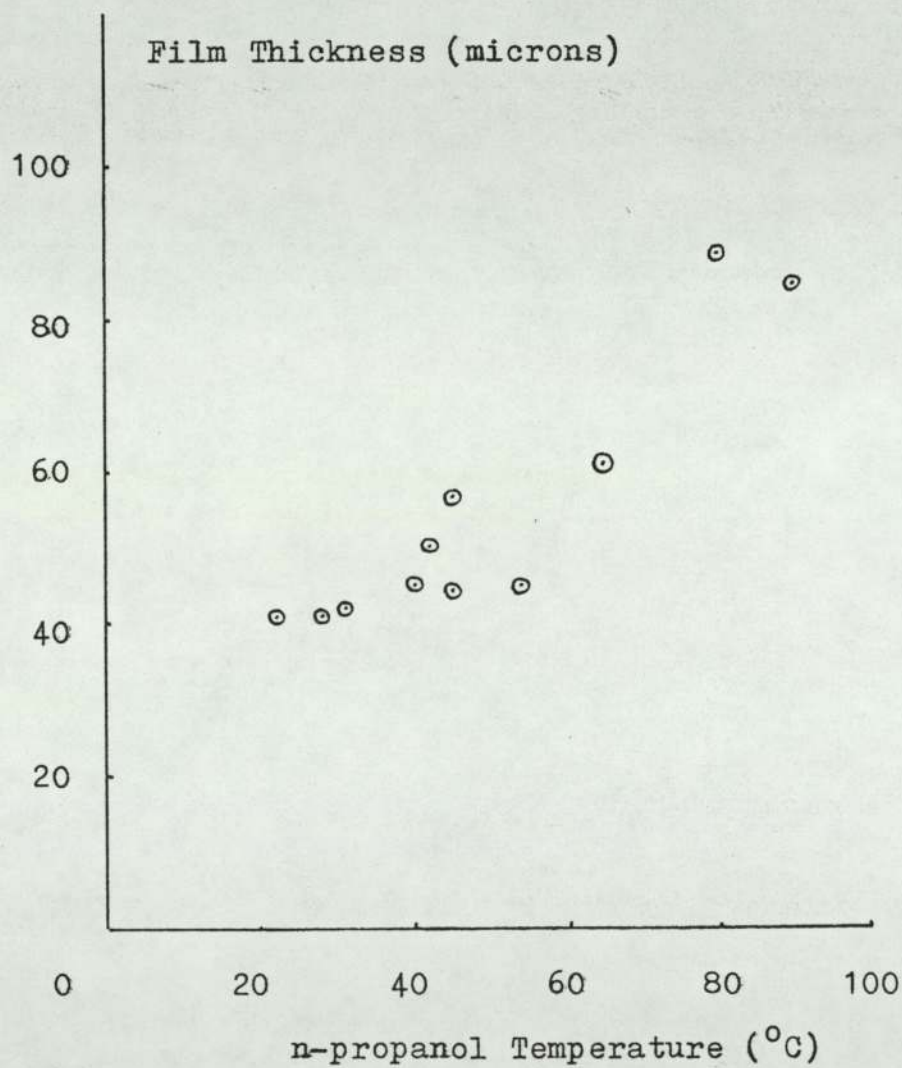
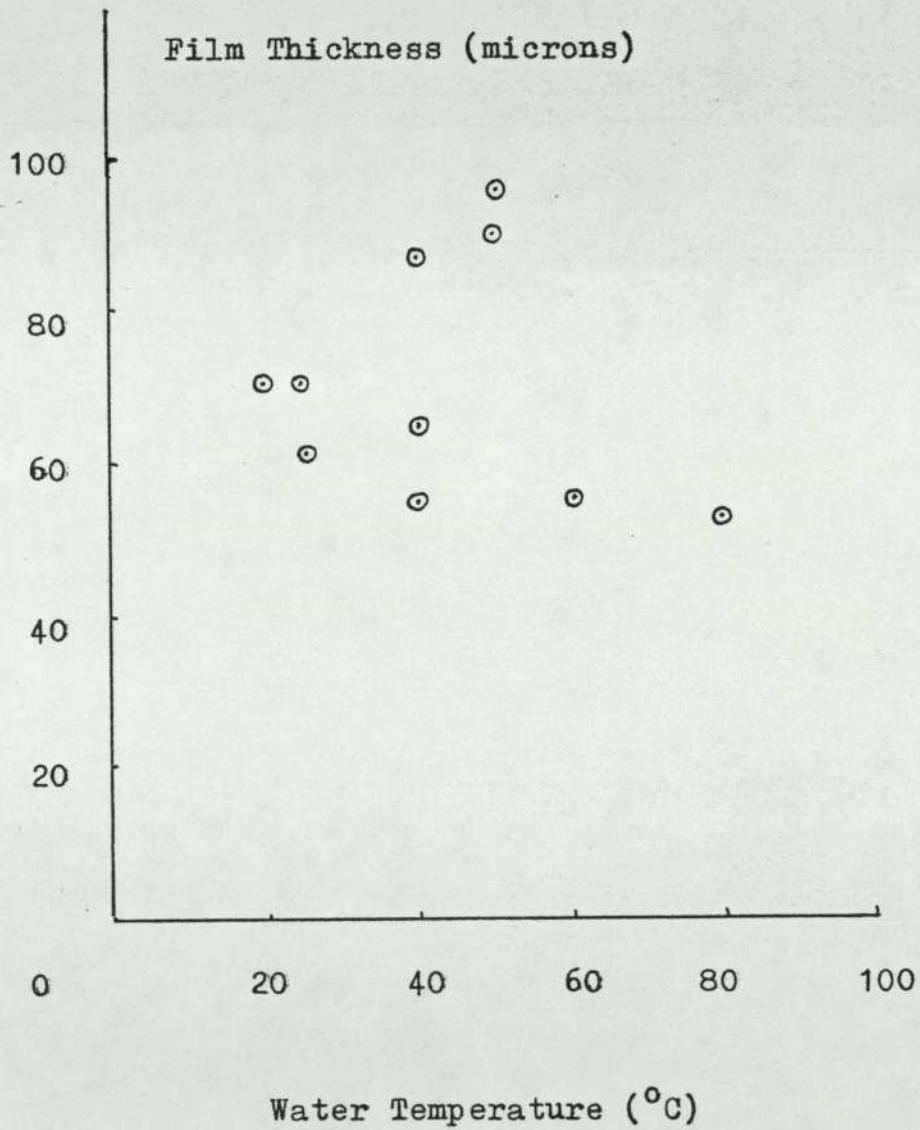


Fig 4.12 The Film Thicknesses At Collapse In Water



#### 4.5 The Effect Of The Transducer

The incorporation of the transducer into the probe experiments did not appear to affect the probe-coolant system. Using the standard equation for the force between the plates of a capacitor, the force  $F$  on the vapour-liquid interface due to the voltage  $V_{Cv}$  across the film is given by

$$F = \frac{1}{2} V_{Cv}^2 \frac{dC_v}{d\delta}$$

From equations (4.2), (4.3) and (4.14), it follows that

$$F = \frac{I_0^2 \cos^2 2\pi f t}{8 \pi^2 f^2 A \xi_0 \xi_r}$$

And thus the average force over each cycle  $\bar{F}$  is

$$\bar{F} = \frac{I_0^2}{16 \pi^2 f^2 A \xi_0 \xi_r}$$

Taking the example of the experiments of the previous subsection,  $\bar{F}$  is found to be about 200 nN ( $I_0$  is approximately  $15 \mu A$ ). This force is negligible compared to the forces present due to hydrostatic pressure.

## CHAPTER FIVE

### A MODEL FOR FILM BOILING

#### 5.1 Introduction

In Chapter Two, it was noted that in order to examine vapour explosions, the way in which heat travels from a metal to a coolant would have to be examined. The film boiling model of Bromley<sup>(23)</sup> considered the situation of a vertical tube undergoing film boiling in a saturated coolant. Experiments in which molten metal-water explosions have been observed have shown that the water subcooling is an important variable. Therefore, in order to make Bromley's model for film boiling more relevant to these experiments, the coolant subcooling must be taken into account. In the model for film boiling presented here, the coolant subcooling is introduced as a variable, and the resulting equations are solved and used to construct the film boiling curves for water. The equations used to describe the movement of vapour in the vapour film are similar to those used by Nusselt (see Monrad and Badger<sup>(24)</sup>) who considered the dynamics of a falling condensing laminar film.

When the dynamics of the vapour are considered, (up to equation 5.3), the presentation is similar to that given by Coulson and Richardson<sup>(26)</sup> in their treatment of Nusselts analysis of a falling condensate.

In this model, the geometry of the metal or heater surface is taken as a vertical plane, firstly because a plane is an easy geometry to define mathematically and secondly, because it is reasonable to expect correlation between the heat fluxes from vertical planes and those from the probe experiments.

## 5.2 Heat Transfer Equations

Consider a vertical surface of unit width undergoing film boiling (see Fig 5.1). Part of the heat leaving the metal is naturally convected away by the coolant, and the rest produces vapour.

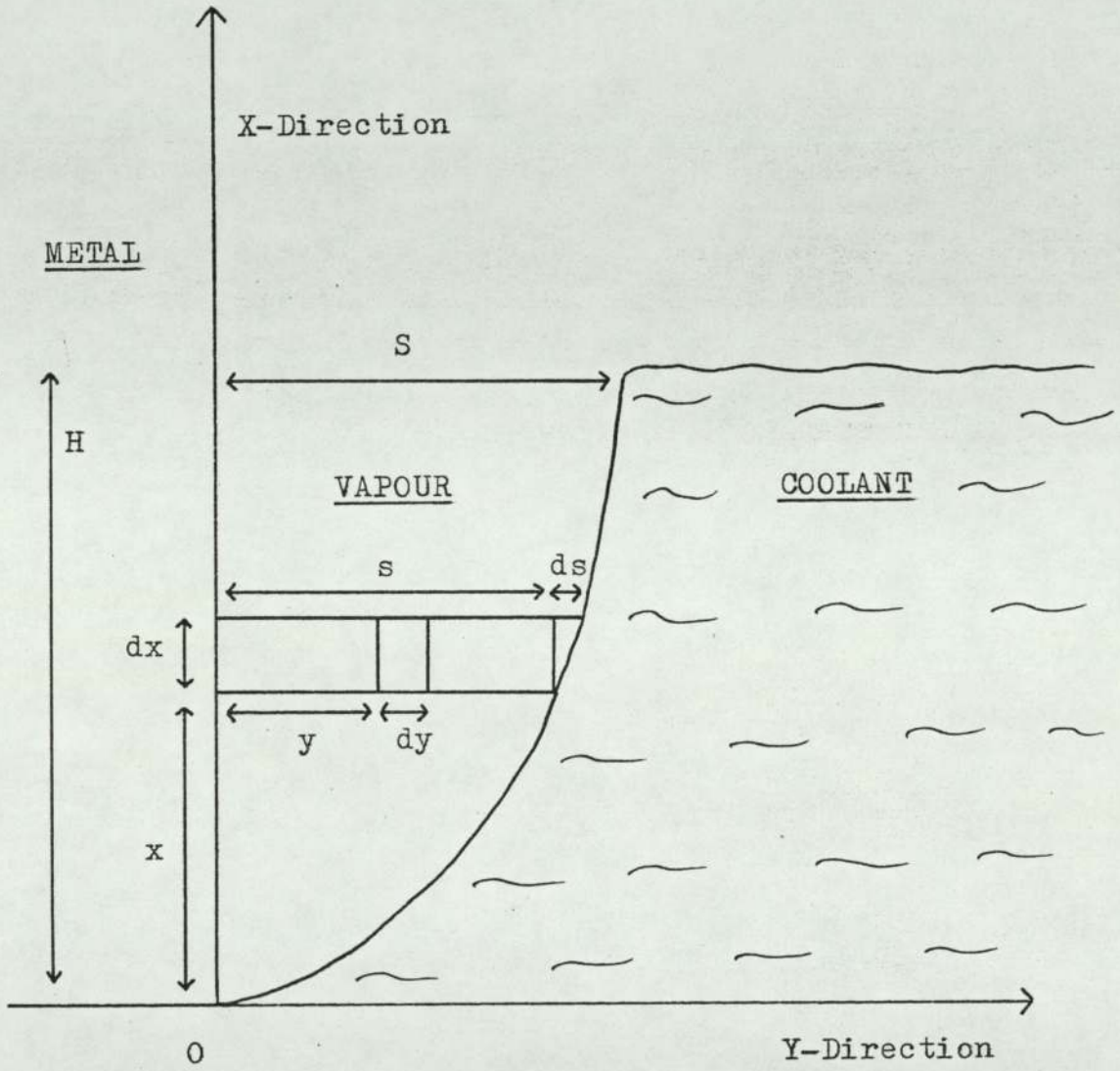
In an element of vapour, thickness  $dx$  at a distance  $x$  from the base of the surface, the buoyant force in the X-direction acting on the vapour at a distance greater than  $y$  from the surface is  $(s-y)(\rho_L - \rho_v)gdx$  where

$s$  = thickness of the film (a variable)

$y$  = a fraction of the film thickness

$\rho_L$  = the density of the coolant

Fig 5.1 A Vertical Surface Undergoing Film Boiling



$\rho_v$  = the density of the vapour estimated at  
the mean vapour temperature ( $T_m$ )  
 $g$  = acceleration due to gravity

The retarding force on the vapour is the viscous drag at the inner boundary of the element. The shear stress at the vapour-liquid interface is neglected. Thus the retarding force in the X-direction is

$$\mu_v \left( \frac{du_y}{dy} \right) dx$$

where  $\mu_v$  is the viscosity of the vapour at the temperature  $T_m$  and  $u_y$  is the velocity of the vapour at a distance  $y$  from the surface.

At equilibrium it follows that

$$(s-y)(\rho_L - \rho_v)g dx = \mu_v \left( \frac{du_y}{dy} \right) dx$$

Thus

$$du_y = \frac{(\rho_L - \rho_v)(s-y) g dy}{\mu_v}$$

And therefore on integration

$$u_y = \frac{(\rho_L - \rho_v)(sy - \frac{1}{2}y^2)g}{\mu_v} \dots(5.1)$$

since the vapour in contact with the metal is at rest, i.e.  $u_y=0$  when  $y=0$

The mass rate of flow  $G$  of vapour over the metal is

$$\begin{aligned}
 G &= \int_0^s \rho_v u_y dy \\
 &= \frac{(\rho_L - \rho_v) \rho_v g s^3}{3 \mu_v} \dots(5.2)
 \end{aligned}$$

The vapour is produced by evaporation, and so the thickness of the film will be zero at the base of the metal and will increase towards the top. Under stable conditions, the difference in the mass rates of flow at distances  $x$  and  $x+dx$  from the base of the metal will result from evaporation over the small element of the surface  $dx$ .

If the thickness of the vapour film increases from  $s$  to  $s+ds$  in the distance  $dx$ , the increase in the mass rate of flow of vapour is

$$\begin{aligned}
 dG &= \frac{d}{ds} \left\{ \frac{(\rho_L - \rho_v) \rho_v g s^3}{3 \mu_v} \right\} ds \\
 &= \frac{(\rho_L - \rho_v) \rho_v g s^2 ds}{\mu_v} \dots(5.3)
 \end{aligned}$$

In an element of surface  $dx$ , the heat flux travelling across the vapour film ( $q_1$ ) to the vapour-liquid interface can be divided into that required to produce and heat the vapour ( $q_2$ ), and that naturally convected away by the coolant ( $q_3$ )

Thus

$$q_1 = q_2 + q_3$$

$q_1$  is given by

$$q_1 = \frac{k_v(T_s - T_b)}{s} = \frac{A}{s} \dots(5.4)$$

where

$k_v$  = thermal conductivity of the vapour at  $T_m$

$T_s$  = temperature of the metal surface

$T_b$  = boiling point of the coolant

$A = k_v(T_s - T_b)$  by definition

Also

$$q_3 = C$$

where

$$C = 0.56 \left\{ \frac{C_{pL} \beta_L g \rho_L^2 k_L^3 \Delta T^5}{H \mu_L} \right\}^{1/4} \dots(5.5)$$

where

$C_p$  = specific heat capacity of the coolant

$\beta_L$  = cubic expansivity of the coolant

$\rho_L$  = density of the coolant

$k_L$  = thermal conductivity of the coolant

$\Delta T$  = subcooling of the bulk of the coolant

$H$  = height of the metal surface

$\mu_L$  = viscosity of the coolant

All the variables associated with the coolant are estimated at the temperature  $T_b - \frac{1}{2} \Delta T$ .

The equation for  $C$  comes from the equation

$$Nu = 0.56 ( Pr \cdot Gr )^{1/4} \dots(5.6)$$

as suggested by Saunders<sup>(45)</sup> for natural convection of heat away from vertical planes.

$Nu$  = the Nusselt group

$Pr$  = the Prandtl group

$Gr$  = the Grashof group

Therefore the heat required to produce and heat the vapour is

$$dx \{q_1 - q_3\} = \left\{ \frac{A}{s} - C \right\} dx \quad \dots(5.7)$$

This is equal to the increase in the mass rate of vapour flow over the distance dx, multiplied by the energy required to produce and heat the vapour.

$$= dG \left\{ L + \frac{C_{p_v}(T_s - T_b)}{2} \right\} \quad \dots(5.8)$$

where

L = latent heat of vapourisation of the coolant  
 $C_{p_v}$  = specific heat capacity of the vapour

This equation has assumed that the vapour produced is heated to the mean film temperature  $T_m$ .

Therefore, combining equations (5.3), (5.7) and (5.8)

$$\left\{ \frac{A}{s} - C \right\} dx = \frac{(p_L - p_v) p_v g s^2}{\mu_v} \left\{ L + \frac{C_{p_v}(T_s - T_b)}{2} \right\} ds \quad \dots(5.9)$$

Defining

$$B = \frac{(p_L - p_v) p_v g}{\mu_v} \left\{ L + \frac{C_{p_v}(T_s - T_b)}{2} \right\}$$

Then

$$\left\{ \frac{A}{s} - C \right\} dx = B s^2 ds$$

Or

$$dx = \frac{Bs^3 ds}{A-Cs} \quad \dots(5.10)$$

Integration gives

$$x = -\frac{B}{C} \left\{ \frac{s^3}{3} + \frac{ps^2}{2} + p^2s + p^3 \ln\left(1 - \frac{s}{p}\right) \right\} \quad \dots(5.11)$$

since  $s=0$  when  $x=0$ . For convenience,  $p$  has been defined as  $A/C$ .

In order to make equation (5.11) easier to understand, the logarithm can be expanded to give

$$x = \frac{B}{A} \left\{ \frac{s^4}{4} + \left(\frac{C}{A}\right) \frac{s^5}{5} + \left(\frac{C}{A}\right)^2 \frac{s^6}{6} \dots \right\} \quad \dots(5.12)$$

It can be seen that if no heat is convected away by the coolant, i.e.  $C=0$ , then

$$x = \frac{Bs^4}{4A} \quad \dots(5.13)$$

which is the result obtained by Bromley for vertical surfaces undergoing film boiling with the coolant at its boiling point.

The mean heat flux from the metal is

$$\bar{q} = \frac{1}{H} \int_0^H q_1 dx \quad \dots(5.14)$$

Changing the variables using equation (5.10) gives

$$\bar{q} = \frac{1}{H} \int_0^S \frac{A}{s} \cdot \frac{Bs^3}{A-Cs} ds \quad \dots(5.15)$$

where S is the thickness of the vapour film at height H from the base of the metal surface.

Therefore

$$\bar{q} = -\frac{AB}{HC} \left\{ \frac{S^2}{2} + pS + p^2 \ln \left( 1 - \frac{S}{p} \right) \right\} \quad \dots(5.16)$$

Taking equation (5.11) and replacing x by H and s by S, and combining with equation (5.16) gives

$$\bar{q} = C + \frac{BS^3}{3H} \quad \dots(5.17)$$

### 5.3 Solution Of The Equations

The equations obtained were used to construct the film boiling curves for water.

- 1 The vertical surface was taken to be 2.5 cm high. This defines the value of  $H$ .
- 2 A water subcooling was chosen and the value of  $C$  was calculated.
- 3 A metal temperature was chosen and the values of  $A$  and  $B$  were calculated.
- 4 The values of  $A, B$  and  $C$  were typed into a computer program (Fig 5.2) written in Basic. The value of  $S$  was found by step increasing the value of  $s$  put into equation (5.11) by one micron until the calculated value of  $x$  was greater than  $H$ . The first value of  $s$  for which  $x$  was larger than  $H$  was taken to be  $S$ . Thus, the calculated thickness is accurate to the nearest micron. The value of  $S$  found was put into equation (5.17) to give  $\bar{q}$ . The program also plotted out the vapour film profile.

Fig 5.2 A Program To Calculate Heat Fluxes

(written in Sinclair ZX81 Basic)

```

10 INPUT A
20 INPUT B
30 INPUT C
40 LET P=A/C
50 LET T=-B/C
60 LET R=0
70 LET R=R+1
80 LET S=R*1E-6
90 IF A < C*S THEN GOTO 130
100 LET X=T*(S**3/3+P*S**2/2+P**2*S+P**3*LN(1-S/P))
110 PLOT 5+R/10,15+1000*X
120 IF X < 2.5E-2 THEN GOTO 70
130 LET Q=C+B*S**3/7.5E-2
140 PRINT AT 16,7;Q

```

The Inputs A, B and C are given by

$$A = k_v(T_s - T_b)$$

$$B = \frac{(\rho_L - \rho_v) \rho_v g}{\mu_v} \left\{ L + \frac{C_{p_v}(T_s - T_b)}{2} \right\}$$

$$C = 0.56 \left\{ \frac{C_{p_L} \beta_L g \rho_L^2 k_L^3 \Delta T^5}{H \mu_L} \right\}^{1/4}$$

The variables associated with the vapour are estimated at the temperature  $\frac{1}{2}(T_s + T_b)$ . The variables associated with the coolant are estimated at the temperature  $T_b - \frac{1}{2}\Delta T$ .

- 5 Other metal and coolant temperatures were chosen and the corresponding heat fluxes calculated, thus constructing the boiling curves.

The film boiling curves that were obtained using these equations are shown in Fig 5.3.

#### 5.4 The Vapour Flow Reynolds Number

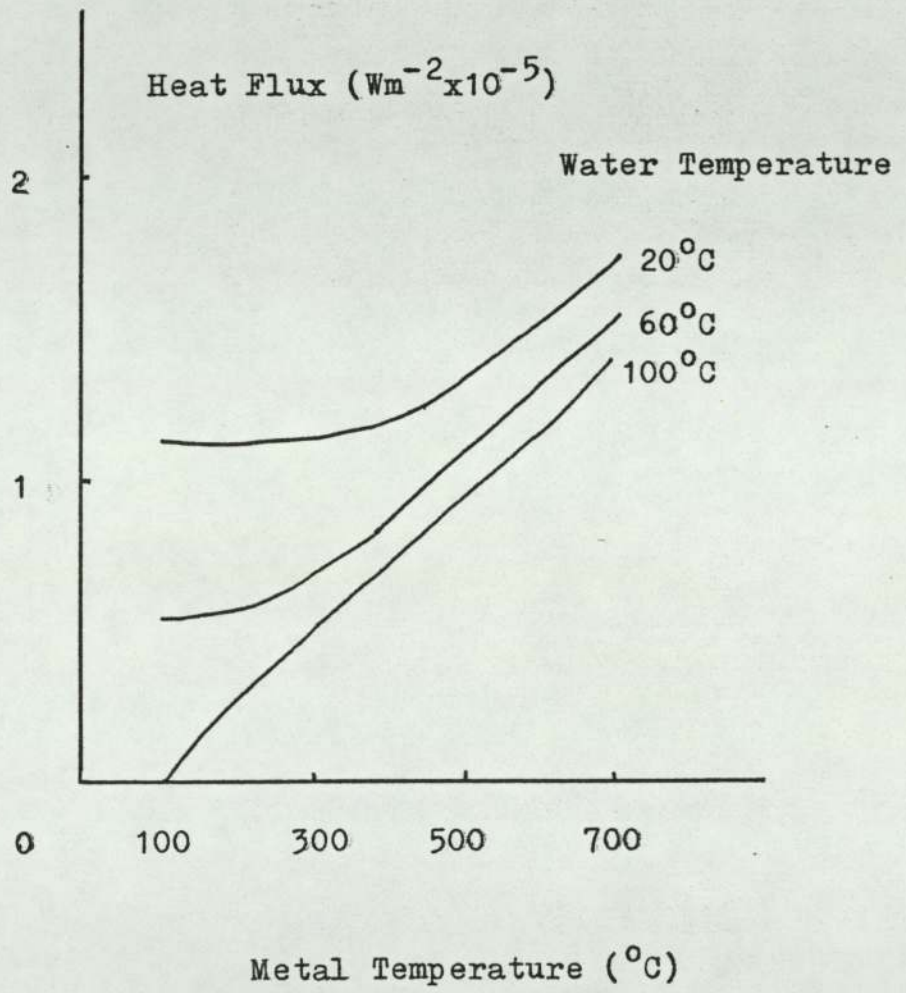
In order to establish the most likely nature of the vapour flow in the temperature regions considered, the Reynolds numbers for the flow were calculated. Hsu and Westwater<sup>(25)</sup> made the approximation that in film boiling, the vapour flow changes from viscous to turbulent at  $Re = 100$ . This approximation was based on the universal velocity profile.

The Reynolds numbers for the vapour leaving the top of the surface ( $x = H$ ) were calculated. The thickness of the vapour film at this point is  $S$ , therefore

$$Re = \frac{U \rho_v S}{\mu_v} \quad \dots(5.18)$$

where  $U$  is the velocity of the vapour at height  $H$  at the vapour-liquid interface.

Fig 5.3 Film Boiling Curves For Water



$$U = \frac{(\rho_l - \rho_v) g S^2}{2 \mu_v} \quad \dots(5.19)$$

Equation (5.19) is obtained by putting  $y=S$  and  $s=S$  in equation (5.1).

Combining equations (5.17), (5.18) and (5.19) gives

$$Re = \frac{3 H (\bar{q} - C)}{2 \mu_v \left\{ L + \frac{C_p (T_s - T_b)}{2} \right\}} \quad \dots(5.20)$$

The Reynolds numbers for the vapour flow at the top of the surface were calculated. The results of these calculations are shown in Fig 5.4.

### 5.5 The Mean Film Thickness

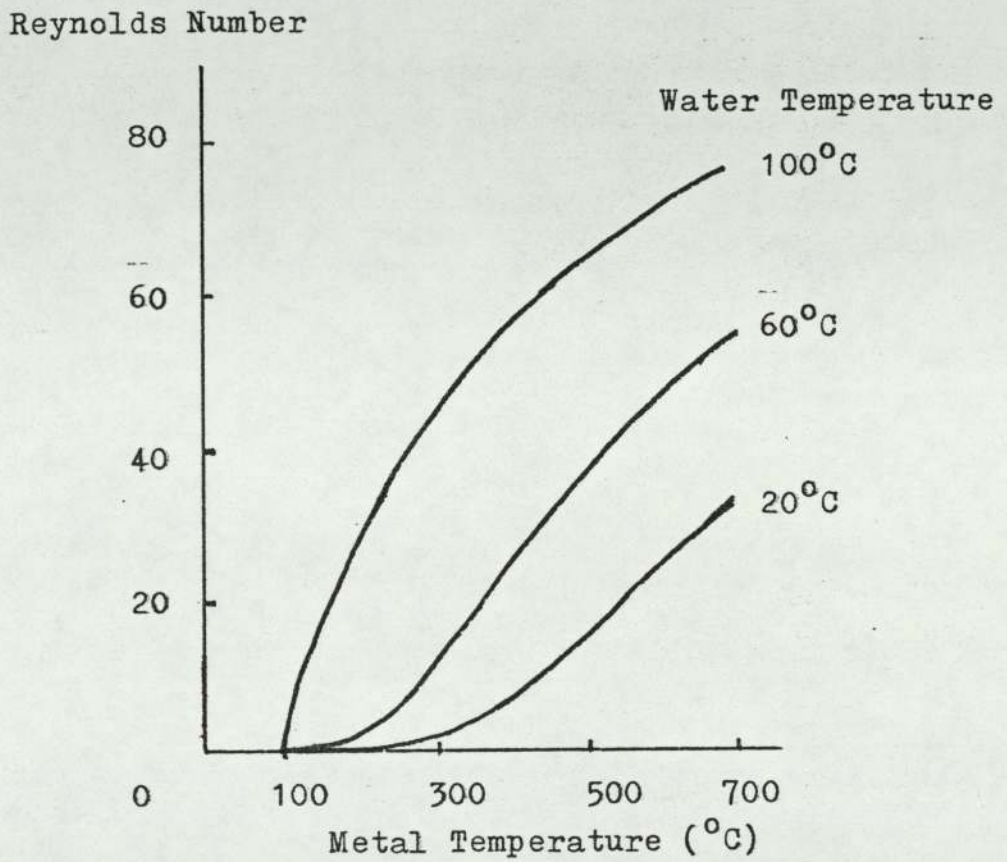
The mean film thickness ( $\bar{s}$ ) is given by

$$\bar{s} = \frac{1}{H} \int_0^H s \, dx \quad \dots(5.21)$$

Changing the variables gives

$$\bar{s} = \frac{1}{H} \int_0^S \frac{B s^4}{A - C s} \, ds \quad \dots(5.22)$$

Fig 5.4 The Vapour Flow Reynolds Numbers



Therefore

$$\bar{s} = \frac{B}{CH} \left\{ \frac{S^4}{4} + \frac{pS^3}{3} + \frac{p^2S^2}{2} + p^3S + p^4 \ln\left(1 - \frac{S}{p}\right) \right\} \quad \dots(5.23)$$

To make this equation easier to understand, the logarithm can be expanded to give

$$\bar{s} = \frac{B}{H} \left\{ \frac{S^5}{5A} + \frac{CS^6}{6A^2} + \frac{C^2S^7}{7A^3} + \dots \right\} \quad \dots(5.24)$$

Taking equation (5.11) and replacing  $x$  by  $H$ , and  $s$  by  $S$ , and combining with equation (5.23) gives

$$\bar{s} = \frac{A}{C} - \frac{BS^4}{4CH} \quad \dots(5.25)$$

Values of  $\bar{s}$  as a function of water and metal temperature are shown in Table 5.1 together with the corresponding values of  $S$ . The surface was again taken to be 2.5 cm high.

### 5.6 Film Boiling Over A Cooling Surface

This film boiling model shows that the values of  $\bar{q}$ ,  $Re$ ,  $S$  and  $\bar{s}$  would all decrease as the metal surface cools. The model also predicts that in subcooled

Table 5.1 Values Of  $\bar{s}$  And S

Mean Film Thickness ( $\bar{s}$ ) (microns)

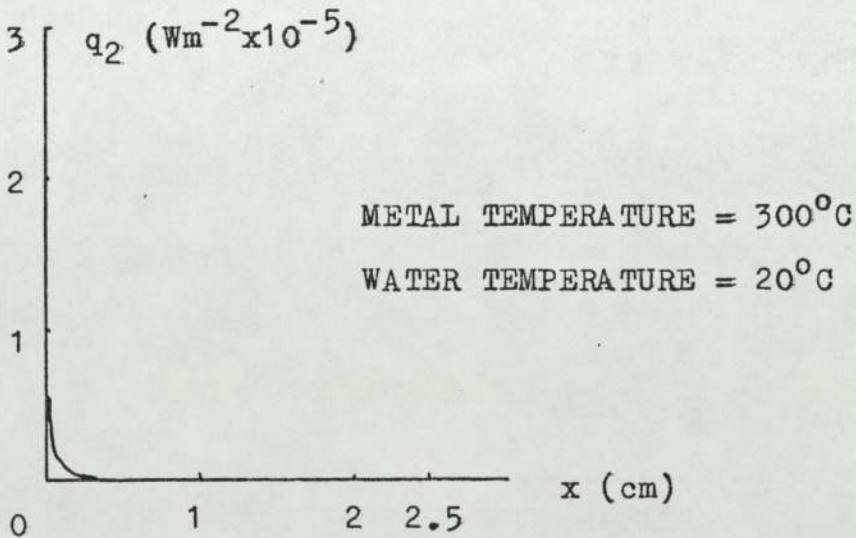
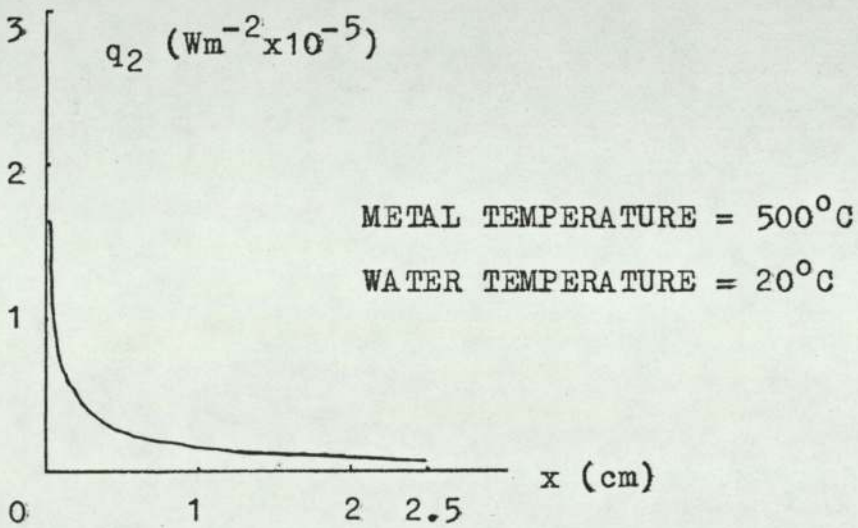
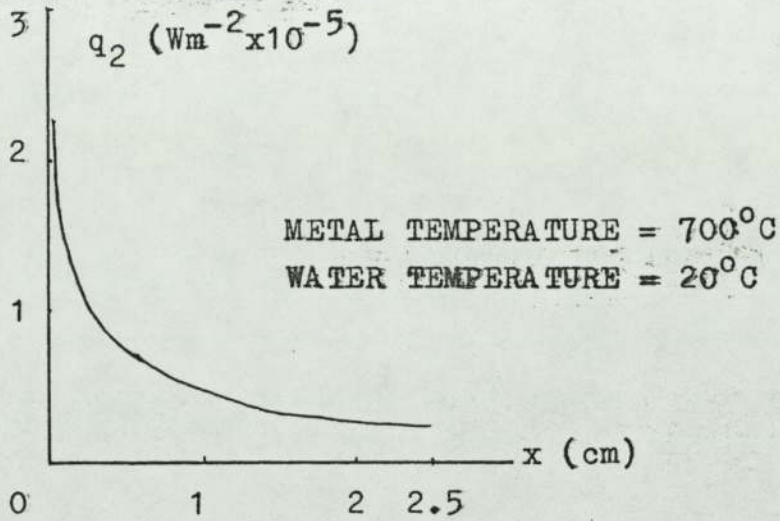
<u>Metal Temperature (<math>^{\circ}\text{C}</math>)</u>	<u>Water Temperature (<math>^{\circ}\text{C}</math>)</u>		
	<u>20</u>	<u>60</u>	<u>100</u>
700	196	219	246
600	166	196	222
500	134	167	197
400	97	137	170
300	58	110	142
200	25	52	109
100	0	0	0

Film Thickness At Height 2.5 cm (S) (microns)

<u>Metal Temperature (<math>^{\circ}\text{C}</math>)</u>	<u>Water Temperature (<math>^{\circ}\text{C}</math>)</u>		
	<u>20</u>	<u>60</u>	<u>100</u>
700	233	275	307
600	194	241	278
500	150	205	246
400	102	164	213
300	59	115	177
200	26	53	137
100	0	0	0

coolants, a drop in surface temperature would result in the bulk of the vapour being produced nearer the base of the surface. This can be seen in Fig 5.5 which shows how  $q_2$  (the heat flux required to produce and heat the vapour) depends on metal temperature and height in 20°C water.

Fig 5.5 The Heat Flux  $q_2$



## CHAPTER SIX

### HEAT TRANSFER FROM LIQUID METALS

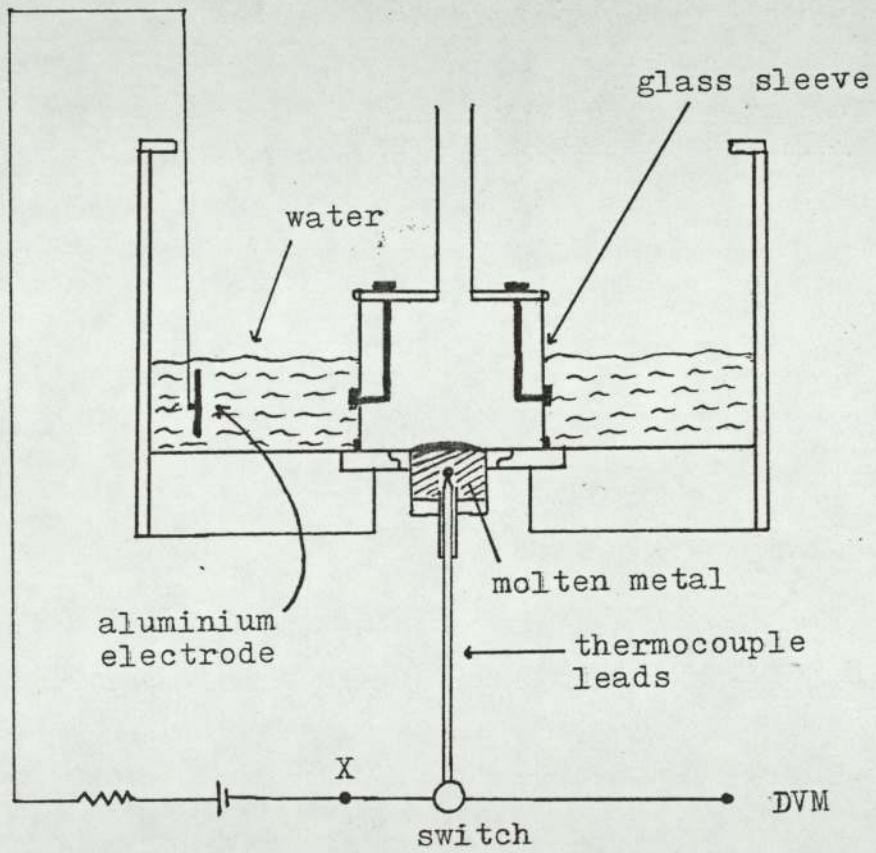
#### 6.1 Vapour Films On Liquid Metals

In this part of the work, the object was to design an experiment capable of extending the results of Boxley<sup>(31)</sup> by measuring the heat transfer rates that exist in the liquid copper-water system.

In order to decide on the type of apparatus best capable of yielding such data, the experimental apparatus used by Boxley was analysed. An account of Boxley's experiment, together with a diagram of Boxley's apparatus, is presented in the Appendix.

The aim of the experiments was to find out whether stable vapour films existed between the molten metal and the water. The experiments employed the D.C. analysis techniques of section 4.1. These experiments were carried out as described by Boxley, except that the thermocouple was used both as an electrical connection to the metal, and as a temperature transducer. A schematic diagram of the experiment is shown in Fig 6.1.

Fig 6.1 D.C. Analysis Of Boxley's Apparatus



By using the switch, the thermocouple in the metal could be connected either to a DVM (to measure the metal temperature), or to point X so that the thermocouple in the metal was connected in series to a resistor, battery and an aluminium electrode submerged in the water coolant. The voltage across the resistor was dependent on the amount of contact between the molten metal and the water.

The first experiment performed was the quenching of molten aluminium (initially  $\sim 900^{\circ}\text{C}$ ) in hot water ( $\sim 80^{\circ}\text{C}$ ). The experimental procedure was as follows;

- 1 About 5g of aluminium was melted into the silica crucible and then allowed to cool.
- 2 The glass sleeve was put into position and water poured into the tank.
- 3 The water was heated by an immersion heater, and the crucible heated by gas. The aluminium in the crucible was under a nitrogen atmosphere.
- 4 When the DVM indicated that the metal temperature was approximately  $900^{\circ}\text{C}$ , the thermocouple was connected to point X (using the switch), the chart recorder drive was switched on, and the bomb release (see Appendix) was fired.

5. As the aluminium cooled, flooded by water, the voltage across the resistor was recorded by the chart recorder.

The chart recorder trace showed that the voltage across the resistor was never zero, indicating that the aluminium was always in contact with the water. During the experiment, it was seen that there was intense boiling on the pyrophyllite ring surrounding the crucible. This boiling sometimes had a "foamy" appearance. The boiling was due to the high temperature attained by the pyrophyllite during the initial heating of the metal. In further experiments, attempts were made to reduce the amount of contact which occurred between the metal and the water. These attempts were made firstly by changing the initial water depths and temperatures, and secondly, by slowly manually raising the glass sleeve instead of using the bomb release. These attempts were unsuccessful. When tin was used as the molten metal, the contact was still found to occur.

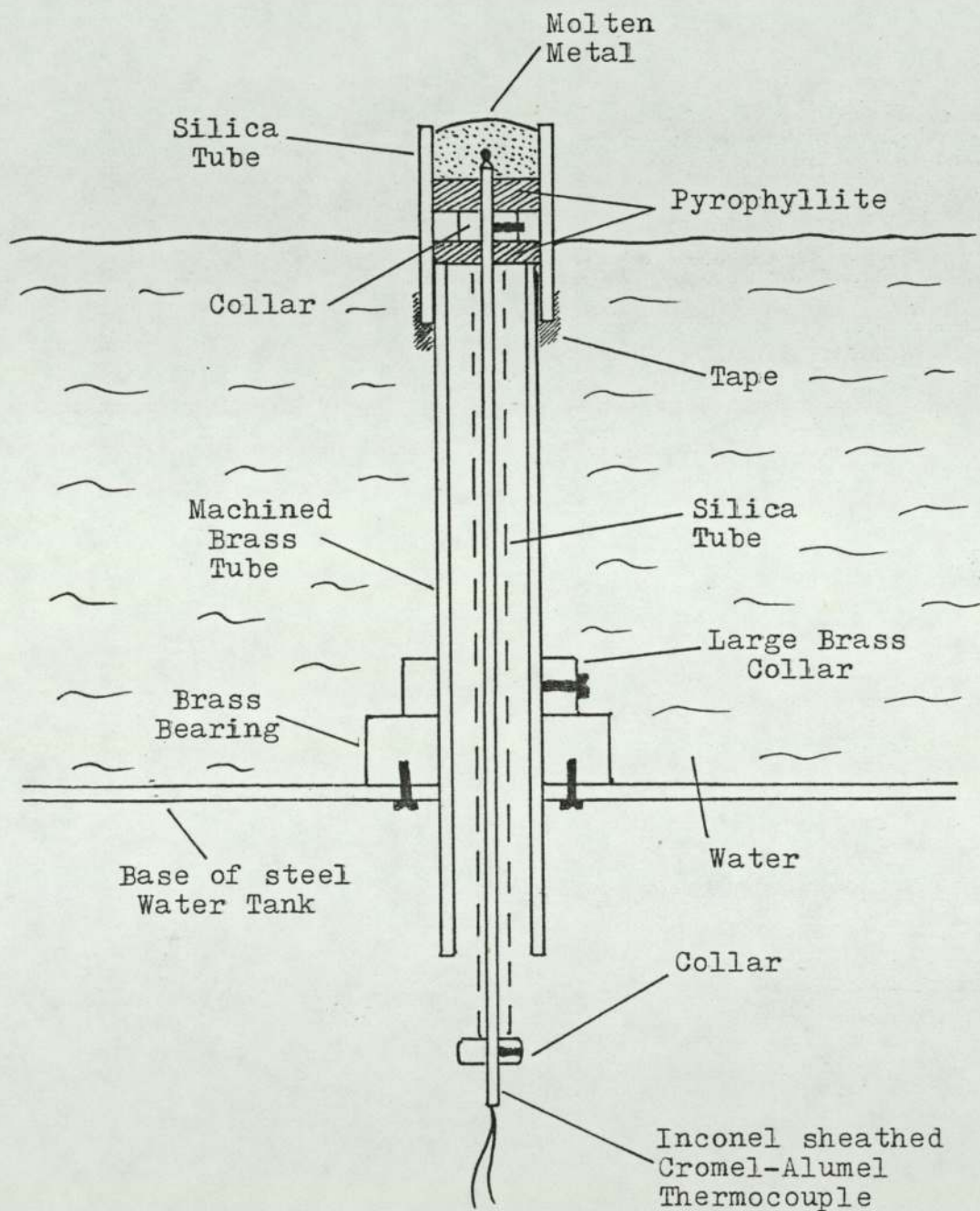
From these experiments, it was concluded that either complete decoupling of the liquid metal and water was not a characteristic of the metal-water system at the temperatures used (metal less than 900°C,

water 20°C to 90°C), or stable vapour film generation was inhibited by the apparatus used. It was considered that the intense boiling on the pyrophyllite ring would not be conducive to stable vapour film generation over the liquid metal.

In an attempt to produce a stable vapour film between the liquid metal and water, apparatus was designed which reduced the amount of hot ceramic in the vicinity of the molten metal. The trial apparatus devised is shown in Fig 6.2. A machined brass tube with a silica/pyrophyllite crucible at its top was constructed. The junction of an inconel sheathed cromel-alumel thermocouple was held in place in the crucible by a collar positioned between two pyrophyllite rings, the lower of which rested on top of the machined brass tube. A silica tube (16 mm bore) was connected to the outside of the brass tube by tape. A small diameter silica tube was held in place around the thermocouple by a collar. The machined brass tube was held in a fixed position in a steel tank by a brass collar around the tube. The brass collar was glued to a brass bearing at the base of the tank.

Water was poured into the tank until the water level

Fig 6.2 The Trial Apparatus



was about an inch below the top of the silica tube. This apparatus was incorporated into a D.C. circuit. The thermocouple and water were connected to a resistor ( $33k\Omega$ ) and a battery (9V) in the same way that the thermocouple and water of Boxley's apparatus were connected (see Fig 6.1). A chart recorder was connected across the resistor.

Approximately 10g of tin was melted into the crucible. The tin was heated to  $800^{\circ}\text{C}$  by gas, and the water heated to about  $80^{\circ}\text{C}$  by an immersion heater. At  $800^{\circ}\text{C}$ , the heating was stopped and the oxidised tin removed with a spatula. The thermocouple was connected into the D.C. circuit using the switch and the chart recorder drive was switched on. The water level was then raised above the crucible top by lowering a large weighted wooden block into the steel water tank. While the tin was cooling in the water, it was noted that the vapour production was mainly limited to the top of the tube above the metal. The chart recorder trace showed that at high tin temperatures, there was no contact between the water and the tin. In further experiments, in which tin was quenched in water, both stable film boiling and film boiling with partial contact were observed.

It was concluded that since the crucible arrangement in the trial experiment had provided stable film boiling, this crucible arrangement should be built into a more refined apparatus. This apparatus was built and used to measure the heat fluxes present in the liquid copper-water system.

## 6.2 The Liquid Copper-Water System

The apparatus shown in Fig 6.3 was used to plunge liquid copper held in a silica/pyrophyllite crucible into water. The crucible arrangement used is shown in Fig 6.4. Tungsten/Tungsten-26% Rhenium thermocouple wires were passed through a recrystallised alumina tube. This tube passed through a 1" diameter brass collar and a machined pyrophyllite cylinder, and was held in place by the collar screw. The lower face of the pyrophyllite cylinder was attached to the upper face of the collar with silicone rubber glue. A cylinder of silica ( $16 \pm 0.8$  mm bore,  $1.4 \pm 0.25$  mm wall thickness) encased the pyrophyllite and was glued to the upper plane face of the collar. The upper plane face of the pyrophyllite and the silica tube formed the crucible. The W/W-Re wires were cased in rubber except for the

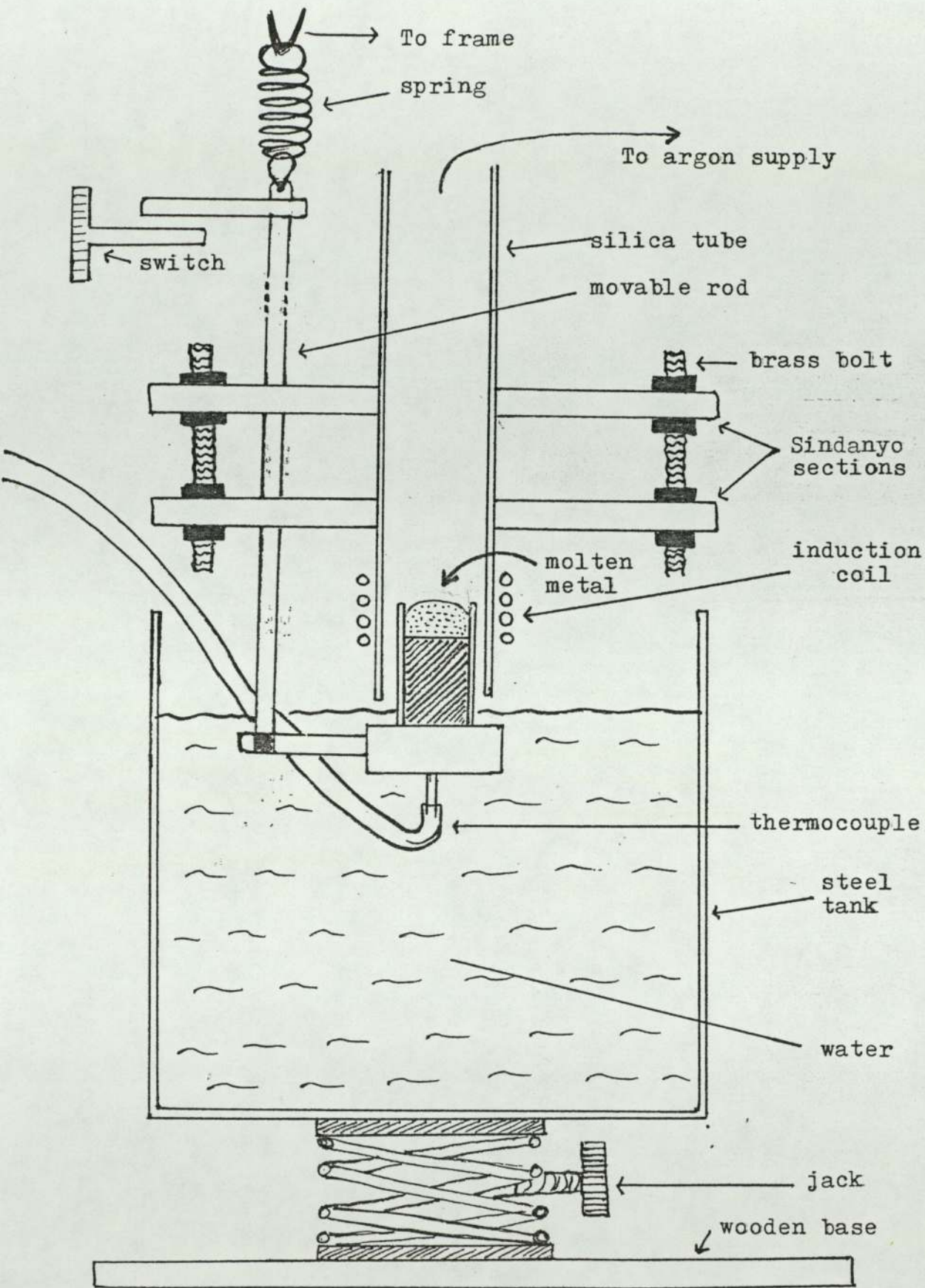
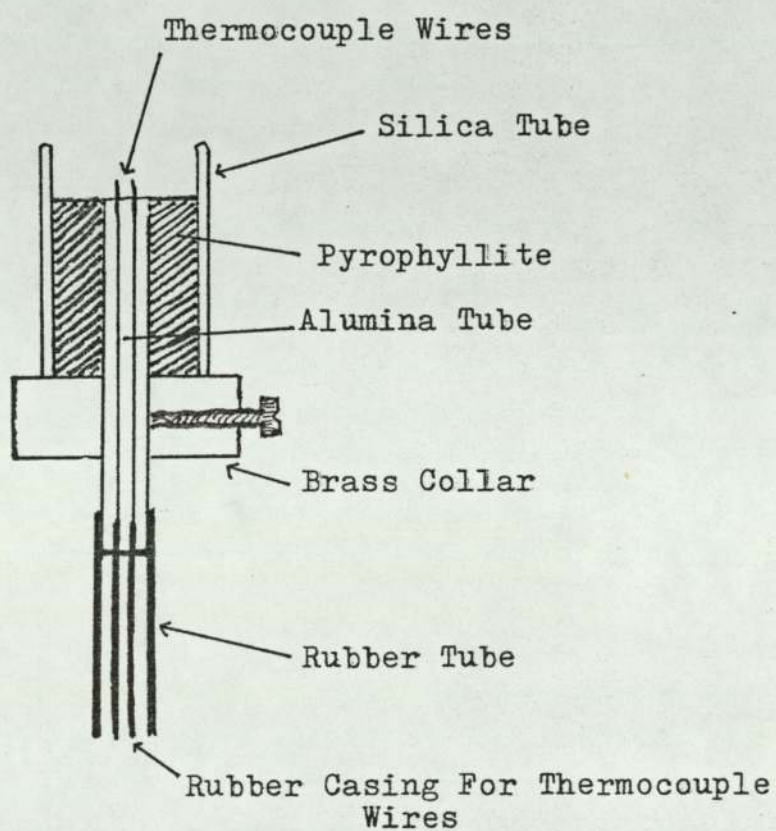


Fig 6.3 Liquid Metal Heat Transfer Apparatus

Fig 6.4 The Crucible Arrangement



lengths within about an inch of the crucible. The lower part of the recrystallised alumina tube and the rubber cased thermocouple wires were surrounded by further rubber casing, held in place with tape.

The crucible was incorporated into the main apparatus by a clamp which held the brass collar. The clamp was connected to a vertical  $\frac{1}{2}$ " diameter weighted rod which could slide through two 10" square  $\frac{1}{2}$ " thick sections of Sindanyo held  $2\frac{1}{2}$ " apart. The travel of the rod was aided by teflon washers set into the Sindanyo sections. By moving the rod, the crucible could be moved between two positions, "up" and "down". In the "up" position, the crucible was held inside a silica tube parallel to the movable rod. This silica tube passed through the axis of the two Sindanyo sections, and was held in position by a clamp resting on the top face of the upper Sindanyo section. Outside this silica, level with the crucible, was an induction coil from a Radyne C50 furnace. The top of the silica tube was connected to a supply of argon.

Thus, in the "up" position, metal in the crucible could be heated in an inert atmosphere. In the

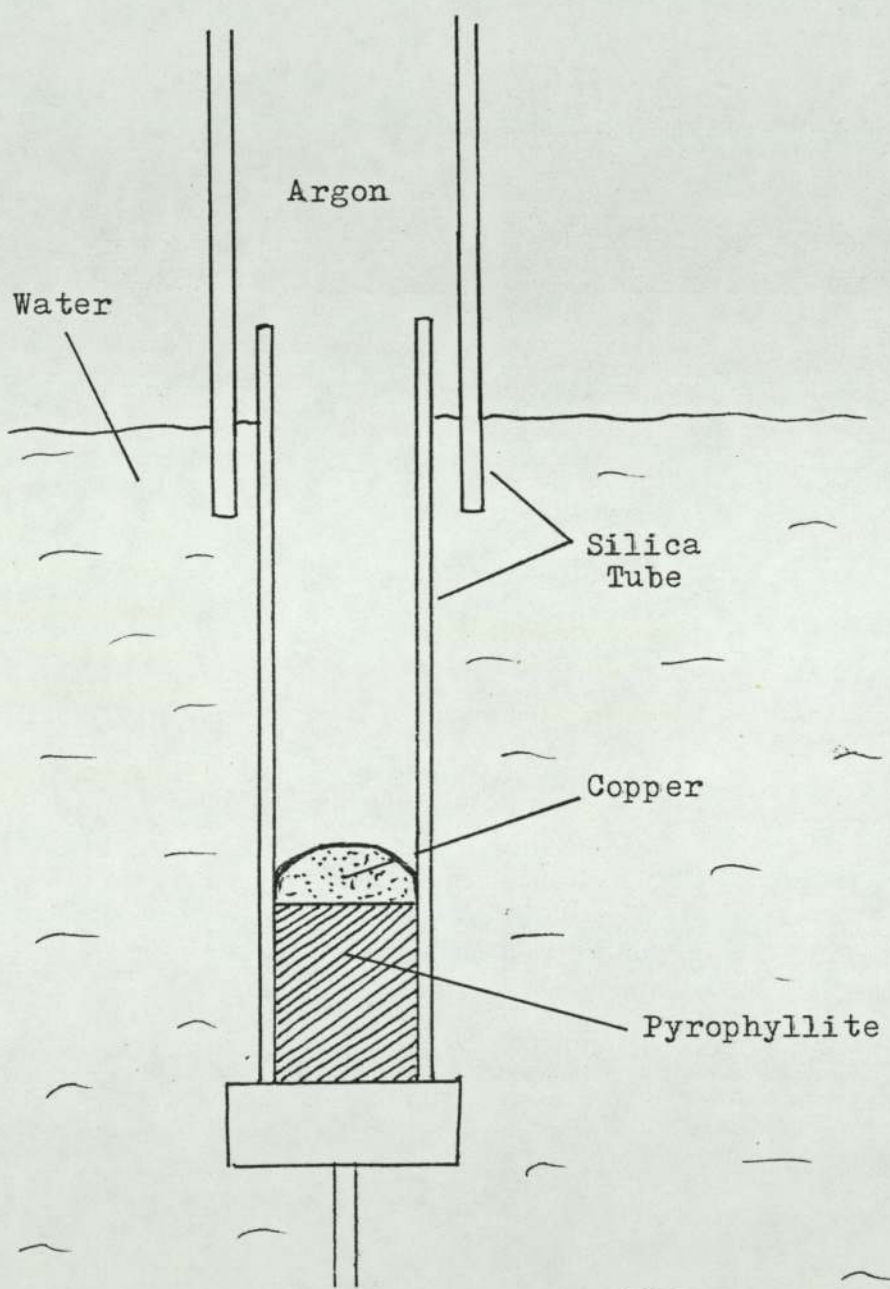
"down" position, the crucible was submerged in water which was held in a steel tank, the top of the crucible being 2" below the water surface. The tank rested on a jack which in turn rested on a wooden base held parallel to the two Sindanyo sections by Dexion frame. The crucible was held in the "up" position by the movable rod, the fall of which was interrupted by a simple manually operated mechanical switch. The fall of the rod, and thus the crucible to the "down" position was damped by a spring connected from the Dexion frame to the rod.

Experiments were performed using this apparatus, in which the cooling rates of 8g of liquid copper in water were recorded. The copper was melted into the crucible and then heated to above 1300°C, the power to the induction coil was cut and the crucible was plunged into the water (25°C). As the copper cooled in the water, the output of the thermocouple was recorded on magnetic tape by an Ampex FR 1300 tape recorder. The recorded signal was replayed to a chart recorder after the quenching. From each of these experiments, a cooling rate ( $\frac{dT}{dt}$ ) of the copper over the temperature range 1120°C to 1220°C was evaluated.

Before these cooling rates were converted into heat fluxes, an attempt was made to take into account the heat lost by the copper to the crucible. The amount of heat that travelled to the crucible was estimated by performing experiments in which 8g of copper, held in a high-walled silica/pyrophyllite crucible was quenched in water (25°C). The dimensions of the crucible used were the same as in the previous experiments, except for the depth (about 3" in these experiments). The copper was melted into the crucible and then heated to above 1300°C in an argon atmosphere. The crucible was plunged into the water, which resulted in the copper being 2" below the water surface, but not in contact with the water (see Fig 6.5). The cooling of the copper was recorded as before. From each of these experiments, a cooling rate  $(\frac{dT}{dt})_2$  of the copper over the temperature range 1120°C to 1220°C in 25°C water was evaluated. The two sets of data which correspond to liquid copper cooling in 25°C water over the temperature range 1120°C to 1220°C were combined using the equation

$$q_1 = \frac{mC_p}{A_1} \left\{ \frac{dT}{dt}_1 - (\frac{dT}{dt})_{av} \right\} \dots(6.1)$$

Fig 6.5 Quenching Of The High-Walled Crucible



where

$q_1$  = heat flux corresponding to the loss of heat directly to the water

$m$  = mass of the copper

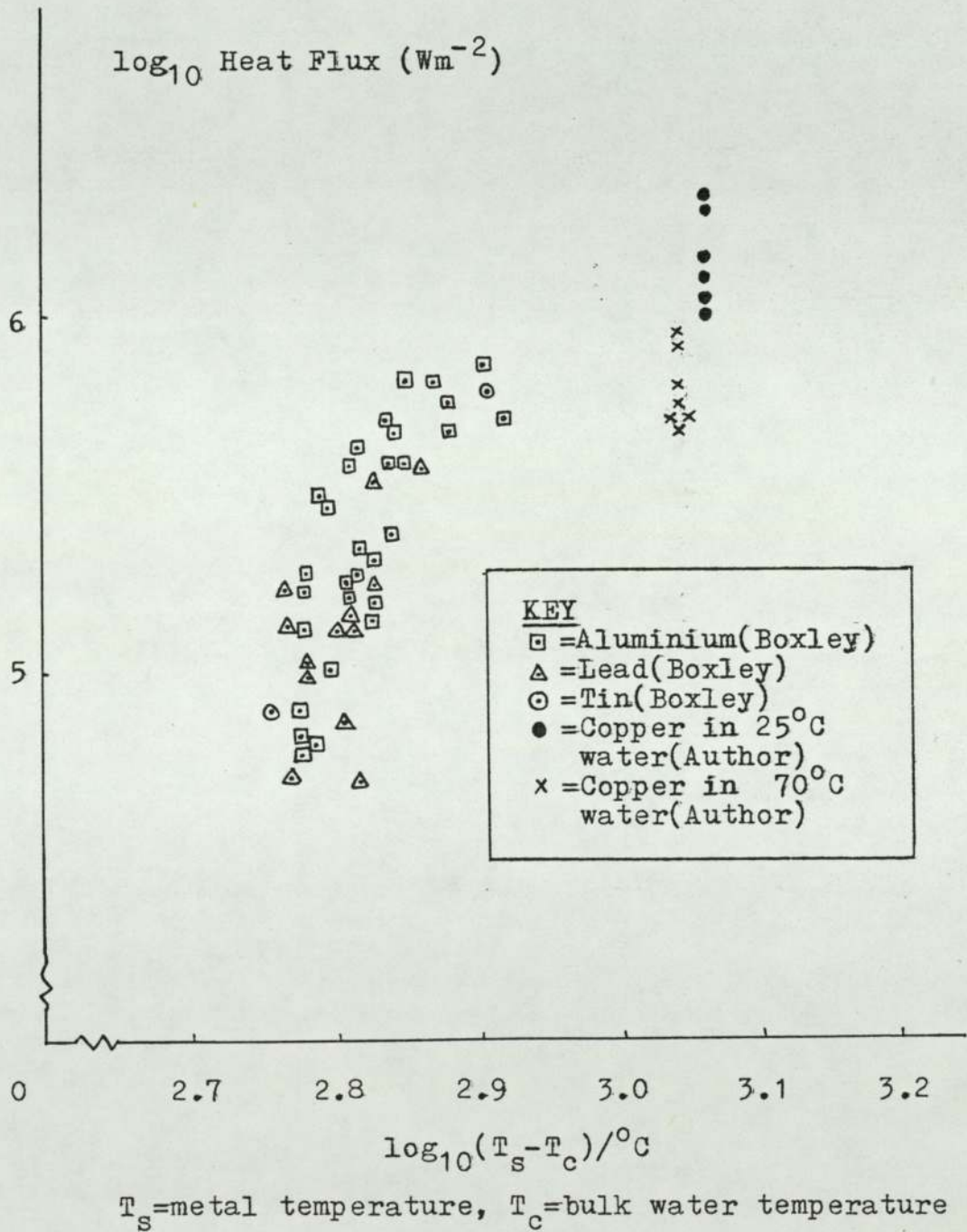
$A_1$  = area of the copper which is directly exposed to the water

$C_p$  = specific heat capacity of copper

The value of  $(\frac{dT}{dt})_{av}$  was obtained by averaging the values of  $(\frac{dT}{dt})_2$  that had been experimentally obtained. The recorded values of  $(\frac{dT}{dt})_1$  were put into equation (6.1) together with the value of  $(\frac{dT}{dt})_{av}$  to give values of  $q_1$ . These heat fluxes ( $q_1$ ) are compared to the heat flux data of Boxley, who recorded heat flux data in liquid metal (tin, lead and aluminium)-water systems.

Fig 6.6 shows the data recorded by Boxley, together with the heat fluxes  $q_1$ . Since the heat fluxes ( $q_1$ ) have been derived from experiments which have recorded the cooling rate of copper over the temperature range 1120°C to 1220°C, the metal temperature ( $T_s$ ) used to plot the data for copper corresponds to the mid-range temperature of 1170°C. Results from experiments which recorded the heat fluxes from copper (over the

Fig 6.6 Heat Transfer Data For Liquid Metal-Water Systems



temperature range 1120°C to 1220°C) to 70°C water are also presented. The experimental method employed in the 70°C water experiments was the same as that used for the 25°C water experiments.

The basis of equation (6.1) is now examined. The heat fluxes  $q_1$  have been taken to be measures of the amount of heat that directly travels from the copper to the water.

When the crucible is fully submerged in the water, the liquid copper loses heat directly to the water and to the crucible. If the copper at a temperature  $T_s$  falls in temperature by a small amount  $\Delta T_1$  in time  $\Delta t$ , an energy equation can be written

$$m C_p \Delta T_1 = q_1 A_1 \Delta t + q_2 A_2 \Delta t \quad \dots(6.2)$$

where

$q_2$  = A heat flux corresponding to the loss of heat to the crucible

$A_2$  = area of copper in contact with the crucible

If the mass  $m$  of copper at a temperature  $T_s$  only lost heat to the crucible, falling in temperature a small amount  $\Delta T_2$  in time  $\Delta t$ , the energy equation becomes

$$m C_p \Delta T_2 = q_2 A_2 \Delta t \quad \dots(6.3)$$

Combining equations (6.2) and (6.3) gives

$$m C_p \Delta T_1 = q_1 A_1 \Delta t + m C_p \Delta T_2 \quad \dots$$

Or

$$q_1 = \frac{m C_p}{A_1} \left( \frac{\Delta T_1}{\Delta t} - \frac{\Delta T_2}{\Delta t} \right) \quad \dots(6.4)$$

Therefore, if  $\Delta t$  is infinitesimally small

$$q_1 = \frac{m C_p}{A_1} \left( \frac{dT_1}{dt} - \frac{dT_2}{dt} \right) \quad \dots(6.5)$$

Equation (6.5), which evaluates  $q_1$  in terms of two cooling rates  $\left(\frac{dT_1}{dt}\right)$  and  $\left(\frac{dT_2}{dt}\right)$ , was the basis for evaluating the experimental results. It is noted that when the copper was cooling in the high-walled crucible, the copper was losing heat vertically by radiation and by natural convection to the argon.

A heat flux ( $q_{RC}$ ) corresponding to these heat losses can be estimated using standard equations. For copper at  $1170^{\circ}\text{C}$ , the value of  $q_{RC}$  is estimated to be approximately  $50 \text{ kWm}^{-2}$ . In this calculation, the characteristic dimension of the copper surface losing heat upwards was taken to be the diameter of the crucible. The emissivity of copper was taken to be 0.15. The heat fluxes ( $q_1$ ) for copper plotted in Fig 6.6 have not taken  $q_{RC}$  into account. If  $q_{RC}$  is taken into account, it is expected that the effect would be to raise each of the heat fluxes for copper in Fig 6.6 by approximately  $50 \text{ kWm}^{-2}$ .

### 6.3 Minimum Temperature Experiments

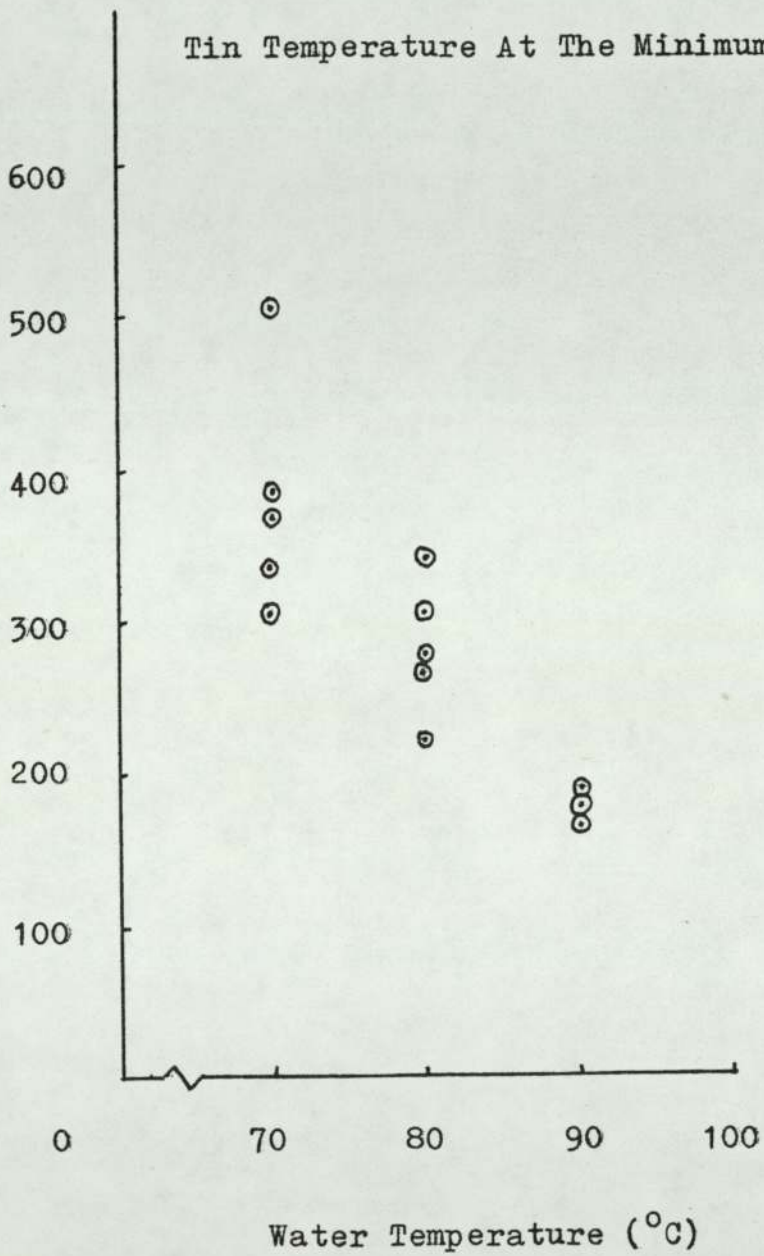
The experimental apparatus used for copper was not found to be suitable for providing heat flux data in the liquid tin-water system. This was because it was found that the recorded values of  $(\frac{dT}{dt})_1$  and  $(\frac{dT}{dt})_2$  were too close together to enable reliable data to be generated. However, the apparatus was capable of measuring the tin temperatures at which the minimum heat fluxes occurred ( $T_{\min}$ ) in the tin-water system.

The thermocouple used was chromel alumel instead of W/W-Re. 5.5g of liquid tin was quenched from approximately 600°C in water, the temperature of which was varied between 70°C and 90°C. The cooling rate of the tin was recorded as in the copper experiments. The recorded minimum heat flux temperatures are plotted as a function of the water temperature in Fig 6.7.

### 6.4 Small Scale Interactions

Liquid tin (2-3g) was heated in air in a nickel crucible to temperatures up to 500°C, and then poured into a variety of room temperature coolants held in a 100ml beaker. In water, explosions were observed

Fig 6.7 Minimum Temperatures In The Tin-Water System



in contrast to the coolants listed in Table 6.1, in which no explosions were recorded. When liquid Wood's metal was used instead of tin with the same coolants, explosions were again only recorded in water.

Table 6.1 Coolants In Which Explosions Were Not Recorded

Acetone  
Benzyl Alcohol  
sec Butyl Alcohol  
Carbon Tetrachloride  
Chloroform  
Ethanol  
Formamide  
Methanol  
Fuming Nitric Acid  
n-propanol  
Concentrated Sulphuric Acid

## CHAPTER SEVEN

### DISCUSSION

#### 7.1 Discussion Of The Experimental Apparatus

Many workers who have used quenching techniques to examine film boiling have recorded the cooling rate of a sphere completely submerged in the coolant. This method was not used in these experiments because importance was placed on creating vapour films which had a smooth simple geometry, uninterrupted by the thermocouple and which were able to freely remove vapour. This simple geometry minimised the possibility of film destabilisation due to geometric effects associated with the heater, and completely removed the possibility of premature film destabilisation on the thermocouple sheath. The simple geometry of the probe enabled an expression for the capacitance of the vapour films to be obtained in terms of the mean vapour film thicknesses.

The probe was made of copper because copper has a high thermal conductivity and a high melting point. Care was taken to ensure that the oxide formation

on the surface was minimised by using an induction furnace to heat the probe when temperatures above 300°C were required. The induction furnace made it possible to design apparatus which kept the probe in an argon atmosphere during its heating and transference.

When performing experiments with liquid copper, cromel-alumel thermocouples could not be used. During the initial heating when solid copper and the thermocouple junction were present in the crucible, it was found that the induction furnace heated the cromel-alumel thermocouple at a significantly faster rate than the copper, which caused the thermocouple to be destroyed before the copper melted. Therefore a Tungsten/Tungsten-26%Rhenium thermocouple was used.

The silica and pyrophyllite used to make the crucible were found to be well able to withstand the high temperatures that were imposed on them. The pyrophyllite ceramic was found to be very useful due to the ease with which it could be machined. However, experiments involving iron could not be used with this apparatus, as liquid iron was found to rapidly

destroy the pyrophyllite. Experiments using nickel were not possible with this apparatus, since liquid nickel was found to adversely affect the W/W-Re thermocouple.

Small quantities of liquid metal were used in these experiments so that any unintentional explosive interaction could be well contained by the perspex safety sheets which were positioned around the apparatus.

## 7.2 Discussion Of Boiling Terminology

Bradfield<sup>(32)</sup> concluded that it was possible to have contact in stable film boiling. This statement is ambiguous and raises the question of what the definition of stable film boiling is. In this thesis, stable film boiling is defined as the condition in which the coolant is totally separated from the metal by a film of vapour. The condition in which the coolant is for the most part separated from the metal, but some contact between the metal and coolant occurs, is referred to here as "film boiling with partial contact", which differs from the term used by Bradfield of "stable film boiling with partial contact". It is thought that the terminology used here is slightly clearer than

that used by Bradfield.

Also, reference to the Leidenfrost point or Leidenfrost temperature is avoided. The Leidenfrost phenomenon strictly speaking occurs when an unconstrained liquid mass does not wet a horizontal heating surface and enters the spheroidal state in which the liquid is prevented from wetting the heater by a cushion of vapour. Many authors refer to the Leidenfrost point as the point at which the minimum heat flux between the metal and coolant occurs. Winter, Merte and Herz<sup>(46)</sup> state that under many conditions, the minimum temperature (the metal temperature corresponding to the minimum heat flux) and the Leidenfrost temperature are about equal. Thus, they do not have to be the same. When describing the quasi-static boiling situations of the quenching experiments performed here, no reference to the Leidenfrost point or temperature is made, so as to avoid any confusion.

The terms that are used here correspond to the following three points which can be identified from the experimental data.

### The Minimum Point

The point at which the minimum heat flux from the metal to the coolant occurs. At this point

$$\frac{dq}{dT_s} = 0 \quad \text{and} \quad \frac{d^2q}{dT_s^2} \text{ is positive}$$

where  $q$  is the heat flux from the metal, and  $T_s$  is the metal temperature. The metal temperature at this point is written as  $T_{\min}$ .

### The Contact Point

The first point (using D.C. analysis) at which the cooling metal first contacts the coolant, allowing a current to flow around the D.C. circuit.

### The Point Of Film Collapse

The point, measured using the transducer, at which the graph of  $V_{\text{chan C}}$  versus time is most curved. At this point,  $\rho$  is a minimum, where

$$\rho = \frac{\left\{ 1 + \left( \frac{dV_{\text{chan C}}}{dt} \right)^2 \right\}^{3/2}}{\left\{ \frac{d^2V_{\text{chan C}}}{dt^2} \right\}}$$

A necessary condition when using this definition is that the graphs of  $V_{\text{chan C}}$  against time should be smoothed, i.e. oscillation of the film is neglected.

### 7.3 Discussion Of The Experimental Results

Information on vapour films over solid and liquid metals has been provided by experiments which have recorded the thermal and electrical properties of various metal-vapour-coolant systems.

#### 7.3.1 Thermal Experiments With The Copper Probe

The experiments of Chapter Three which recorded the cooling rates in the film boiling regime of a copper probe in water and organic coolants show that no fundamental difference between the behaviour of water and the organic coolants was observed. The data trends observed in the experimental results for each coolant were the same. These trends were

1. In the film boiling regime, higher metal temperatures and higher coolant subcoolings resulted in higher heat fluxes.
2. The values of  $T_{\min}$  (the temperature corresponding to the minimum heat flux) and  $q_{\min}$  (the heat flux at  $T_{\min}$ ) were generally found to increase as the coolant subcooling increased.

The difference between water and the organic coolants

lay in the magnitude of the heat fluxes during film boiling, and the ranges of  $T_{\min}$ . The values of  $T_{\min}$  for the organic coolants were in the range  $110^{\circ}\text{C}$  to  $220^{\circ}\text{C}$ , the corresponding range for water being  $240^{\circ}\text{C}$  to  $570^{\circ}\text{C}$ .

### 7.3.2 Electrical Experiments With The Copper Probe

The D.C. analysis was only able to supply a limited amount of information concerning the film boiling regime. The main observations that were made, were that firstly, the contact point was observed at probe temperatures in excess of  $T_{\min}$ , contact between the probe and coolant always being observed below  $T_{\min}$ ; and secondly, that in some cases contact was electrically recorded even though careful visual observation suggested that the probe and coolant were totally decoupled. It is suggested that care should be taken when concluding that stable vapour films exist on the basis of visual or photographic observation.

The D.C. analysis showed that it was reasonable to consider vapour films as capacitors. On this basis, apparatus was designed which was capable of estimating mean vapour film thicknesses by firstly estimating the capacitances of the vapour films and then con-

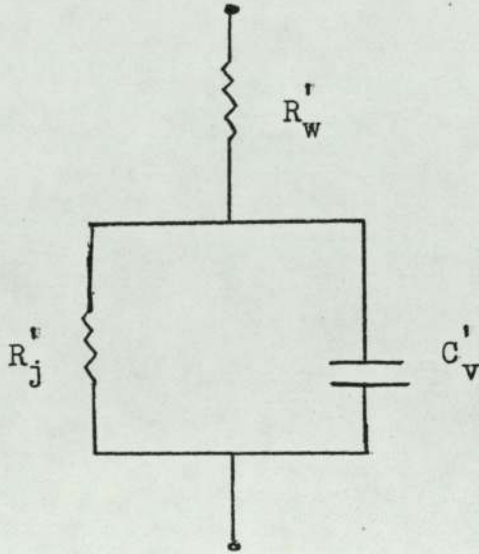
verting the capacitances into mean film thicknesses. Estimation of film thicknesses by this electrical method requires that the coolant should be a reasonable conductor of electricity. It has the advantage that the vapour film does not have to be visible, and therefore this technique can be used with coloured coolants. The film capacitances were estimated using a transducer which was built up after the trial experiment of section 4.2. A theoretical examination of the operations performed by the transducer was carried out.

The first series of experiments performed using the transducer recorded the behaviour of vapour films over an oxidised stainless steel probe cooling in water. These experiments were performed to gain experience in using the transducer, and to make basic observations on the nature of vapour films. Since many experiments on vapour films were required to do this, oxidation of the probe surface was considered at this stage to be of secondary importance to the need for the experiments to be simple and quick to perform. Figs 4.7 and 4.8 showed the general behaviour of vapour films as the probe cooled. The capacitative data showed that the vapour films thin and tend to oscillate less as the probe cools.

The graph of Fig 4.9 simultaneously recorded the outputs of the resistance and capacitance channels as the probe cooled. It can be seen that just before the point of film collapse, there was a small step increase in the output of the resistance channel. It was suggested that this corresponded to a small amount of contact between the probe and the water being made across the vapour film. The electric circuit corresponding to this situation is shown in Fig 7.1. A.C. theory can be used to estimate the values of  $R_j'$  and  $C_v'$  from the values of the resistance and capacitance outputs shown in Fig 4.9. Analysis shows that in the case considered here,  $R_j'$  has a very high resistance, indicating that the area of contact between the probe and the water was very small compared to the area covered by the vapour film.

The transducer could be conveniently incorporated into the quenching experiments of Chapter Three. From these experiments, estimates of the film thicknesses at the point of film collapse were made. The results showed that the film collapse thicknesses in n-propanol were similar to those observed in water. Collapse occurred between approximately 40 and 90 microns in n-propanol, the range in water being 50 to 100 microns.

Fig 7.1 The Electric Circuit Corresponding To  
Contact Across The Vapour Film



$R_w^r$  = resistance of the main bulk of the water  
 $C_v^r$  = capacitance of the vapour film  
 $R_j^r$  = resistance of the water bridging the  
vapour film

### 7.3.3 Experiments With Liquid Metals

It was noted that Boxley's apparatus did not provide stable film boiling, whereas the trial apparatus of Fig 6.2 did. This observation is important since, as previously noted with the copper probe experiments, visual observation of the film can be misleading.

It was decided that the crucible arrangement of Fig 6.2 should be used to measure the heat fluxes present in the liquid copper-water system. This crucible arrangement together with the induction heating of the metal was an improvement on the apparatus used by Boxley, since the boiling was limited to the vicinity of the liquid metal. The disadvantage of the apparatus compared to Boxley's was that an estimate of the heat flow from the copper to the crucible had to be made.

Work on Boxley's apparatus and the apparatus of Fig 6.3 showed that measuring heat fluxes in liquid metal-water systems is more complicated than it might at first appear. The difficulty stems from the fact that since the metal is liquid, it has to be supported. If it is supported, there will be heat loss through the support and an involvement of the support in the boiling process.

The experiments performed here have identified a problem that should be considered when attempting to measure heat fluxes in liquid metal-coolant systems, and have gone some of the way to overcoming the problem.

Although the scatter of the heat flux data for liquid copper was large, it can be seen that the heat fluxes were a function of the water subcooling. It is not clear if the heat fluxes recorded by Boxley exhibited the same dependence. The values of the heat fluxes recorded for copper are slightly lower than would be expected from extrapolation of Boxley's data. Whilst extrapolation is not always valid, this may be an indication of the differing stabilities of film boiling in the two sets of apparatus. That is, higher heat fluxes may be expected in Boxley's apparatus due to the less stable nature of the vapour films generated.

When experiments with molten tin were performed, it was noted that the values of  $T_{\min}$  recorded (Fig 6.6) were significantly lower than those recorded by Boxley (average value quoted by Boxley, 610°C). It is suggested that this observation is a reflection of the difference in stability of vapour films generated in the two sets of apparatus.

#### 7.4 Discussion Of The Model For Film Boiling

The model for film boiling enabled theoretical estimates of heat fluxes to be made for vertical surfaces undergoing film boiling in subcooled coolants.

The heat fluxes predicted by the model for water were lower than those recorded in the probe experiments. This discrepancy could be due to the vapour flow in the probe experiments not being totally laminar. The theoretical Reynolds numbers for the vapour flow (Fig 5.4) were found to be less than 100, and using the approximation made by Hsu and Westwater<sup>(25)</sup>, the vapour flow would be expected to be laminar. However, it is noted that the choice of a critical Reynolds number at 100 is based on the assumption that the vapour exists either in a totally laminar or totally turbulent condition, i.e. the existence of a buffer zone is neglected. In order to develop the film boiling model presented, effects associated with the buffer zone would need to be considered.

In subcooled water, the model shows that for mean vapour film thicknesses up to approximately 50 microns, the mean film thickness ( $\bar{\delta}$ ) takes values very close to

those of  $(S)$ , the film thickness at the top of the surface. When  $\bar{s}$  is close to  $S$ , the bulk of the vapour production occurs at the base of the surface.

If the bulk of the vapour production occurs at the base of the surface, i.e. becomes localised, it might be possible for the system to remove vapour by vapour bubbles at the base of the surface, instead of allowing the vapour to rise over the metal surface and leave the system.

It is noted that in the experiments with water, the film collapse thicknesses (Fig 4.12) were all above 50 microns. Visual observation showed that film collapse always started at the base of the probe.

Such observations would be expected if vapour film collapse was linked with a localisation of vapour production.

## 7.5 Discussion Of The Results In The Context Of Vapour Explosion Phenomena

### 7.5.1 Spontaneous Explosions

The experiments of Pool<sup>(9)</sup> showed that spontaneous explosions could occur when liquid tin (mpt 232°C) was dropped into room temperature water, but not when liquid tin was dropped into n-propanol. Similarly, the experiments of section 6.4 show that liquid tin and liquid Wood's metal (a Pb-Bi-Sn-Cd alloy, mpt 70°C) spontaneously exploded in room temperature water, but not in organic coolants.

Visual observation and capacitative vapour film analysis showed that in room temperature coolants, the point of film collapse was near to  $T_{\min}$ .

If the observations made on the probe-coolant system are applicable to the small scale interactions of section 6.4, then from the data of Figs 3.10 and 3.14, it would be expected that in the small scale interactions, film collapse in n-propanol would have occurred over Wood's metal when the metal was molten, and over tin when the tin had just frozen. Also, film collapse

in water would have occurred over Wood's metal and tin when they were both molten.

Explosions were only observed when water was the coolant. This implies that direct molten metal-coolant contact following a vapour film collapse is not a sufficient condition for the initiation of a vapour explosion. It may however be a necessary condition.

### 7.5.2 Externally Triggered Explosions

In this subsection, the externally triggered explosion experiments of Alexander, Chamberlain and Page<sup>(6)</sup> are examined. Heat flux data from Chapter Six is incorporated into a model which considers one of their explosions in terms of a simple steam explosion.

In their experiments with copper, 4 kg of liquid copper (at temperatures up to about 200°C above its melting point) was poured into a steel tank (dimensions 30x30x30 cm) containing cold water. When the copper was in the water, a length of cordtex attached to the outside of the tank was detonated, the resulting explosion causing the copper-water system to undergo a vapour explosion.

Taking the example of 4 kg of copper at 1200°C being triggered, the time taken for the copper to fragment can be estimated if it is assumed that

- 1 The interaction is a simple steam explosion
- 2 The fragmentation process stops when the copper starts to freeze.

- 3 The area of copper directly exposed to the water increases exponentially during the fragmentation.
- 4 The heat transfer data of Chapter Six are applicable to this system

If the explosion is a simple steam explosion, then the time taken for fragmentation is equal to the time taken for the liquid copper to lose its superheat by boiling heat transfer to the water.

The superheat energy ( $Q$ ) of the copper is given by

$$Q = m C_p \Delta T \quad \dots(7.1)$$

where

$m$  = mass of copper

$C_p$  = specific heat capacity of copper

$\Delta T$  = superheat of the copper

During the fragmentation, in a small amount of time  $dt$ , the copper loses a small quantity of heat  $dQ$  given by

$$dQ = q A dt \quad \dots(7.2)$$

where

$q$  = the heat flux from the copper to the water  
(assumed to be a constant during the fragmentation).

$A$  = the area of the copper exposed to the  
water at time  $t$ .

The total amount of heat lost by the copper during  
the fragmentation is  $Q$  which is given by

$$Q = \int_0^{t^*} q A dt \quad \dots(7.3)$$

where  $t^*$  is the time taken for the fragmentation.

The area of the copper exposed to the water, the area  
taking part in boiling heat transfer, is assumed to  
increase exponentially during the fragmentation, and  
therefore

$$A = A_0 \exp kt \quad \dots(7.4)$$

where

$A_0$  = the initial area of the copper exposed  
to the water i.e. the area of the copper  
exposed when the trigger is applied.

$k = \text{a constant}$

If the final area of the copper (the area of the copper exposed to the water when the fragmentation is completed) is  $A^*$ , then

$$A^* = A_0 \exp kt^* \quad \dots(7.5)$$

Combining equations (7.1), (7.3) and (7.4) gives

$$\begin{aligned} m C_p \Delta T &= q A_0 \int_0^{t^*} \exp kt \, dt \\ &= \frac{q A_0}{k} \left\{ \exp kt^* - 1 \right\} \quad \dots(7.6) \end{aligned}$$

From equation (7.5) it follows that

$$\exp kt^* = \frac{A^*}{A_0} \quad \dots(7.7)$$

and

$$k = \frac{\ln(A^*/A_0)}{t^*} \quad \dots(7.8)$$

Substituting the values of  $\exp kt^*$  and  $k$  from equations (7.7) and (7.8) into equation (7.6) gives

$$m C_p \Delta T = \frac{q A_0 t^*}{\ln(A^*/A_0)} \left\{ \frac{A^*}{A_0} - 1 \right\}$$

and therefore

$$t^* = \frac{m C_p \Delta T \ln(A^*/A_o)}{q (A^* - A_o)} \quad \dots(7.9)$$

Equation (7.9) is now used to make an estimate of the time taken for the copper to fragment.

The initial area of the copper exposed to the water is estimated by assuming that when the trigger is applied, the copper covers the base of the water tank (base area =  $0.09 \text{ m}^2$ ). It is assumed that at this stage, the copper is losing heat upwards as a horizontal plate.

The final area of the copper is estimated by assuming that the final form of the copper is  $100 \mu\text{m}$  diameter particles. This assumption is supported by Pool<sup>(9)</sup> who noted that the debris collected after the explosions in these large scale copper experiments was "very finely divided with metal particles below  $10^{-2}$  cm being common". Also, Zyskowski<sup>(41)</sup> who observed the debris from experiments in which liquid copper particles (0.5 to 2 g) exploded in room temperature water found that the most likely mean diameter of a debris particle was approximately  $100 \mu\text{m}$ .

The heat flux ( $q$ ) from the copper to the water is taken to be  $1.5 \text{ MWm}^{-2}$ , this result being taken from the experimental data of Chapter Six. This result corresponds to the average value of the heat fluxes ( $q_1$ ) that were recorded from liquid copper to  $25^\circ\text{C}$  water

Summarising the data

$$m = 4 \text{ kg}$$

$$C_p = 495 \text{ Jkg}^{-1} \text{ K}^{-1}$$

$$\Delta T = (1200 - 1083) = 117^\circ\text{C}$$

$$A^* = 30 \text{ m}^2$$

$$A_o = 0.09 \text{ m}^2$$

$$q = 1.5 \text{ MWm}^{-2}$$

Substituting into equation (7.9) gives the value of  $t^*$  to be 30 ms. The time taken for these particles to freeze is given by  $t_f$ , where

$$t_f = \frac{mL}{qA^*} \quad \dots(7.10)$$

where  $L$  is the latent heat of fusion of copper ( $2.1 \times 10^5 \text{ Jkg}^{-1}$ ). Thus this time is 19 ms. The time ( $t^* + t_f$ ), is assumed to be the time taken for the

interaction. This time is 49 ms.

This time is about a factor of ten too high. It is likely that the value of  $q$  taken, whilst being appropriate for the initial state of the system, is too low as the interaction proceeds.

Though there is a large difference between the calculated and observed times for the interaction, the results are within an order of magnitude of each other, and this strengthens the belief that the interaction is a simple steam explosion.

The model is capable of development if more data on the liquid copper-water system is generated. These data would need to involve firstly measurement of the heat fluxes in the system at pressures in excess of atmospheric, and secondly measurement of heat fluxes when there is relative motion between the two liquids.

## 7.6 Suggestions For Further Work

The Capacitance-Resistance transducer is capable of monitoring vapour film thicknesses with high time resolution. It is suggested that the transducer would be a useful method of observing the behaviour of vapour films in the presence of externally applied pressure transients.

## APPENDIX

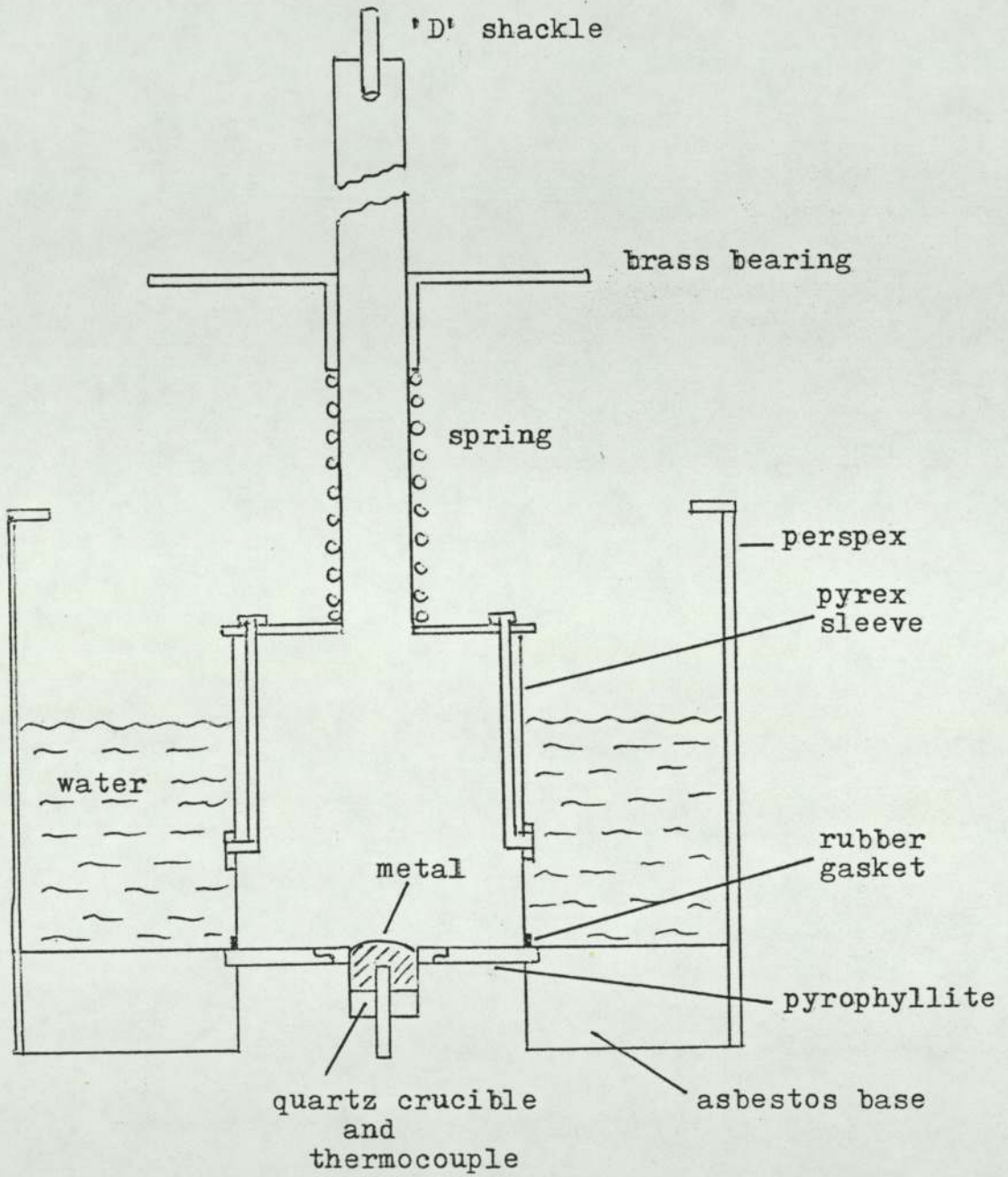
### The Apparatus Used By Boxley

The following account of the apparatus used by Boxley is taken from reference (6)

"The apparatus used (see figure 8.1) was based on one used by Nelson and measured the temperature history of a small crucible of molten metal when it was flooded with water. The apparatus consisted of a spring loaded glass sleeve which pressed against the container bottom, through a rubber gasket to ensure that the system was watertight. A sufficient quantity of water was placed between the glass sleeve and the container wall to ensure that the tank could be flooded to the desired depth. The glass sleeve was connected through a stirrup and a sash cord to a heavy weight normally held in a bomb release catch. To flood the tank, the bomb release was fired electrically and the weight fell, pulling the glass sleeve up against its stirrup and letting the water flow under the sleeve to flood the metal.

The metal was held in a nickel or silica crucible set into the pyrophyllite base of the container with

Fig 8.1 Apparatus for measuring heat flux from a liquid surface



the top flush with the base. A fast response (base) thermocouple passed through the bottom of the crucible to within 1mm of the top. The amount of metal needed to fill the crucible completely when molten, was weighed and melted in the crucible by external heat. When it stabilised at the desired temperature, the sleeve was raised and the output of the thermocouple recorded on a Datalab model 905 transient recorder, and subsequently transferred to a chart recorder."

## REFERENCES

The references 47,48,49,50 and 51 are data references. The data that was taken from these references is listed below.

Reference 47 Calibration table for the Tungsten/  
Tungsten-26%Rhenium thermocouple.

Reference 48 Specific heat capacities of liquid  
and solid copper.

Reference 49 Thermal conductivity of steam,  
Viscosity of steam,  
Specific heat capacity of steam.

Reference 50 Calibration table for the Cromel-  
Alumel thermocouple,  
Specific heat capacity of water,  
Cubic expansivity of water,  
Density of water,  
Viscosity of water.

Reference 51 Latent heat of fusion of water,  
Latent heat of fusion of copper.

## List Of References

- 1 Letter in the Sheffield City Archives, 26  
July 1826
- 2 Health and Safety Executive, "The Explosion at  
the Appleby-Frodingham Steelworks, Scunthorpe,  
4 November 1975", HMSO 1976
- 3 Private Communication
- 4 Long G., "Explosions of Molten Aluminium in  
Water - Cause and Prevention", Metal Progress,  
71, 107-112 (1957)
- 5 Epstein L.F., "Analytical Formulations for the  
Reaction Rate of Metal Water Reactions", USAEC  
Report, GEAP 3272, (1958)
- 6 Alexander W.O., Chamberlain A.T. and Page F.M.,  
"Melt-Coolant Interactions", A Report, Research  
Agreement 7205-16/801/08, University of Aston  
in Birmingham, April (1982)
- 7 Konuray M., Ph.D Thesis, University of Aston  
in Birmingham (1975)
- 8 Dullforce T.A., Buchanan D.J., and Peckover R.S.,  
"Self-triggering of Small Scale Fuel-Coolant  
Interactions", J.Phys., Appl.Phys., Vol 9 (1976)
- 9 Pool G., Ph.D Thesis, University of Aston in  
Birmingham (1980)

- 10 Nelson L.S., and Duda P.M., "Steam Explosion. Experiments with Single Drops of Iron Oxide Melted with a CO<sub>2</sub> Laser", Sandia National Laboratories, NUREG/CR-2295, SAND81-1346, R3 (1981)
- 11 Nukiyama S., "The Maximum and Minimum Values of Heat Transmitted from Metal to Boiling Water under Atmospheric Pressure", J.Soc. Mech.Eng. Japan 37, 367 (1934)
- 12 Farber E.A., and Scoria R.L., "Heat Transfer to Water Boiling under Pressure", Trans.Am. Soc.Mech.Eng., 70, 369-384 (1948)
- 13 Cole R., "Boiling Nucleation", Adv. Heat Trans., 10, 85-166 (1974)
- 14 Kenrick F.B., Gilbert C.S. and Wismer K.L., "The Superheating of Liquids", J.Phys.Chem. 28, 1297 (1924)
- 15 Buchanan D.J. and Dullforce T.A., "Fuel-Coolant Interactions, Small Scale Experiments and Theory", Culham Laboratory, CLM-P362 (1973)
- 16 Rohsenow W.M. and Clark J.A., "A Study of the Mechanism of Boiling Heat Transfer", Trans ASME, 73, 609-620 (1951)
- 17 Cryder D.S. and Finalborgo A.C., "Heat Transmission from Metal Surfaces to Boiling Liquids", Trans.Am.Inst.Chem., 33, 346 (1937)

- 18 Berenson P.J., "Experiments on Pool Boiling Heat Transfer", *Int.J.Heat Mass Transfer*, 5, 985-999 (1962)
- 19 Zuber N., "On the Stability of Boiling Heat Transfer", *Trans ASME*, 711-714, April (1958)
- 20 Ded J.S. and Lienhard J.H., "The Peak Pool Boiling Heat Flux from a Sphere", *AIChE Journal*, 18, No.2, 337-342 (1972)
- 21 Westwater J.W. and Santangelo J.G., "Photographic Study of Boiling", *Ind.Eng.Chem.*, 47, 1605-1610 (1955)
- 22 Leidenfrost J.G., "De Aquae Communis Nonnullis Qualitatibus, Disburg on Rhine (1756)
- 23 Bromley L.A., "Heat Transfer in Stable Film Boiling", *Chem.Eng.Prog.*, 46, 221-227 (1950)
- 24 Monrad C.C. and Badger W.L., "The Condensation of Vapours", *Trans.Am.Inst.Chem.Eng.*, 24, 84 (1930)
- 25 Hsu Y.Y. and Westwater J.W., "Approximate Theory for Film Boiling on Vertical Surfaces", *Chem. Eng.Prog.Symp.Ser.*, 56, No.30, 15-24 (1962)
- 26 Coulson J.M. and Richardson J.F., "Chemical Engineering", Vol.1, 3<sup>rd</sup> Edition, Pergamon Press (1977)
- 27 Awberry J.H., "A Note on the Theory of Quenching", *J.Iron and Steel Inst.*, 144, 119-129 (1941)

- 28 Berenson P.J., "Film Boiling Heat Transfer from a Horizontal Surface", J. Heat Transfer, 83, 351-358 (1961)
- 29 Spiegler P., Hopenfeld J., Silberberg M., Bumpus Jnr C.F. and Norman A., "Onset of Stable Film Boiling and the Foam Limit", Int.J.Heat Mass Transfer, 6, 987-989 (1963)
- 30 Dullforce T.A., Ph.D Thesis, University of Aston in Birmingham (1981)
- 31 Boxley G., Ph.D Thesis, University of Aston in Birmingham (1981)
- 32 Bradfield W.S., "Liquid Solid Contact in Stable Film Boiling", I and E.C. Fund.,5, 200-204 (1966)
- 33 Walford F.J., "Transient Heat Transfer from a Hot Nickel Sphere Moving Through Water", Int. J.Heat Mass Transfer,12, 1621-1625 (1969)
- 34 Board S.J., Clare A.J., Duffey R.B., Hall R.S. and Poole D.H., "An Experimental Study of Energy Transfer Processes Relevant to Thermal Explosions", Int.J.Heat Mass Transfer, 14, 1631-1641 (1971)
- 35 Duffey R.B., Clare A.J., Poole D.H., Board S.J. and Hall R.S., "Measurements of Transient Heat Fluxes and Vapour Generation Rates in Water", Int.J.Heat Mass Transfer,16, 1513-1525 (1973)

- 36 Hinze J.O., "Critical Speeds and Sizes of Liquid Globules", *App.Sci.Res.A1.*, 273-288 (1948)
- 37 Witte L.C. and Cox J.E., "Thermal Explosion Hazards", *Adv.Nuc.Sci.Tech.*, 7, 329-364 (1973)
- 38 Epstein M., "Thermal Fragmentation - A Gas Release Phenomena", *Nucl.Sci.Eng.*, 55, 462 - 467 (1974)
- 39 Johnson G.W. and Shuttleworth R., "The Solubility of Krypton in Liquid Lead, Tin and Silver", *Phil.Mag.*, 957-963 (1959)
- 40 Hsiao K.H., Cox J.E., Hedgcoxe P.G. and Witte L.C., "Pressurisation of a Solidifying Sphere", *J.App.Mech.*, 39, 71-77 (1972)
- 41 Zyskowski W., "Study of Thermal Explosion Phenomena in the Molten Copper-Water System", *Int. J.Heat Mass Transfer*, 19, 849-867 (1976)
- 42 Flory K., Paoli R. and Mesler R.B., "Molten Metal-Water Explosions", *Chem.Eng.Prog.*, 65, 50-59 (1969)
- 43 Fauske H.K., "On the Mechanism of Uranium Dioxide-Sodium Explosive Interactions", *Nuc.Sci.Eng.*, 95-101 (1973)
- 44 Buchanan D.J. and Dullforce T.A., "Mechanism of Vapour Explosions", *Nature* 245, No.5419, 32-34 (1973)

- 45 Saunders O.A., "Natural Convection in Liquids",  
Proc.Roy.Soc., A, 172, 55(1939)
- 46 Winter R.F., Merte H. and Herz H.M., "Recent  
Developments in Boiling and Condensation",  
Reprotext, Verlag Chemie, Weinheim, New York(1977)
- 47 "Temperature, its measurement and Control in  
Science and Industry", Vol 4 Part 2, Proceedings  
of the 5<sup>th</sup> Symposium on Temperature, Washington  
D.C. June (1971), Edited by H.H.Plumb
- 48 Smithells C.J., "Metals Reference Book" 5<sup>th</sup>  
Edition, Butterworth (1976)
- 49 Touloukian Y.S., "Thermophysical Properties of  
Matter", The TPRC Data Series.
- 50 Handbook of Chemistry and Physics, 62<sup>nd</sup> Edition  
The Chemical Rubber Company, 1981-1982
- 51 Science Data Book, Edited by R.M.Tennent, Oliver  
and Boyd (1979)